New off-line ion source infrastructure at IGISOL

Master's thesis, 26.7.2016

Author:

Markus Vilén

Supervisor:

Sami Rinta-Antila

JYVÄSKYLÄN YLIOPISTO
FYSIIKAN LAITOS

ABSTRACT

Vilén, Markus
New off-line ion source infrastructure at IGISOL
Master's thesis
Department of Physics, University of Jyväskylä, 2016, 83 pages

A new off-line ion source infrastructure has been commissioned at the IGISOL facility at the University of Jyväskylä. This thesis presents technical details of hardware and software of the new system. The system includes a new stretch of beam line, a glow discharge ion source and a control system for both of them. Mass separation of a beam from the new system revealed ions of the cathode material as expected. However, the yield was lower than what was hoped for. Solutions to improve the situation are proposed. The beam line was found to be functional as far as current testing opportunities make it possible to determine. The control system based on EPICS software package was found to be fully functional.

Keywords: glow discharge, off-line, IGISOL, EPICS

TIIVISTELMÄ

Vilén, Markus
Uusi off-line ionilähdeinfrastruktuuri IGISOL laitteistolla
Pro gradu -tutkielma
Fysiikan laitos, Jyväskylän yliopisto, 2016, 83 sivua

Uusi off-line ionilähdeasema on otettu käyttöön IGISOL-laitteistolla Jyväskylän yliopistossa. Tämä opinnäytetyö esittää kyseiseen laitteistoon ja ohjelmistoon liittyvät tekniset yksityiskohdat. Käyttöön otettu järjestelmä sisältää uuden suihkulinjan, uuden glow discharge -tyyppisen ionilähteen sekä ohjausjärjestelmän näille molemmille. Laitteistolla tuotetun hiukkassuihkun massahajotelma paljasti suihkun sisältävän katodimateriaalia odotetusti. Kuitenkin tämän materiaalin määrä oli toivottua pienempi. Työssä esitetään ratkaisuehdotuksia tilanteen parantamiseksi. Suihkulinja todettiin toimivaksi niin suurilta osin kuin tähänastiset testaamismahdollisuudet sallivat todeta. EPICS ohjelmistopakettiin perustuvan ohjausjärjestelmä todettiin täysin toiminnalliseksi.

Avainsanat: glow discharge, off-line, IGISOL, EPICS

Contents

1 INTRODUCTION **5**

2 THEORETICAL CONSIDERATIONS **7**
2.1 Ion optics . . . 7
2.1.1 Lenses . . . 7
2.1.2 Electrostatic quadrupole triplet . . . 13
2.1.3 Condensers . . . 18
2.2 Glow discharge ion source . . . 21

3 HARDWARE **25**
3.1 Introduction to IGISOL . . . 25
3.2 The new off-line set-up . . . 28

4 SOFTWARE **41**
4.1 EPICS . . . 41
4.1.1 Introduction to EPICS . . . 41
4.1.2 EPICS with the off-line ion source . . . 45
4.2 Graphical User Interface . . . 50

5 EQUIPMENT TEST RESULTS **58**

6 DISCUSSION **66**

References **69**

A EPICS configuration files **71**

B Graphical user interface source code **82**

1 INTRODUCTION

The IGISOL (Ion Guide Isotope Separator On-Line) facility at the University of Jyväskylä is used to study exotic nuclei using a wide range of different beams. Under normal operating conditions the IGISOL facility uses a primary beam of particles accelerated with a cyclotron. This beam is collided with a thin target foil. Collisions between incoming particles and the target material produce a range of reaction products that have sufficient energy to pass through the remaining thickness of the target. These reaction products then enter a gas cell filled with a buffer gas through a thin window. The products are thermalized via collisions with the gas. The gas cell has a small hole on one side which is used to bleed helium out of the cell. Thermalized reaction products leave the gas cell through the small hole along with a flow of helium. After this the products are gathered and accelerated using both RF and DC voltages to form a secondary beam that can be made of a variety of ions, even exotic ones. This mode of operation has come to be known as on-line.

Naturally, on-line operation of system relies on the availability of a primary beam from an accelerator. There are times a beam is not available. To make the most of such periods of time, the IGISOL facility has an ion source that can be placed in the target area instead of the gas cell and target. This mode of operation has come to be known as off-line. Installation of the off-line source requires a person to enter the irradiated target area. This has resulted in the need to wait for radiation levels to drop after each experiment, which undesirably has increased downtime of the set-up. This situation is improved with the new off-line set-up commissioned as a part of this thesis work.

This project included two main parts, installing necessary pieces of hardware for a new ion source and a stretch of beam line, the hardware part, and designing and implementing a control system for both of them, the software part. The hardware side of this work was mainly focused on the ion source, a glow discharge ion source, and ion optics needed to operate it. The ion source is in its simplicity made of two needles pointing towards each other that have a buffer gas in between them. Given a suitable gas pressure, the electrodes can be used to produce a glow discharge by applying a voltage between them. The discharge sputters material from the cathode electrode which can be then extracted and accelerated. The new ion source was constructed one floor higher than the target area, which removes the need to enter the target area right after on-line operations.

The second part, the control system, was built on a software package called EPICS. It provided a reliable and flexible software architecture to control the set-up over a local area network. This core part of the control system was complemented with a new graphical user interface implemented using LabVIEW. This system allows for multiple user interfaces to be operated simultaneously in parallel so that each of them have up-to-date information on the status of the system. These two parts come together to form a replacement for the previously used off-line ion source as well as provide two free mounting points for additional off-line ion sources.

Altogether, the new ion source and its control system improve the ease of use of an off-line ion source and enable a higher utilization rate of the entire IGISOL set-up. In addition, the new system can be used to provide necessary calibration masses for other pieces of equipment in the IGISOL facility in a way that was not possible previously. Therefore, the new system introduces improvements in personnel radiation safety, system's user friendliness and capability to perform accurate measurements.

2 THEORETICAL CONSIDERATIONS

There is a large variety of different kinds of devices that are used together to form the off-line ion source set-up. Therefore, it is necessary to have an understanding of the physics behind a wide range of phenomena that are related to the set-up. There are, for instance, ion optical elements in the system that are simple to install and operate once the system is up and running. However, it is highly beneficial to have a solid theoretical understanding of these pieces of equipment so that possible problems with the system are easier to mend. It is also crucial for scientists using the IGISOL facility to have an understanding of the operating principles of the entire system as a whole in order to be able to reliably evaluate results obtained using the system. Therefore, aiming towards these goals this chapter is dedicated to discussing relevant phenomena.

2.1 Ion optics

Ion optical elements make up most of the pieces of equipment in the off-line set-up that are adjustable during normal operations. These elements are mainly such that they are adjusted by altering the voltage applied to them without affecting the physical positioning of the elements. It is necessary for personnel using the set-up to understand what kind of effect each element has on ions traversing the system. In the following subsections several ion optical elements are discussed with an aim to provide users with a qualitative understanding to the optical properties of the off-line set-up. The method of transfer matrices is adopted as a mathematical tool along with studying motion of charged particles in electric fields using basic electrodynamical equations.

2.1.1 Lenses

In this project several ion optical elements are used that have similar properties on a beam of charged particles as a traditional lens has on a ray of light. This offers a good starting point for a discussion on ion optics. The adopted method of transfer matrices is a powerful tool for treating traditional optical lenses. It turns out that the same method can be applied to ion optics as well. Naturally, some modifications to transfer matrices are needed but the method remains the same. The mathematical treatment of ion optical lenses shall be started with studying transfer matrices of traditional optical lenses and then making a transition into ion optics. After this a matrix for a simple ion optical lens shall be used to describe more complex pieces of optics.

A lens is an optical element defined by its property of deflecting a ray of light a certain amount $\Delta r'$ depending on the distance r between the ray and the axis of the element. In addition, the deflection is independent of the angle at which the ray impacts the lens [1]. A simplifying assumption is made in this text of treating lenses as thin lenses, which in practice means that each ray of light can be thought to make a sharp bend at the middle of the lens and pass through each edge of the lens without changing direction. This is illustrated in figure 1 where the solid line passing through the lens represents a ray of light. Denoting properties of the ray before the lens with the index

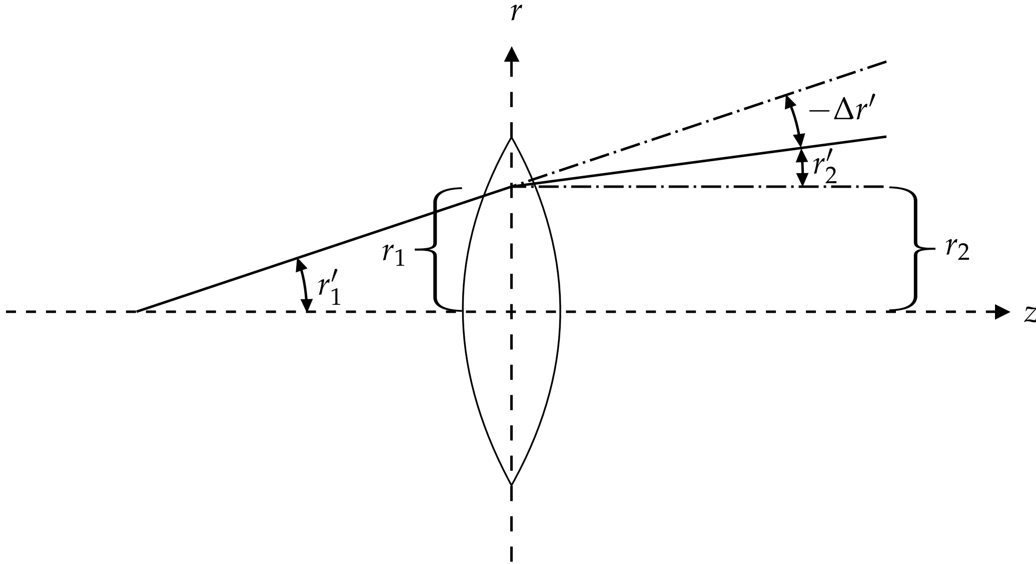

Figure 1: Schematic of a thin lens bending a ray of light.

1 and after the lens with the index 2 one can write

$$r_1 = r_2. \tag{2.1}$$

The slope after the lens can be written as

$$r_2' = r_1' + \Delta r', \tag{2.2}$$

with such a choice of signs that $\Delta r' < 0$. Due to the basic defining property of a lens the change in the slope $\Delta r'$ can be written as

$$-\Delta r' = cr_1, \tag{2.3}$$

where c is a constant of proportionality. It can be presented in a more familiar form by inspecting a special case in figure 2 where the deflected ray of light is parallel to the axis of the lens. In such a case $r_2' = 0$, which means that

$$-\Delta r' = cr_1 = r_1' \tag{2.4}$$

$$c = \frac{-\Delta r'}{r_1} \equiv \frac{1}{f_1}. \tag{2.5}$$

This notation defines the entrance focal length f_1 of the lens. A ray of light that originates a distance f_1 before the lens on the z-axis, i.e. focal point, and passes through the lens appears as a ray parallel to the z-axis after the lens [1]. Focal length can be determined for the exit side similarly as for the entrance side. If the two sides of a lens are symmetric, entrance and exit focal lengths are equal $f_1 = f_2 \equiv f$. By solving equation (2.5) for $\Delta r'$ and inserting it into equation (2.2) one arrives at the expression

$$r_2' = r_1' - \frac{r_1}{f}. \tag{2.6}$$

This, along with equation (2.1), can be presented in an alternative form using matrices as

$$\begin{pmatrix} r_2 \\ r_2' \end{pmatrix} = \begin{pmatrix} 1 & 0 \\ -\frac{1}{f} & 1 \end{pmatrix} \begin{pmatrix} r_1 \\ r_1' \end{pmatrix} \equiv M_L \begin{pmatrix} r_1 \\ r_1' \end{pmatrix}. \tag{2.7}$$

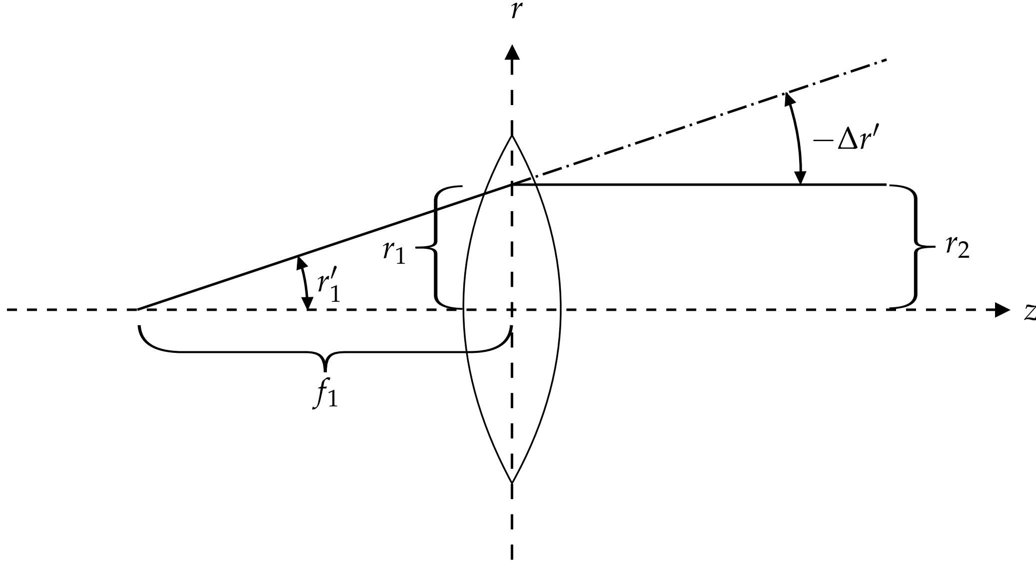

Figure 2: Schematic of a thin lens bending a ray of light originating from entrance focal point.

Here M_L is the transfer matrix of a thin lens. Other optical elements can be similarly represented with transfer matrices. A most beneficial aspect of using transfer matrices to describe optical elements is the fact that a system of optical elements can be described as a whole by multiplying matrices of individual elements. This makes it possible to break down a complex system into smaller more manageable pieces.

In addition to this, there is also another very important property of transfer matrices: they can be used to describe ion optical elements such as apertures of different shapes, Einzel lenses, quadrupole multiplets, etc. For example, in the case of a round aperture that separates two volumes with different uniform electric fields it is possible to utilize the transfer matrix M_L derived earlier. The difference between light optics and ion optics can be accounted for by replacing the focal length f in light optics by

$$f = \frac{4V_a}{E_2 - E_1}, \tag{2.8}$$

where E_1 and E_2 are the electric fields before and after the aperture, respectively, and V_a is the absolute value of voltage of the aperture compared to the voltage of the source of ions [1]. In other words the energy of the ions is $E_{ions} = qV_a$ where q is the charge of an ion. Equations (2.7) and (2.8) can be used to determine whether an aperture focuses or defocuses a beam of ions. These equations result in

$$\begin{pmatrix} r_2 \\ r_2' \end{pmatrix} = \begin{pmatrix} 1 & 0 \\ \frac{E_1 - E_2}{4V_a} & 1 \end{pmatrix} \begin{pmatrix} r_1 \\ r_1' \end{pmatrix} \tag{2.9}$$

$$\begin{cases} r_2 = r_1 \\ r_2' = \frac{E_1 - E_2}{4V_a} r_1 + r_1'. \end{cases} \tag{2.10}$$

From this it can be read that if $E_1 < E_2$ the aperture acts as a focusing lens and if $E_1 > E_2$ is acts as a diverging lens. In the case of a round aperture, this applies separately to both x and y directions. The same qualitative behavior applies also to a slotted aperture. It can be thought as a round aperture that has been stretched in one direction. Given that the slot is much smaller in one direction, the beam diverges or focuses in

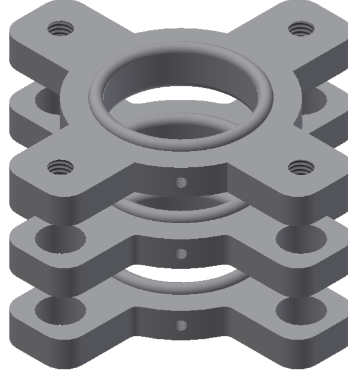

Figure 3: Einzel lens used as a part of the off-line set-up

the direction with smaller separation between opposing edges of the slot and experiences only a negligible focusing action in the other direction. The focusing action in the narrower direction is characterized by a focal length

$$f = \frac{2V_a}{E_2 - E_1}, \tag{2.11}$$

which is differs from the case of round aperture by a factor of 2 [1]. This means that the focusing action is twice as strong in the slotted case.

There remains one more case in which the transfer matrix of a thin lens is important within the scope of this work. That is an ion optical element known as an Einzel lens. It is a set of three round apertures separated by a length of free space between each aperture. A drawing of an Einzel lens used in the off-line set-up is presented in figure 3. A voltage is applied to each aperture in such a way that the voltage of the first is equal to the voltage of the third aperture and the one in the middle is adjusted according to desired focusing effect. In order to be able to give an expression that can be used to gain a qualitative understanding to the effect an Einzel lens has on a beam of particles, a transfer matrix for a unifrom field is necessary. An approximate transfer matrix M_F describing a uniform field can be found in literature [1],

$$M_F = \begin{pmatrix} 1 & \frac{2L}{\sqrt{V_1/V_2}+1} \\ 0 & \sqrt{V_1/V_2} \end{pmatrix}, \tag{2.12}$$

where V_1 and V_2 are voltages at the beginning and end of the field, respectively, and L is the separation between these points in space. The validity of this matrix is restricted by the angle at which the particles enter the field. In deriving this matrix it was assumed that the angle α between the velocity of particles and electric field direction is small enough that $\sin(\alpha) \approx \alpha$ and $\cos(\alpha) \approx 1$. It is worth noting that if $V_1 = V_2$ the transfer matrix for uniform field M_F reverts to a more simple one which describes a drift of length L,

$$M_D = \begin{pmatrix} 1 & L \\ 0 & 1 \end{pmatrix}. \tag{2.13}$$

Accepting the limitation of entry angle, one can write the transfer matrix of an Einzel M_E lens as a product of of five matrices, one for each aperture and length of uniform

field. Here it is assumed that the electric field between apertures is uniform. This is a simplifying assumption that in the case of the off-line set-up is not a very accurate one. If the distance between apertures is large compared to the diameter of the apertures, the approximation is a good one. However, as can be seen in figure 3 the diameter of apertures is large compared to the distance between them. The aim of this text is to provide a qualitative measure of understanding to the ion optics of the set-up and therefore this shortcoming is accepted.

Let us examine a special case where the entrance field of the first aperture and exit field of the last are zero and the first and last apertures are at a voltage $V_{1,3}$. Let us denote the field between first and second aperture E_1 and between second and third E_2 and voltage of the middle aperture V_2. This leads to a transfer matrix M_E for an Einzel lens,

$$M_E = M_{L1} \cdot M_{F1} \cdot M_{L2} \cdot M_{F2} \cdot M_{L3}. \tag{2.14}$$

$$M_E = \begin{pmatrix} 1 & 0 \\ \frac{-E_1}{4V_{1,3}} & 1 \end{pmatrix}_{L1} \begin{pmatrix} 1 & \frac{2L}{\sqrt{V_{1,3}/V_2}+1} \\ 0 & \sqrt{V_{1,3}/V_2} \end{pmatrix}_{F1} \begin{pmatrix} 1 & 0 \\ \frac{E_1-E_2}{4V_2} & 1 \end{pmatrix}_{L2} \begin{pmatrix} 1 & \frac{2L}{\sqrt{V_2/V_{1,3}}+1} \\ 0 & \sqrt{V_2/V_{1,3}} \end{pmatrix}_{F2} \begin{pmatrix} 1 & 0 \\ \frac{E_2}{4V_{1,3}} & 1 \end{pmatrix}_{L3}. \tag{2.15}$$

Table 2.1: Values used to estimate the operation of an Einzel lens

variable	value
$V_{1,3}$	$-800\,\mathrm{V}$
V_2	$-400\,\mathrm{V}$
L	$17 \cdot 10^{-3}\,\mathrm{m}$
E_1	$-23500\,\mathrm{V/m}$
E_2	$23500\,\mathrm{V/m}$

Inputting values in table 2.1 into equation (2.15) one obtains the final transfer matrix for the Einzel lens

$$M_E = \begin{pmatrix} 0.7197 & 0.0182\,\mathrm{m} \\ -33.2571\,\frac{1}{\mathrm{m}} & 0.5481 \end{pmatrix} \tag{2.16}$$

Focal length of the system can be solved using this matrix by setting

$$\begin{pmatrix} r_2 \\ r_2' \end{pmatrix} = \begin{pmatrix} 0.7197 & 0.0182\,\mathrm{m} \\ -33.2571\,\frac{1}{\mathrm{m}} & 0.5481 \end{pmatrix} \begin{pmatrix} r_1 \\ r_1' \end{pmatrix} \tag{2.17}$$

and solving for r_2 and r_2' using values $r_1 = r$ and $r_1' = 0$. This is a corresponding calculation to the one used to obtain the focal length of a thin lens. We get

$$\begin{pmatrix} r_2 \\ r_2' \end{pmatrix} = \begin{pmatrix} 0.7197 \cdot r_1 \\ -33.2571\,\frac{1}{\mathrm{m}} \cdot r_1 \end{pmatrix}. \tag{2.18}$$

Now the focal length can be solved using the fact that r_2' was defined as a slope. This means that

$$r_2' = -\frac{r_2}{f} \tag{2.19}$$

$$f = -\frac{r_2}{r_2'}. \tag{2.20}$$

In the case of our example, this leads to a focal length of $0.0216\,\mathrm{m} \approx 2\,\mathrm{cm}$. This result reproduces the correct lensing effect, i.e. converging, but the magnitude of the focal length does not agree with tests done with the system. The length was found to be several tens of centimeters with voltages close to the ones used in this calculation. However, the derived transfer matrix (2.15) successfully reproduces certain known properties of Einzel lenses, such as the fact that they are always focusing elements regardless whether the middle aperture is at a higher or lower voltage than the rest. Focal length of the system with $V_{13} = -800\,\mathrm{V}$ and $L = 17\,\mathrm{mm}$ is presented in figure 4 for different V_2 values.

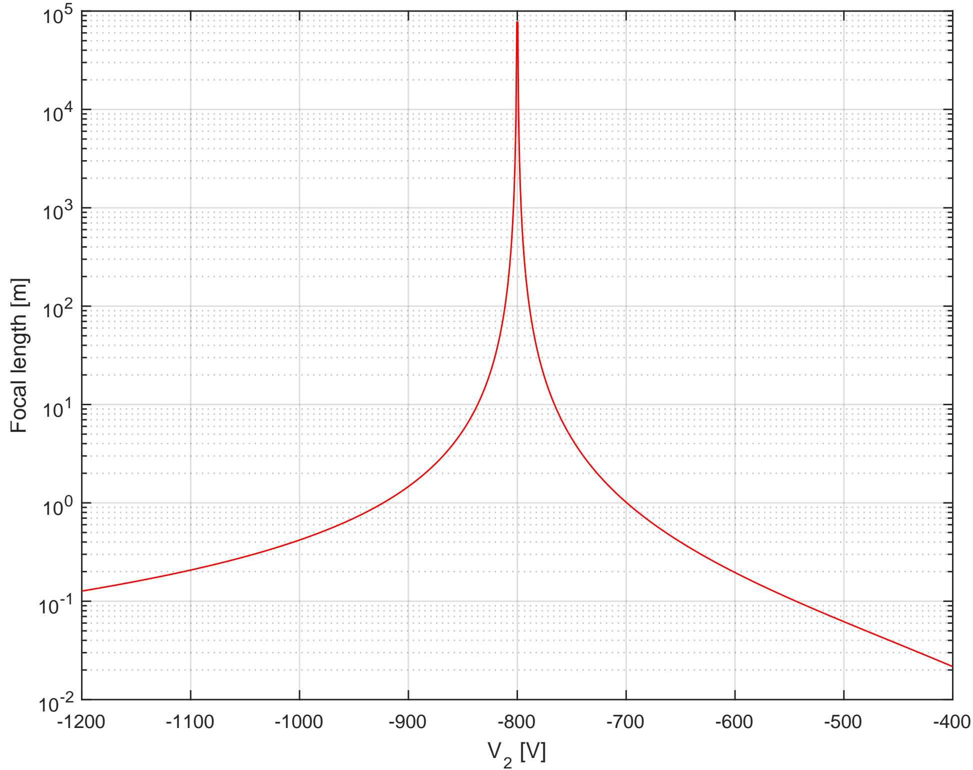

Figure 4: Focal length of an Einzel lens

Another property that is correctly reproduced is that the focal length is larger with any given electric field strength if the middle aperture is at a lower voltage than the first and last aperture rather than at a higher voltage. In other words the system is a more powerful diverging lens if the particles are decelerated in the first gap between apertures and accelerated in the second. For example, comparing two V_2 values $-400\,\mathrm{V}$ and $-1200\,\mathrm{V}$, an equal distance from V_{13}, it can be seen that there is a difference of almost one order of magnitude between focal lengths. The possibility of using either positive or negative voltage in the middle aperture relative to the first and third aperture offers a practical benefit in the sense that a power supply of either sign is accept-

able. However, there are also ion-optical pros and cons to both configurations; The acceleration-deceleration mode offers a longer focal length but it also produces less aberrations than deceleration-acceleration mode [1]. Mathematical treatment of these is outside the scope of this text. Figure 4 also correctly shows that the focal lenght grows rapidly as the voltage of the middle aperture approaches V_{13}. The figure shows the focal length reaching only roughly 10^5 m, but this is merely due to finite amount of computed data points which were evenly distributed around -800 V. The focal length is infinite at exactly -800 V, meaning that the Einzel lens does not focus the beam at all at that voltage.

2.1.2 Electrostatic quadrupole triplet

In addition to the previously introduced lenses, there are also other designs that can be used as electromagnetic lenses. One property an optical design must have in order to qualify as a lens is that the bend particles experience as they traverse the lens has to be proportional to the distance from the optical axis. One way to fulfill this requirement is to search for designs that produce either electric or magnetic field with linearly changing field strength in radial direction. One commonly used choice is quadrupole lenses. They are made of four hyperbolically shaped pole faces that are arranged according to figure 5. This kind of arrangement is focusing in one direction and defocusing in the other. Refraining to electrical lenses henceforth, the choice of axis in figure 5 leads to focusing or defocusing in x and y directions depending on voltages applied to the electrodes [2]. Quadrupole lenses can be treated with transfer matrices analogously to

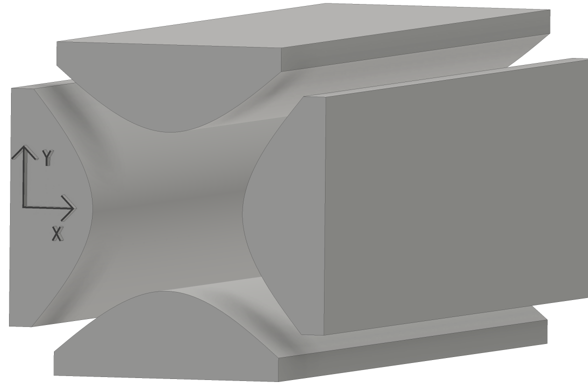

Figure 5: Quadrupole lens with hyperbolical pole faces

other lenses. Naturally, elements of the transfer matrix will be different to previous examples but the method remains the same. Derivation of the transfer matrix is available in literature. For details of the derivation the reader is referred to [2]. A first order approximation of the transfer matrix can be presented as

$$M_{QP,x} = \begin{pmatrix} \cos(kw) & k^{-1}\sin(kw) \\ -k\sin(kw) & \cos(kw) \end{pmatrix} \tag{2.21}$$

$$M_{QP,y} = \begin{pmatrix} \cosh(kw) & k^{-1}\sinh(kw) \\ -k\sinh(kw) & \cosh(kw) \end{pmatrix}, \tag{2.22}$$

separately for x and y direction, where w is the length of the poles and

$$k = \sqrt{\frac{2V_T(ze)}{R_0^2 m v_z^2}} = \sqrt{\frac{V_T(ze)}{R_0^2 E_{kin,z}}} = \sqrt{\frac{V_T(ze)}{R_0^2 (ze) V_a}} = \sqrt{\frac{V_T}{R_0^2 V_a}}. \tag{2.23}$$

Here V_T is the voltage of poles in either in x or y direction depending on which equation (2.21) or (2.22) is being used. Voltages are applied usually in such a way that both electrodes in x direction are at the same voltage V and both electrodes in y direction are at voltage $-V$. Charge of the particle is expressed as ze, its mass is m, speed in z direction v_z and R_0 is the radius between the optical axis and tips of the pole faces, i.e. the shortest distance between any pole and the optical axis. Even though voltages in x and y directions are of different sign, the calculations are done using a positive V_T value for both directions. The difference between polarities is accounted for by the different matrcies for x and y directions. Here the choice of directions is such that x direction has positive and y direction negative voltage.

Let us calculate an example and inspect a similar special case as with Einzel lenses, one where the incoming particles are parallel to the optical axis. All necessary input values are presented in table 2.2.

Table 2.2: Values used to estimate the operation of an electrostatic quadrupole lens.

variable	value
w	82 mm
$V_{T,x}$	400 V
$V_{T,y}$	400 V
V_a	30000 V
R_0	18 mm

Inputting the values the transfer matrices (2.21) and (2.22) become

$$M_{QP,x} = \begin{pmatrix} \cos(k_x w) & k_x^{-1}\sin(k_x w) \\ -k_x \sin(k_x w) & \cos(k_x w) \end{pmatrix} \tag{2.24}$$

$$M_{QP,x} = \begin{pmatrix} 0.8648 & 0.0783\,\mathrm{m} \\ -3.2210\,\frac{1}{\mathrm{m}} & 0.8648 \end{pmatrix} \tag{2.25}$$

$$M_{QP,y} = \begin{pmatrix} \cosh(k_y w) & k_y^{-1}\sinh(k_y w) \\ -k_y \sinh(k_y w) & \cosh(k_y w) \end{pmatrix} \tag{2.26}$$

$$M_{QP,x} = \begin{pmatrix} 1.1416 & 0.0858\,\mathrm{m} \\ 3.5323\,\frac{1}{\mathrm{m}} & 1.1416 \end{pmatrix}. \tag{2.27}$$

Using these it is possible to compute the position vector after the element for both directions,

$$\begin{pmatrix} r_{2,x} \\ r'_{2,x} \end{pmatrix} = \begin{pmatrix} 0.8648 & 0.0783\,\mathrm{m} \\ -3.2210\,\frac{1}{\mathrm{m}} & 0.8648 \end{pmatrix} \begin{pmatrix} r_{1,x} \\ 0 \end{pmatrix} = \begin{pmatrix} 0.8648 \cdot r_{1,x} \\ -3.2210\,\frac{1}{\mathrm{m}} \cdot r_{1,x} \end{pmatrix} \tag{2.28}$$

$$\begin{pmatrix} r_{2,y} \\ r'_{2,y} \end{pmatrix} = \begin{pmatrix} 1.1416 & 0.0858\,\mathrm{m} \\ 3.5323\,\frac{1}{\mathrm{m}} & 1.1416 \end{pmatrix} \begin{pmatrix} r_{1,y} \\ 0 \end{pmatrix} = \begin{pmatrix} 1.1416 \cdot r_{1,y} \\ 3.5323\,\frac{1}{\mathrm{m}} \cdot r_{1,y} \end{pmatrix}. \quad (2.29)$$

Using equation (2.20) it is possible to determine the focal length of the quadrupole lens for the two directions,

$$f_x = -\frac{r_{2,x}}{r'_{2,x}} = -\frac{0.8648}{-3.2210\,\frac{1}{\mathrm{m}}} = 0.2685\,\mathrm{m} \approx 27\,\mathrm{cm} \quad (2.30)$$

$$f_y = -\frac{r_{2,y}}{r'_{2,y}} = -\frac{1.1416}{3.5323\,\frac{1}{\mathrm{m}}} = -0.3232\,\mathrm{m} \approx -32\,\mathrm{cm}. \quad (2.31)$$

Clearly the matrices (2.24) and (2.26) produce the effect that was expected before the calculation, a quadrupole lens focuses the beam in one direction and diverges it in the other, as can be seen from the different signs in focal lengths in equations (2.30) and (2.31).

Using a single quadrupole lens produces a net effect of focusing in one direction and defocusing in the other one. However, a common way to use quadrupole lenses is to combine three lenses into one triplet so that there is a small insulating gap between each lens. This kind of system can be adjusted to have such voltages that the net effect of the triplet is to focus the beam in both directions. Let us examine an example where the dimensions of the system are the same as in the triplet used in the off-line set-up. Values in table 2.2 are taken from the first lens of the triplet. In addition to those values specifications of the remaining two lenses are needed. Necessary input values for all three lenses are presented in table 2.3. The triplet used in the system is presented in figure 6. It differs from figure 5, which was the starting point of our calculations, by the shape of the poles used. The poles are cylindrical instead of hyperbolical in the off-line set-up. This is due to the fact that cylindrical shape is much more convenient from a manufacturing point of view than hyperbolical. Therefore, following calculations are not to be considered entirely accurate, but merely a tool for studying the general behaviour of the triplet.

Table 2.3: Values used to estimate the operation of an electrostatic quadrupole triplet.

variable	value
$w_{1,3}$	82 mm
w_2	163 mm
w_d	28 mm
$V_{T,x1}$	400 V
$V_{T,y1}$	400 V
$V_{T,x3}$	400 V
$V_{T,y3}$	400 V
V_a	30000 V
R_0	18 mm

In order to achieve a net focusing effect in both directions it is necessary to rotate the middle lens by 90° compared to the first and third lens. Naturally, the system is symmetrical in 90° rotations, and therefore, the effective rotation is achieved by changing

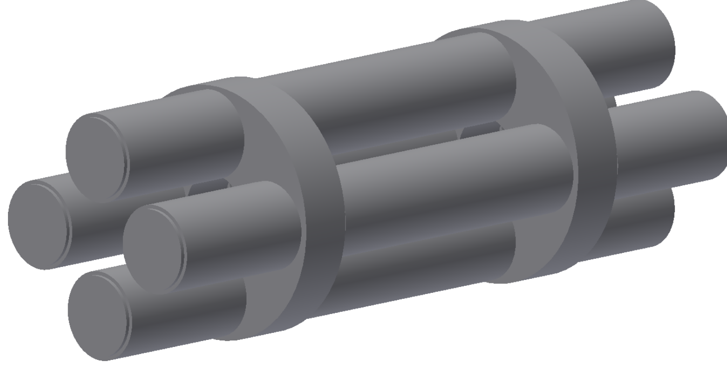

Figure 6: Quadrupole triplet used in the off-line set-up

the polarity of electrodes in the middle lens. This results in polarities in x direction being plus-minus-plus and in y direction minus-plus-minus. Mathematically this corresponds to using a transfer matrix for y direction when computing the x direction behavior of particles through the middle lens and vice verse for treating the y direction. Using the same choice of axis as in figure 5, the transfer matrix for the entire triplet including the insulators can be written as a combination of three quadrupole lenses and two drift lengths. Transfer matrices for the system become

$$\begin{cases} M_{triplet,x} = M_{QP,x} \cdot M_D \cdot M_{QP,y} \cdot M_D \cdot M_{QP,x} \\ M_{triplet,y} = M_{QP,y} \cdot M_D \cdot M_{QP,x} \cdot M_D \cdot M_{QP,y}. \end{cases} \tag{2.32}$$

These can be expressed using equations (2.13), (2.21) and (2.22) as

$$\begin{aligned} M_{triplet,x} = & \begin{pmatrix} \cos(k_{x1} w_{1,3}) & k_{x1}^{-1} \sin(k_{x1} w_{1,3}) \\ -k_{x1} \sin(k_{x1} w_{1,3}) & \cos(k_{x1} w1,3) \end{pmatrix} \begin{pmatrix} 1 & w_{drift} \\ 0 & 1 \end{pmatrix} \cdot \\ & \begin{pmatrix} \cosh(k_{x2} w_2) & k_{x2}^{-1} \sinh(k_{x2} w_2) \\ -k_{x2} \sinh(k_{x2} w_2) & \cosh(k_{x2} w_2) \end{pmatrix} \begin{pmatrix} 1 & w_{drift} \\ 0 & 1 \end{pmatrix} \cdot \\ & \begin{pmatrix} \cos(k_{x3} w_{1,3}) & k_{x3}^{-1} \sin(k_{x3} w_{1,3}) \\ -k_{x3} \sin(k_{x3} w_{1,3}) & \cos(k_{x3} w_{1,3}) \end{pmatrix}, \end{aligned} \tag{2.33}$$

$$\begin{aligned} M_{triplet,y} = & \begin{pmatrix} \cosh(k_{x1} w_{1,3}) & k_{x1}^{-1} \sinh(k_{x1} w_{1,3}) \\ -k_{x1} \sinh(k_{x1} w_{1,3}) & \cosh(k_{x1} w1,3) \end{pmatrix} \begin{pmatrix} 1 & w_{drift} \\ 0 & 1 \end{pmatrix} \cdot \\ & \begin{pmatrix} \cos(k_{x2} w_2) & k_{x2}^{-1} \sin(k_{x2} w_2) \\ -k_{x2} \sin(k_{x2} w_2) & \cos(k_{x2} w_2) \end{pmatrix} \begin{pmatrix} 1 & w_{drift} \\ 0 & 1 \end{pmatrix} \cdot \\ & \begin{pmatrix} \cosh(k_{x3} w_{1,3}) & k_{x3}^{-1} \sinh(k_{x3} w_{1,3}) \\ -k_{x3} \sinh(k_{x3} w_{1,3}) & \cosh(k_{x3} w_{1,3}) \end{pmatrix}. \end{aligned} \tag{2.34}$$

These can be computed for different voltages $V_{T,2x}$ and $V_{T,2y}$ to find values where the focusing effect is equally strong in both directions. This kind of setting would result in parallel-to-point focusing effect. Focal lengths for the transfer matrices (2.33) and (2.34) are presented in figure 7 for a range of middle electrode voltages. The figure has two distinct voltages at which one of the focal lengths approaches $\pm\infty$, the sign

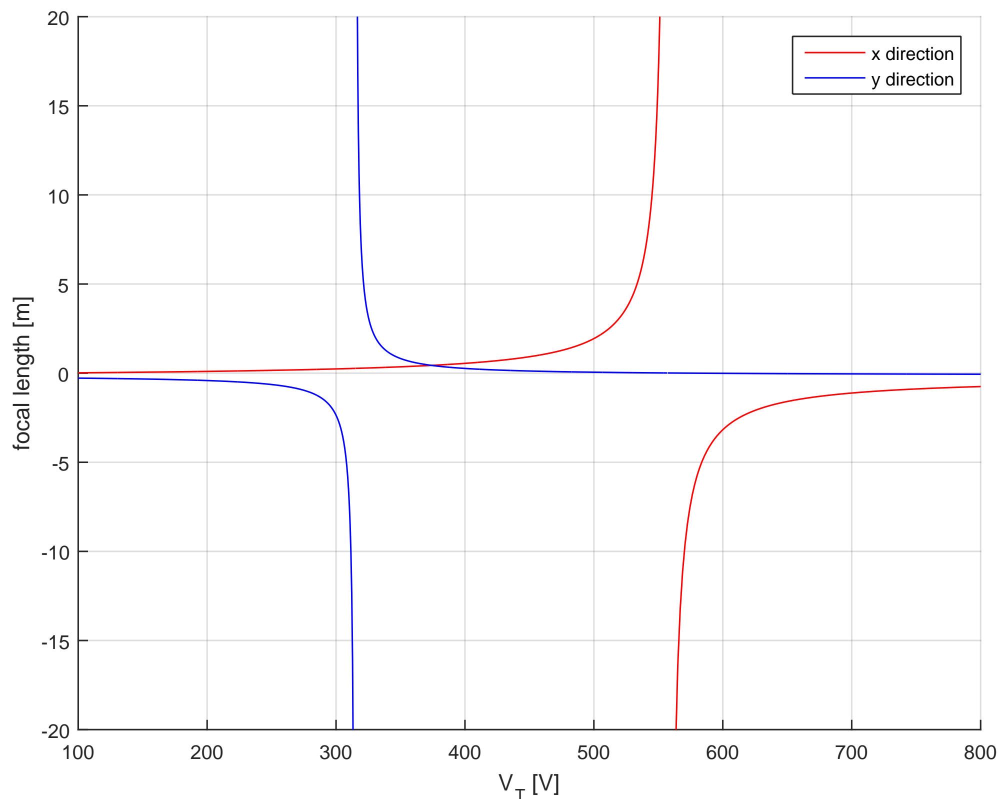

Figure 7: Focal length of a quadrupole triplet as a function of middle electrode voltage V_T in x and y directions

depending on the direction of approach. Figure 7 shows that it is possible to find a common voltage for x and y directions that provides the same focal length for both directions. With the numerical values used in this calculation, that voltage is slighty below 400 V. However, there is no reason that prevents using different voltages in x and y directions. This is beneficial since the two voltages of infinite focal length, i.e. no focusing or defocusing, move farther away from each other with increasing voltages in first and third lens. This means that the common voltage for equal focal length slowly becomes smaller. If moderate voltages are used this is a property that can be used in tuning the system. A good starting point for tuning a triplet would seem to be slightly below the voltages applied to the first and third lens. Figure 7 provides a rule of thumb for choosing the voltages in the middle lens, but it should be noted that the figure is a result of an approximate treatment of the system.

2.1.3 Condensers

Lenses have been at focus in previous subsections due to the fact that they can be used to mathematically treat a large portion of ion optics used in the off-line set-up. However, there remains one more category of ion optical elements that have an important role in the system and remain undiscussed. These are condensers. In its most simple form a condenser consists of two conducting parallel plates.

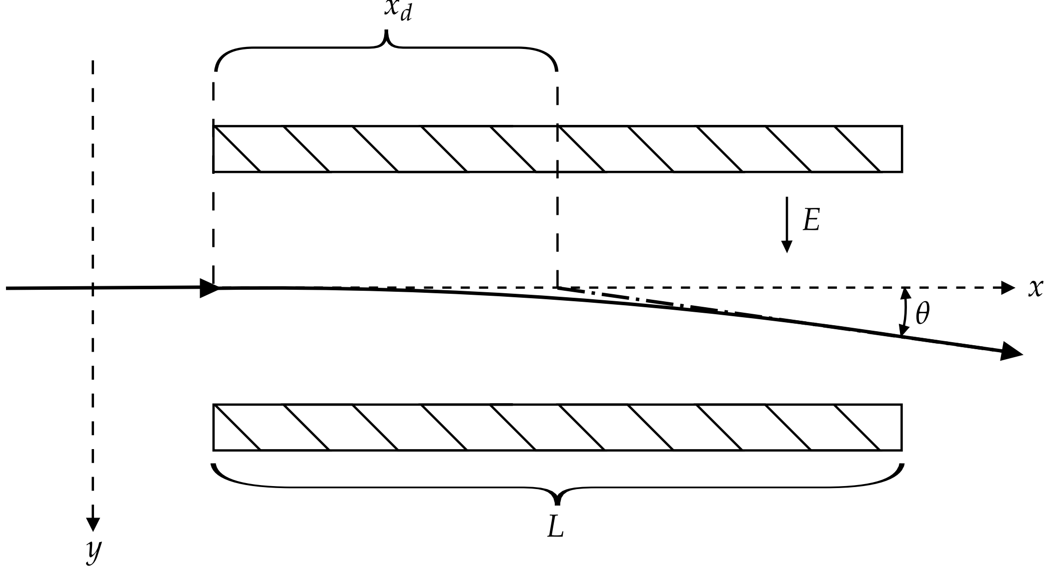

Figure 8: Parallel plate condenser as a beam deflector

If a voltage is applied between the plates of a condenser and a beam of particles traverses through the condenser as in figure 8, the beam is deflected by an angle θ. This angle can be solved starting with forces acting on the particles. The particles experience a force due to the electric field,

$$qE = m\ddot{y}, \tag{2.35}$$

where $y = y(t)$. This differential equation can be solved for y, $\dot{y}$ and $\ddot{y}$. Let us impose a set of boundary conditions that simplify the problem. Let us require $y(0) = 0$ and $\dot{y}(0) = 0$. This leads to

$$\ddot{y} = \frac{qE}{m} \tag{2.36}$$

$$\dot{y} = \frac{qE}{m}t \tag{2.37}$$

$$y = \frac{qE}{2m}t^2. \tag{2.38}$$

Let V_0 be the voltage at which the incoming particles have been initially accelerated. Thus their velocity is $v_0 = \sqrt{2qV_0/m}$. Expressing time as $t = x/v_0$ equations (2.37) and (2.38) can be written at $x = L$ as

$$\dot{y}_L = \frac{EL}{2V_0}v_0 \tag{2.39}$$

$$y_L = \frac{EL^2}{4V_0}. \tag{2.40}$$

To an outside observer the beam coming out of the condenser would seem like coming from a single point on the x axis. This point is called the virtual deflection center [1]. The position of the deflection center can be solved by inspecting the slope formed by v_0 and $\dot{y}$, i.e. the angle at which the beam seems to have intersected the optical axis. This slope y' can be written using equation (2.39) as

$$y' = \frac{\dot{y}_L}{v_0} = \frac{EL}{2V_0}. \tag{2.41}$$

This result allows writing the position of the virtual deflection center x_{center} as

$$x_{center} = \frac{y_L}{y'} = \frac{L}{2}. \tag{2.42}$$

It is worth noting that the use of slope y' in solving for the position x_{center} is justified since we are dealing with a virtual deflection center rather than a real one. It is tempting to think that using a slope solved using a derivative of position to determine another position is incorrect. However, this procedure is justified and it is what makes the deflection center virtual. The angle θ between the exiting beam and the optical axis can be expressed as

$$\tan\theta = \frac{y_L}{L/2}. \tag{2.43}$$

A useful approximation is to assume that θ is small enough so that

$$\tan\theta = \frac{\sin\theta}{\cos\theta} \approx \frac{\theta}{1} = \frac{y_L}{L/2}. \tag{2.44}$$

Using this relation along with equation (2.40) leads to an expression for the angle θ,

$$\theta = \frac{EL}{2V_0}. \tag{2.45}$$

Parallel plate condensers are used in the off-line set-up as beam deflectors and also as a way of moving the beam parallel to the optical axis. This requires two condensers to be used in series. The first condenser deflects the beam by an angle ϕ. After this the beam is allowed to drift for a distance and then finally there is another condenser which deflects the beam back to its initial angle compared to the optical axis. In addition to adjusting the beam position parallel to the optical axis this system can, naturally, be used to give an additional net deflection. This system has come to be known as double xy-plates at the IGISOL facility.

There is one more type of condenser that is necessary in the off-line set-up. This is a cylindrical condenser. In general these can be used as energy spectrometers and thick lenses, but in the case of this work, one is used to bend a beam of particles from a vertical beam line to a horizontal beam line. Here only a part of the properties of cylindrical condenser shall be discussed with a primary focus in determining necessary voltages for bending particles of given energy.

Let us start with determining voltages to be applied to the condenser plates in order to bend a particle that arrives at the middle of the entrance gap parallel to the vertical axis. This kind of situation is presented in figure 9. In such a case the force exerted on the particles by the electric field must be equal to the centrifugal force. This requirement can be written as

$$qE = \frac{mv^2}{r_c} = \frac{2\frac{1}{2}mv^2}{r_c} = \frac{2qV_0}{r_c}. \tag{2.46}$$

This leads to

$$E = \frac{2V_0}{r_c} = -\frac{\mathrm{d}V(r)}{\mathrm{d}r}. \tag{2.47}$$

Here the last equality is merely the definition of electric field. Potential V corresponding to this field can solved by integrating equation (2.47). The potential becomes

$$V(r) = -2V_0 \ln \frac{r}{r_c}, \tag{2.48}$$

where $V_0 = E_{kin}/q$, i.e. the acceleration voltage, and r_c is the radius of the center line of the condenser. Expanding in a Taylor series the potential becomes

$$V(r) = -2V_0 \ln\left(\frac{r_c}{r_c}\right) - 2V_0\frac{r - r_c}{r_c} + V_0\frac{(r - r_c)^2}{r_c^2} - \frac{2}{3}V_0\frac{(r - r_c)^3}{r_c^3} + \cdots \tag{2.49}$$

$$V(r) = -2V_0\left(\frac{r}{r_c} - 1\right) + V_0\left(\frac{r}{r_c} - 1\right)^2 - \frac{2}{3}V_0\left(\frac{r}{r_c} - 1\right)^3 + \cdots \tag{2.50}$$

$$V(r) = -2V_0\left(\left(\frac{r}{r_c} - 1\right) - \frac{1}{2}\left(\frac{r}{r_c} - 1\right)^2 + \frac{1}{3}\left(\frac{r}{r_c} - 1\right)^3 + \cdots\right). \tag{2.51}$$

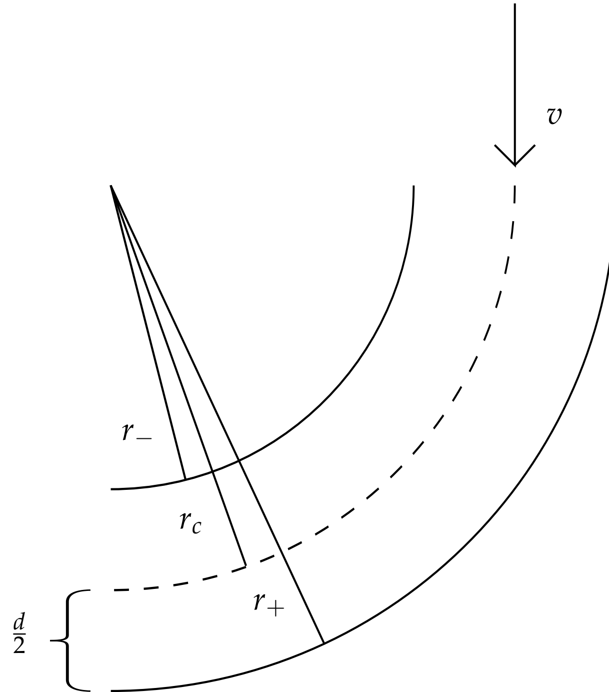

Figure 9: Schematic of a cylindrical condenser

If the cubic term and the ones after it are now cut off and a new variable, $\rho = \frac{r}{r_c} - 1$, is introduced, the expression becomes

$$V(r) = -2V_0 \left(\rho - \frac{\rho^2}{2} \right). \tag{2.52}$$

Now all that remains before voltages for the condenser plates can be solved is to express the position of the electrodes using the new variable ρ. Let us denote the radial distance between electrodes d. This leads to an expression

$$r_\pm = r_c \pm \frac{d}{2} \tag{2.53}$$

$$\frac{r_\pm - r_c}{r_c} = \pm \frac{d}{2r_c} = \rho. \tag{2.54}$$

Plugging this into equation (2.52) results in potentials

$$\begin{cases} V_+ = -2V_0 \left(\frac{d}{2r_c} - \frac{d^2}{8r_c^2} \right) \\ V_- = -2V_0 \left(-\frac{d}{2r_c} - \frac{d^2}{8r_c^2} \right), \end{cases} \tag{2.55}$$

and finally in the voltage between the electrodes

$$V_+ - V_- = 2\frac{dV_0}{r_c}. \tag{2.56}$$

There is one cylindrical condenser in the off-line set-up. It is 400 mm in radius and has electrode separation of 19 mm. The system is designed to operate using an acceleration voltage of 30 kV. Using these values equation (2.56) gives a voltage of 2850 V to be applied between the electrodes. A more thorough discussion on condensers along with the derivation presented above can be found in [1].

2.2 Glow discharge ion source

The main purpose of this thesis work was to commission an ion source and a beam line necessary to transport a generated ion beam to the rest of the experimental set-up. As will be discussed in the next section, the new beam line design offers a possibility to install three off-line ion sources to the system at the same time. However, only one ion source was commissioned as a part of this work. This ion source was chosen to be a glow discharge ion source. This decision was motivated by the fact that another source of the same type has been routinely used at the IGISOL facility.

A glow discharge, the phenomenon upon which the ion source is built on, can be generated by applying a voltage between two electrodes in a gas. Given suitable gas pressure, electrode separation and applied voltage, a current will flow between the electrodes. In favorable conditions this results in a glow discharge with multiple distinct regions between the electrodes that can be seen with a naked eye. However, the discharge starts off as a more subtle phenomenon, a small current between the electrodes that does not produce any visible effects. This can be achieved with relatively low inter-electrode voltages, tens of volts. This process relies on external radiation to get started. Cosmic radiation and natural radioactivity work as sources of ionizing

radiation that create the first ions between the electrodes. The applied voltage then pulls these ions to electrodes of opposite signs, creating a small current. The amount of current is too small in these conditions to emit any visible light [3].

The discharge is still at this stage a non-self-sustaining one, meaning that it needs an external source of ionization or a source of electrons or ions that is not a result of the discharge itself in order to exist. Current flowing in the discharge can be increased by raising the voltage. An increase in voltage makes the transportation of electrons and ions to the electrodes faster, which in turn helps to minimize recombination of opposite charges. This leads to an increase in current. However, there is a limit to the increase set by the amount of ionization due to the external sources. Once the voltage is high enough that no significant amount of recombination takes place the current saturates.

If the voltage is raised even further the discharge rapidly changes at a certain voltage from a non-self-sustaining to a self-sustaining one. This is due to a breakdown taking place in the discharge. The breakdown results in even higher current and emission of light. The phenomenon can be explained by considering individual electrons. A breakdown occurs once the electric field gives a sufficient amount of kinetic energy to free electrons to knock another electron loose from a neutral atom when the two collide. After this the two electrons repeat the process resulting in an electron avalanche.

In general, this situation can develop in two directions at higher voltages. It can turn into a glow discharge, as it will in the case of this thesis work, or it can become an arc discharge. Which one of these possibilities is realized is determined by conditions surrounding the breakdown. If the pressure is high, roughly atmospheric level, and the external circuit powering the discharge has a low impedance, the breakdown turns into an arc discharge. This type of discharge is characterized by a low voltage over the formed discharge, high current of the order of 1 A and high thermal power. The other alternative, a glow discharge, is formed in lower pressure with higher voltage between electrodes and high impedance of the external circuit. In this case the high impedance in necessary to limit the current in the discharge. One typical set of condition conditions for a stable glow discharge in the ion source commissioned as a part of this work is a pressure of 5 mbar and a voltage of 700 V with 0.1 mA of current.

As mentioned, both of these discharges are self-sustaining. However, the mechanism of electron emission from the cathode is different in these cases. An arc discharge heats up the cathode due to a high current and electrons are termionically emitted. In the case of the glow discharge the cold cathode emits electrons due to impacts of positive ions [3]. If the system is used to sputter material, the cathode also serves as the sputtering target [4]. The difference in electron emission mechanisms is something to bear in mind when choosing a power source for a glow discharge ion source.

In the case of this work, a breakdown between electrodes develops into a glow discharge. This type of discharge has an internal structure which consists of several separate regions with different sets of properties. These shall be discussed next. The structure of a typical glow discharge is presented in figure 10. Different regions of the discharge are visible in the figure. They can be roughly divided into three main categories, dark spaces, glow regions and a positive column.

Formation of these regions can be understood by considering the behavior of electrons inside the discharge. Electrons needed to sustain the discharge are ejected from the

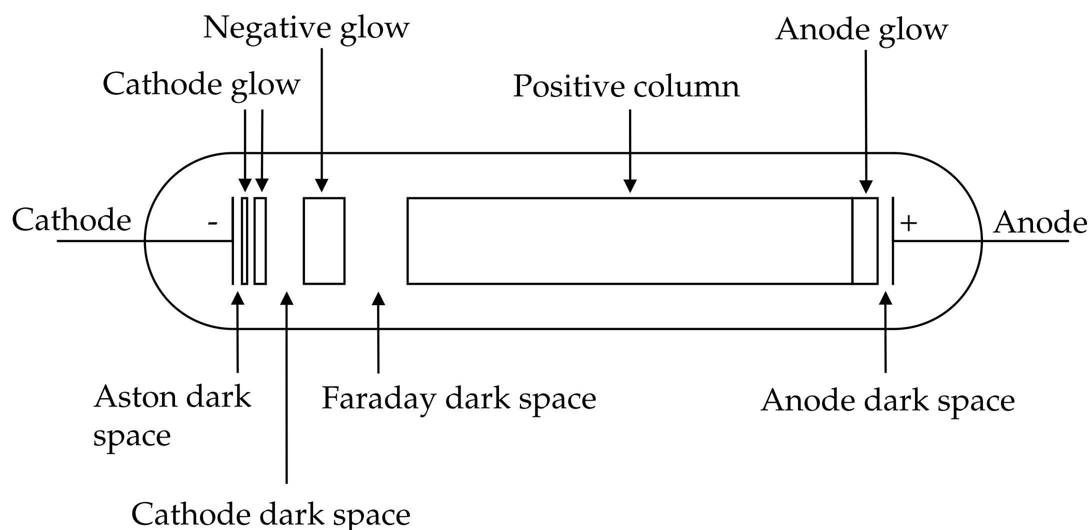

Figure 10: Structure of a glow discharge [3]

cathode. These electrons do not have sufficient energy to excite atoms right after their ejection. This gives rise to the Aston dark space. Given that electrons and the cathode have the same sign of electrical charge, the electrons are accelerated away from the cathode. Once the electrons gain enough energy to excite atoms the Aston dark space gives away to the cathode glow. A glow discharge may have several layers of cathode glow. Each of these is due to separate excitations of electrons bound to atoms. The layers are ordered in such a way that the one corresponding to the lowest excitation energy is closest to the cathode. Electrons gain additional energy passing a dark space after each glow layer, which enables the formation of the following glow layer.

The cathode glow comes to an end once the energy of electrons becomes so high that excitation cross section between electrons and atoms starts to fall off. This gives rise to the cathode dark space. Even though excitations are unlikely in this dark space there are still collisions in this region. These collisions are the mechanism behind the majority of ionization which happens via electron avalanche. The created ions are much more massive than electrons and therefore they also move much more slowly. This results in a build-up of positive space charge. This space charge reduces the strength of the electric field created by the cathode and effectively slows down electrons that go past it. Nature of electron avalanche is such that the amount of ionization increases the farther the electrons travel from the starting point of the avalanche. Therefore, the amount of positive space charge within the dark space also increases with distance from the cathode. This also means that the deceleration of electrons increases. Once the energy of electrons drops back to the region where excitation cross section is significant, the cathode dark space ends and the negative glow begins.

Similarly to the cathode glow, the negative glow exhibits different colors of light depending on the distance the electrons have traveled. In this case excitations that have the highest energy are visible first. Due to collision inside the negative glow the electrons gradually lose their energy. This results in dominance of excitations of lower energies as distance from the cathode increases. Eventually the negative glow fades away and the Faraday dark space begins. Electrons continue to lose their energy within

the Faraday dark space. Gradually the amount of electrons that can penetrate the distance grows smaller and the electric field rises, pointing towards the cathode. This can be understood similarly as the reduction of the field strength inside the cathode dark space.

Eventually the Faraday dark space gives away to the positive column which is a region of a low level of ionization and electrical neutrality. In this region the electrical field is not high enough to enable all electrons to excite atoms. However, the electrons have a distribution of velocities. This means that some of the electrons have sufficiently high energy for excitations. This creates a luminescence that is used in many commercial applications. For example, many glowing tubes that make up street advertisements utilize this luminescence.

The positive region is followed by an anode dark space. This is a result of the anode attracting negative charges and pulling them out of the positive column. At the same time all positive ions are repelled by the anode. This results in the build-up of negative space charge next to the anode which decreases the electric field in between the space charge and positive column. The result is the anode dark space. It is followed by a region of higher electric field between the space charge and anode. This gives rise to the anode glow.

These are the main, in some cases visible, regions of a glow discharge. However, not all of these are present in all situations. The positive column is the most flexible region, in a sense. It can vanish altogether or it can extend very long distances. If the electrodes are brought closer together the column shrinks and eventually vanishes. On the other hand, if the electrode separation is increased, it is the positive column that expands to cover the distance. The only purpose of the positive column is to close the electrical circuit between electrodes. If the electrodes are brought close enough the Faraday dark space also vanishes. Beyond this point, the negative glow starts to contract. If the negative glow disappears completely the entire glow discharge is extinguished. This can be compensated by increasing the voltage or pressure. An increase in pressure causes all the layers to become thinner and shift closer to the anode, bar the Faraday dark space and positive column.

In the framework of this thesis work, a most important piece of knowledge regarding glow discharges is the fact that most of the ionization takes place in the cathode dark space, which causes ions to accelerate towards the cathode and sputter material from its surface. An important aspect to notice is also the fact that the cathode dark space is terminated due to a build up of positive space charge. This results in a large potential difference between the location where positive ions are created and the cathode. This enables the ions to gain a large amount of kinetic energy along their way to the cathode. A majority of the potential difference between the electrodes is usable by the ions created in the cathode dark space [3]. Another useful piece of knowledge is that the layers taking part in accelerating the ions shrink with increasing pressure. Therefore, increasing pressure and voltage are expected to aid in sputtering and then ionizing material from the cathode which, in the end, is what the glow discharge ion source is built for.

For a more detailed discussion on the topics covered in this subsection and aspects of glow discharges that remain thus far to be discussed, the reader is referred to [3].

3 HARDWARE

Now that the most important theoretical topics have been introduced, it is time to put them to context. All phenomena discussed in the previous section have their place in the hardware set-up. In this section the hardware will be covered in more detail. The pre-existing parts of the IGISOL facility shall be covered first followed by a discussion on the part of the system commissioned during this thesis work.

3.1 Introduction to IGISOL

The off-line set-up can be described simply as an extension to the previously used IGISOL facility that provides the infrastructure necessary for operating a number of off-line ion sources. The IGISOL facility is primarily located on two floors. The upper floor was used previously by the IGISOL research group only for housing and operating laser related equipment. The lower floor houses the majority of equipment. This includes, among other things, the front end, RFQ cooler buncher and Penning traps. Naturally, the lower floor also houses necessary beam transport lines to and from these pieces of equipment. Layout of the lower floor along with the vertical beam line is presented in figure 11.

The flow of particles in figure 11 is from left to right. Any on-line measurement at IGISOL starts with a beam of particles from one of the cyclotrons at the Accelerator Laboratory. This particle beam is then directed to collide with a thin target. This happens at the front end labeled C in figure 11. A characteristic property of the IGISOL technique is the following step in the process. The reactions products produced in collisions between the beam and thin target are transported into a gas cell. This relies on the momentum the products receive from the primary beam hitting the target. The gas cell is filled with low pressure helium in order to thermalize the reaction products. The helium is then allowed to flow out of the cell through a small aperture. After this the reaction products that remain electrically charged are separated from neutral material with the help of alternating electrical fields. This is followed by an electrostatic acceleration of the remaining products to form the secondary beam of particles.

The secondary beam can also be produced using an alternative method, an off-line ion source. The acceleration of ions and their extraction from the neutral material remain the same as in the on-line case, but the difference lies in the way the ions for the secondary beam are produced. In the off-line case, the gas cell is not used and it is replaced by a glow discharge ion source which was discussed in section 2.2. This provides a way to use the IGISOL facility even without an available cyclotron. This type of off-line ion source is the part of the IGISOL system that will be made obsolete by the new off-line set-up.

After the secondary beam has been accelerated it is directed to pass through a dipole magnet which is used to perform a first stage mass separation of the beam. After the dipole the beam enters the switchyard. It is a vacuum chamber that houses ion

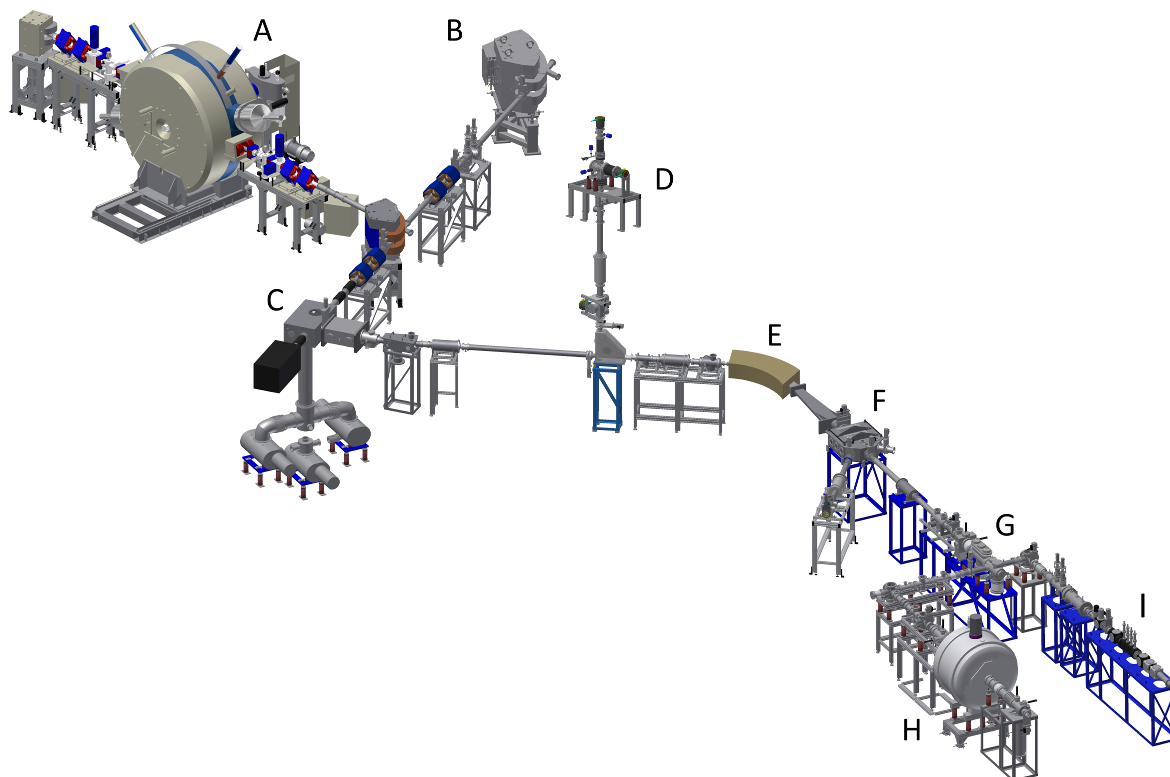

Figure 11: Layout of the IGISOL facility along with the MCC30 cyclotron

A	MCC30 cyclotron	F	switchyard
B	line from K130 cyclotron	G	RFQ
C	front end	H	Penning traps
D	vertical line	I	laser specrtoscopy line
E	dipole magnet		

optical elements used to bend the beam in a chosen direction. Currently the beam can be directed towards the spectroscopy line or passed on to an RFQ (Radio Frequency Quadrupole) cooler buncher. It is a device that can be used to turn the continuous secondary beam into a bunched beam. In addition, the RFQ is capable of reducing the energy spread and cross sectional spatial spread of the beam, i.e. it can cool the beam.

The RFQ achieves this using both a static electric field and an alternating one. The structure of RFQ cooler buncher is presented in figure 12. The RFQ consists of a number of sets of four electrodes placed around the beam axis. Each of these can be adjusted to a desired DC voltage in order to form a potential well in the axial direction for the incoming beam. Trapping of the ions in the radial direction is achieved using alternating electric potentials applied to the electrodes. An RF voltage is applied to each set of four electrodes in such a way that each two opposing electrodes at different sides of the beam axis are always at the same potential. These doublets within a set of four are at sinusoidally oscillating potential so that there is a phase shift of π rad between the doublets. The net effect this has on charged particles depends on the frequency and amplitude of the oscillating voltage. With suitable settings the particles are driven towards the beam axis, i.e. they are radially confined.

The RFQ is filled with low pressure helium which, together with the axial and radial potential wells, enables bunching of the beam. The axial well is first set up so that the

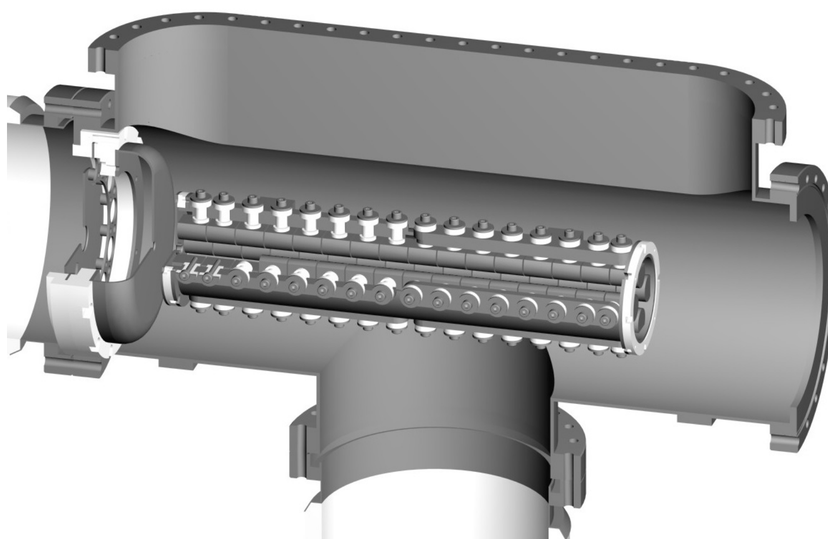

Figure 12: Internal structure of the RFQ cooler buncher

incoming particles can enter the RFQ but do not have sufficient energy to pass through it. During the time the ions spend inside the RFQ they dissipate their kinetic energy via collisions with the buffer gas. In a case where the neutral buffer gas is made up of lighter elements than an incoming beam of particles the net effect is that the beam experiences viscous drag due to the buffer gas. This is referred to as collisional cooling [5]. It causes the ions to gradually fall deeper into the well and become axially confined to the well. Once the beam has accumulated for a period of time the potential at the end of the RFQ is lowered so that the particles are once again accelerated forward. Then the potential is brought back up. This cycle is then repeated as long as a bunched beam is necessary. For a more detailed discussion on the RFQ the reader is referred to [6].

Once the beam has been bunched and cooled it can be directed to one of two alternative routes. One is towards the Penning traps and the other is a laser spectroscopy line. For further details on these the reader is referred to [7] and [8], respectively. However, these will not be discussed further in this text due to the fact that the RFQ has one more important property that has not been covered thus far. Since the RFQ bunches and cools the beam, a beam released from the RFQ does not have any properties that are traceable to the ion optics before the RFQ. In other words, the beam does not remember anything that preceded the cooler. Naturally, the beam has some properties such as intensity that are in some way dependent on the preceding system, for example the ion source, but the relevant point is that if a given amount of a certain type particles is trapped in a cooling and bunching cycle, it does not matter what kind of properties the incoming beam had before the cooler since the beam is going to be identical after the cooler compared to any other bunch with the same amount of particles. Therefore, given the motivation behind this thesis project, the remaining parts of the system are of little importance to discussion in this text.

3.2 The new off-line set-up

As mentioned in the previous section the new off-line set-up is going to replace the current off-line ion source system. The way this is achieved is through commissioning a new stretch of beam line that extends to the second floor and is connected to the pre-existing horizontal beam line after the point at which the secondary beam is accelerated. The new beam line joins the horizontal line before the dipole magnet so that the capability to mass separate the beam remains unchanged.

The new vertical portion of beam line that extends between the floors is merely a tool for transporting particles from one to the other. The important property of being able to use multiple off-line ion sources is provided by the structure above the second floor. The vertical beam line along with one ion source is presented in figure 13.

Figure 13: The newly commissioned vertical beam line

As mentioned, the second floor houses the part of the new system that enables the use of multiple off-line sources. The core part of the second floor set-up is presented in figure 14. The main body of the system is formed by a vacuum chamber that is an intersection of three straight pieces of pipe. This results in a chamber that has six flanges that can be connected to other pieces of equipment. One of these is used to connect to the vertical beam line that runs down to the lower floor. Another flange is needed to connect the chamber to the lower set of vacuum pumps, a turbomolecular pump in series with a scroll pump. Only the turbomolecular pump is visible in figure 14. The remaining three flanges in the horizontal plane remain free for use for other pieces of equipment. One of these is connected to a vacuum gauge in figure 14 but the gauge can be easily connected in another way so that that direction of the chamber becomes available. The direction opposite to the pump cannot be used to attach a ion source due to limitations set by ion optics inside the chamber. This flange could be used as a mounting point for the vacuum gauge, for example. The last flange is used to connect the glow discharge ion source and necessary vacuum pumps to operate it.

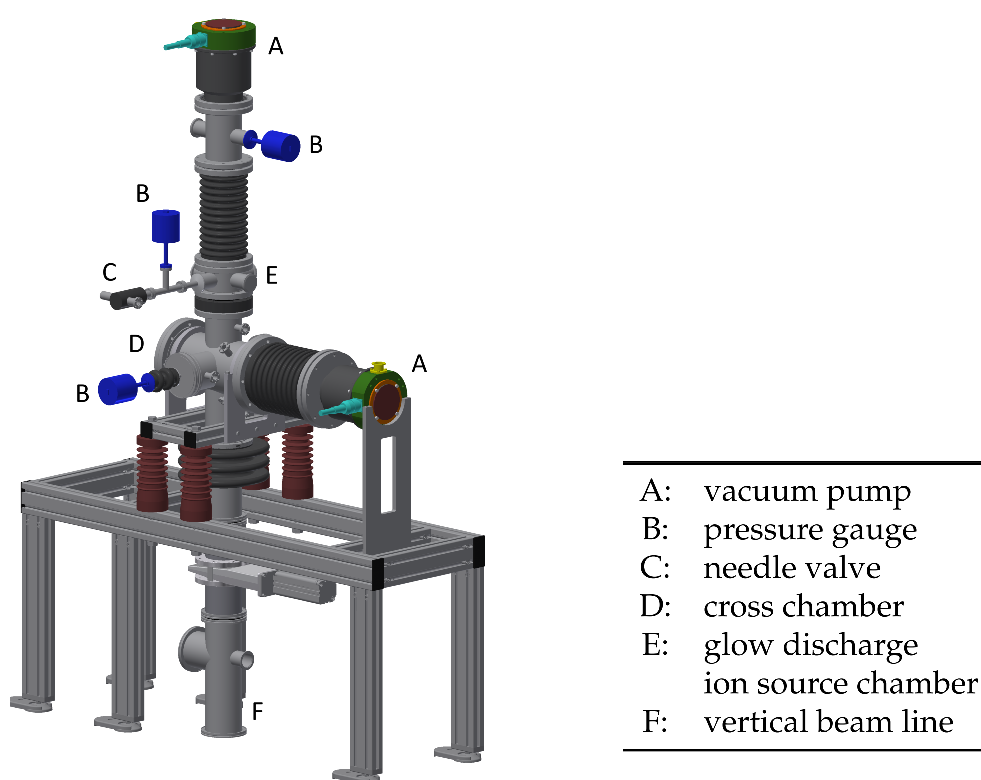

A:	vacuum pump
B:	pressure gauge
C:	needle valve
D:	cross chamber
E:	glow discharge ion source chamber
F:	vertical beam line

Figure 14: Core parts of the second floor set-up

The set-up in figure 14 contains most of the ion optics commissioned as a part of this thesis work. Some of it is packaged together with the glow discharge ion source and some of it is attached to the cross chamber and parts of vacuum system below it. This makes it possible to remove the current ion source and replace it with another source, if necessary.

The first pieces of ion optics are attached to the same chamber as the ion source itself. All ion optical elements located above the second floor level are presented in figure 15. To get an idea on the scale of the optical system the figure can be compared to figure

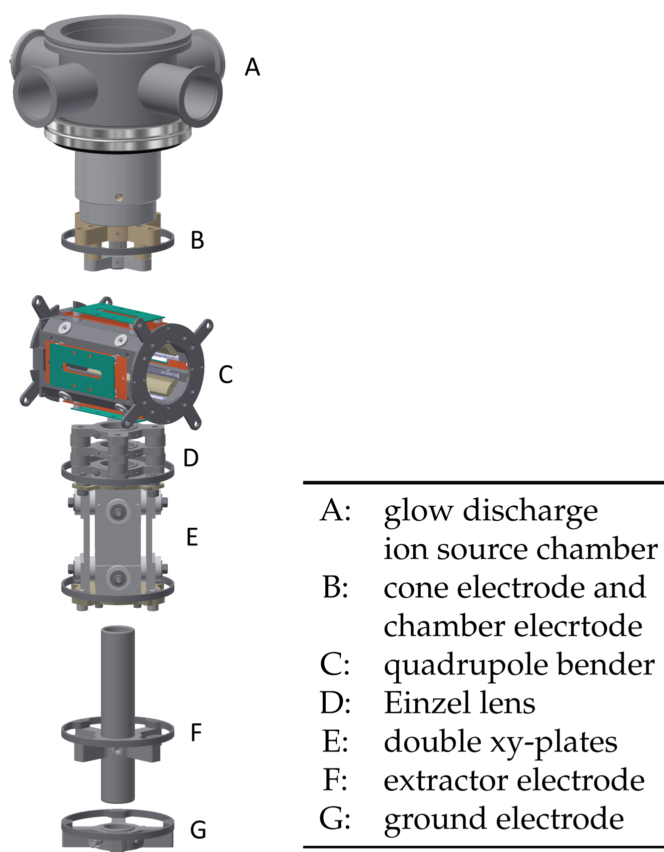

Figure 15: Ion optical elements located above the second floor level

14. The glow discharge ion source chamber is visible in both figures. Additionally, the ground electrode in figure 15 is located right below the black wavy insulator underneath the cross chamber in figure 14. Orientation of the elements is the same in both figures.

The ion source is located inside chamber A in figure 15. A closer view of the ion source and its surrondings is presented in figures 16 and 17. The latter figure is in false colors in order to make different elements more distinguishable. In the figures gas input line is labeled A. This is used to provide the ion source the gas pressure it needs to operate, as explained in section 2.2. All gas that passes the needle valve in figure 14 flows through this connector into the ion source. Needles inside the source that are to be ionized, are connected to the BNC connectors labeled C. Ionization takes place inside a small block of aluminum labeled B. It works as a container for the gas and holds the BNC connectors in place. The internal structure of the ion source is visible in figure 18. In the figure gas flows down from the top along a long channel and gets ionized between the needles attached to the yellow BNC connector tips. After the needles the gas slowly flows out of the ion source through a small circular aperture at the bottom of the ion source. Ions from two materials, gas and needle tips, are transported through the aperture into a volume between the source and skimmer electrode, visible in figures 16 and 17.

The first place where ion optics becomes relevant is the volume that separates the ion source and skimmer. Ions created in the source are electrostatically accelerated for the

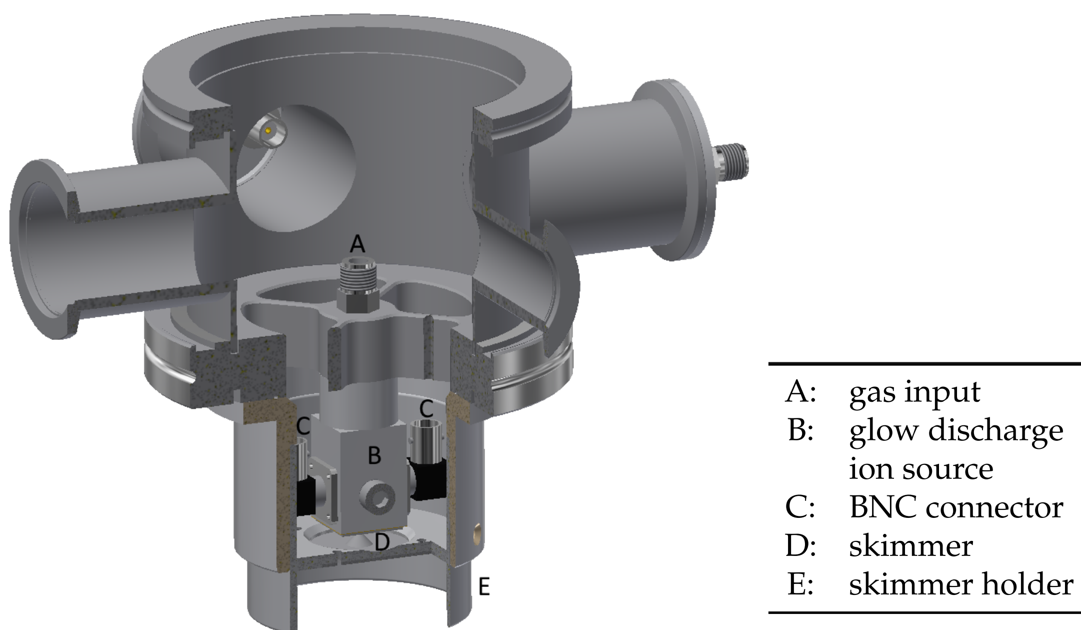

A:	gas input
B:	glow discharge ion source
C:	BNC connector
D:	skimmer
E:	skimmer holder

Figure 16: Structure of the glow discharge ion source and its surrondings and their attachment to vacuum chamber

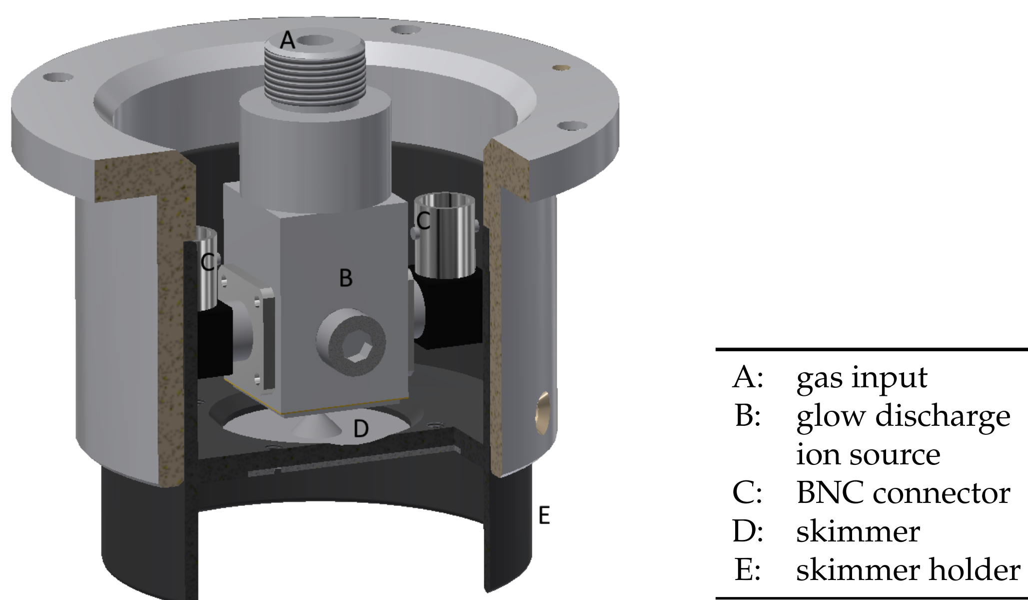

A:	gas input
B:	glow discharge ion source
C:	BNC connector
D:	skimmer
E:	skimmer holder

Figure 17: Structure of the glow discharge ion source and its surroundings

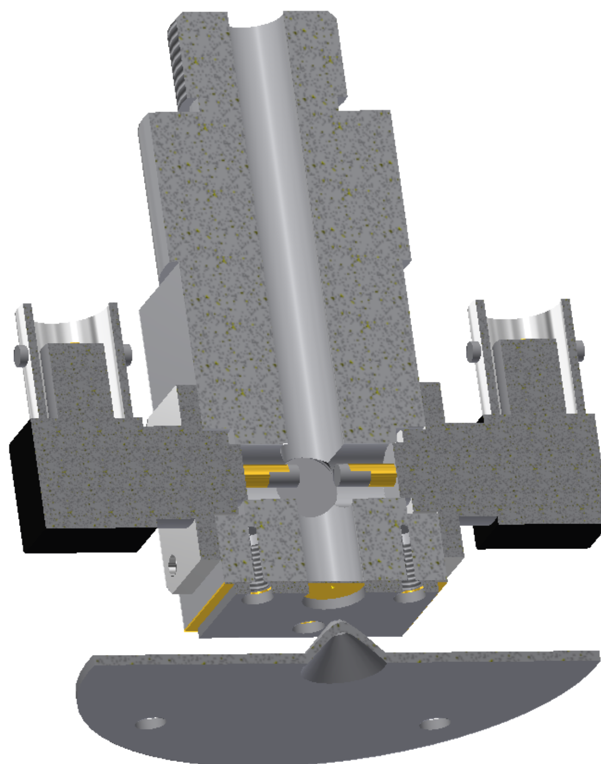

Figure 18: Internal structure of the glow discharge ion source

first time in this gap. The skimmer is held at a negative potential compared to the source, which provides the ions an increase in momentum. Shape of the skimmer is such that the electric field guides the ions towards an aperture at the tip of the cone which can be seen in figure 18. The skimmer is held typically at roughly $-290\,\mathrm{V}$ compared to the ion source.

The skimmer itself is perhaps the most important ion optical element near the ion source. However, it is not sufficient by itself. The skimmer holder in figure 17 also plays an important role. It serves as a protecting element to the electric field between the tip of the skimmer and the ion source. The skimmer and its holder are kept in place by a cylindrical piece of plastic. This plastic, being an insulator, is a possible location for problematic surface charge build-up due to the fact that the ion source is designed to continuously release electrically charged particles into the surrounding volume. These ions may get attached to the surface of any insulating material that they come in contact with. This possibly results in varying surface charge densities that may be high enough to have an effect on beam formation. The ion source was initially tested with a different version of the skimmer holder that did not have as long cylindrical sections above and below skimmer level as the current design. That structure was also simulated and it was found that the plastic holder might negatively affect the beam. Therefore, the skimmer holder was redesigned and the structure in figures 16 and 17 was introduced. According to simulations the new structure is considerably more robust when it comes to adverse effects due to charge build-up in surrounding plastic parts. This will be discussed further later in this section.

Once ions created in the ion source pass through the aperture in the skimmer they enter a volume of much lower pressure. A typical pressure in the volume above the skimmer

is roughly $5 \cdot 10^{-5}$ mbar during operation with a helium feed pressure of 4.5 mbar. This pressure drops down to roughly $6 \cdot 10^{-6}$ mbar below the skimmer. It should be emphasized that the pressure reading from the upper volume is measured rather close to the turbomolecular pump at the top of the set-up. Since the upper volume houses the ion source which partially blocks the path from the skimmer to the pump, the flow of gas from the ion source to the vacuum gauge is reduced to some extent. Therefore, pressure right next to the skimmer aperture is higher than what is detected by the vacuum gauge. Given that structure of the lower chamber is more spacious than that of the upper one, the vacuum is considerably better in the lower parts of the system. This is beneficial for transporting the beam, since it reduces the scattering of ions.

The next piece of ion optics after the skimmer are the cone and chamber electrodes labeled B in figure 15. These are presented in more detail in figure 19. Voltage of the cone electrode can be adjusted independently of other optical elements whereas the chamber electrode is connected to the cross chamber voltage. These form the following stages of acceleration after the skimmer. Typically the cone is held at roughly -100 V and the chamber electrode at -800 V. Therefore, voltages between ion source, skimmer and cone electrode are rather small compared to the voltage between cone and chamber electrodes. The reason behind leaving most of the acceleration to be after the cone electrode lies in focusing the beam. If the cone voltage gets much higher the beam starts to diverge after the tip of the cone. By leaving a large potential difference between the chamber and cone electrodes, a focusing effect is achieved between the two electrodes. This can be seen very clearly in simulations. Software used for simulating ion optics was SIMION [9]. The system was simulated from the ion source to the end of the chamber electrode. Beyond this point simulations were no longer practically feasible due to a lack of rotational symmetry in the ion optics. This increased computation burden proved to be beyond available computational capacity. Rotational symmetry in simulating the ion source was achieved my approximating the ion source as a cylinder rather than a rectangular piece with BNC connectors attached on the sides. Two examples of acquired simulation results are presented in figures 20 and 21.

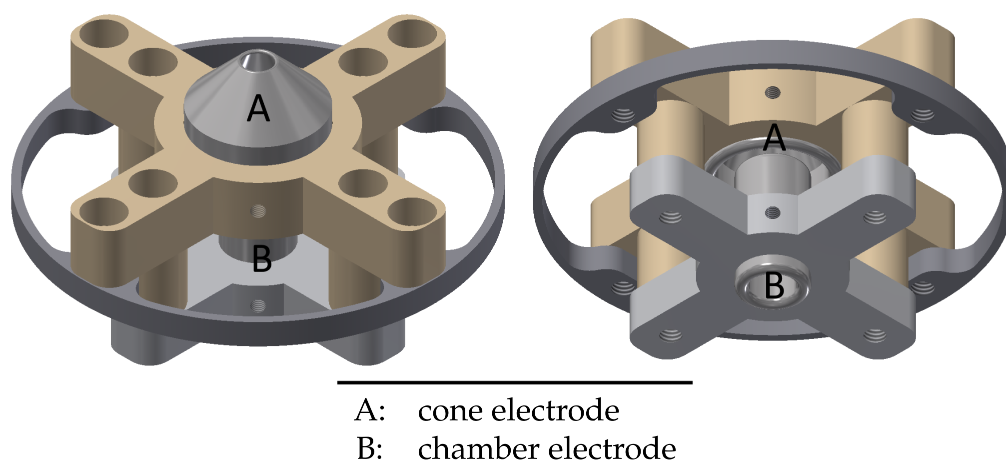

Figure 19: Cone and chamber electrodes in their mounts

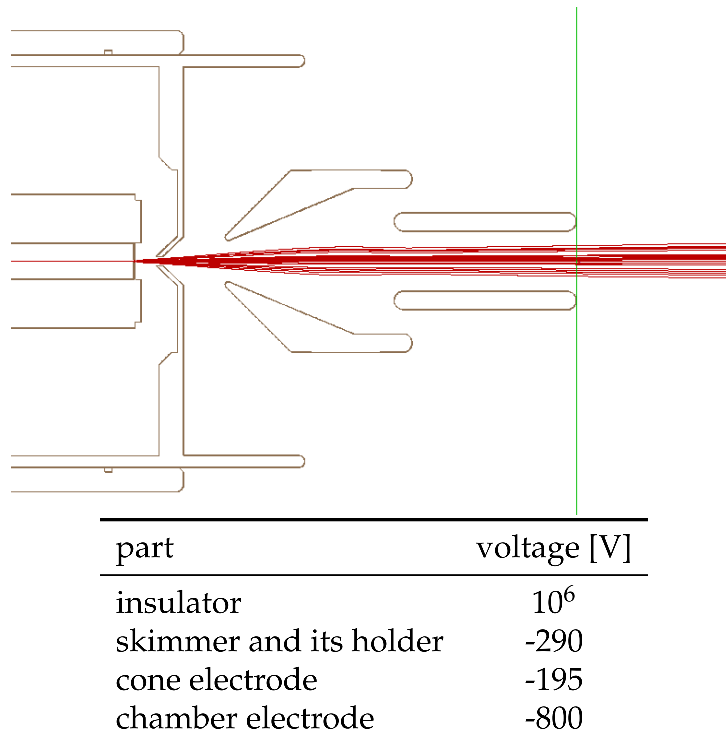

part	voltage [V]
insulator	10^6
skimmer and its holder	-290
cone electrode	-195
chamber electrode	-800

Figure 20: Simulated ion trajectories with higher cone voltage

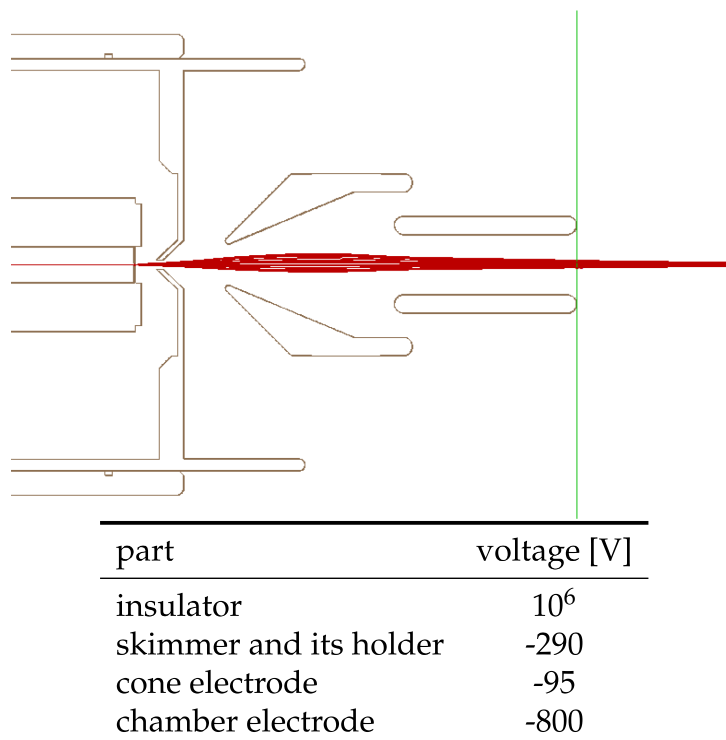

part	voltage [V]
insulator	10^6
skimmer and its holder	-290
cone electrode	-95
chamber electrode	-800

Figure 21: Simulated ion trajectories with lower cone voltage

These simulations were done in three dimensions with the set-up in figure 17, with the exception of the ion source shape. The figures are two dimensional cross sections of the system.

The effect of raising the cone electrode voltage can be seen in figures 20 and 21. The first figure has a potential of -195 V applied to the cone whereas the second has only -95 V. All other voltages were the same in the simulations. It can be seen that in the first case the beam is diverging after the chamber electrode, but in the latter figure it is converging. It was found that simulated optimal voltages do not quite match optimal values in tests with the actual set-up. However, similar behavior can be reproduced with the physical set-up as in simulations, i.e. that increasing the cone electrode voltage reduces measured beam current. These simulation show one more important property of the current design. The plastic insulator that holds the skimmer and its mount in place can have a voltage of up to 1 MV without the beam being adversely affected. After this value the beam starts to quickly deteriorate and eventually it does not even reach the cone electrode but it is reflected back just before it.

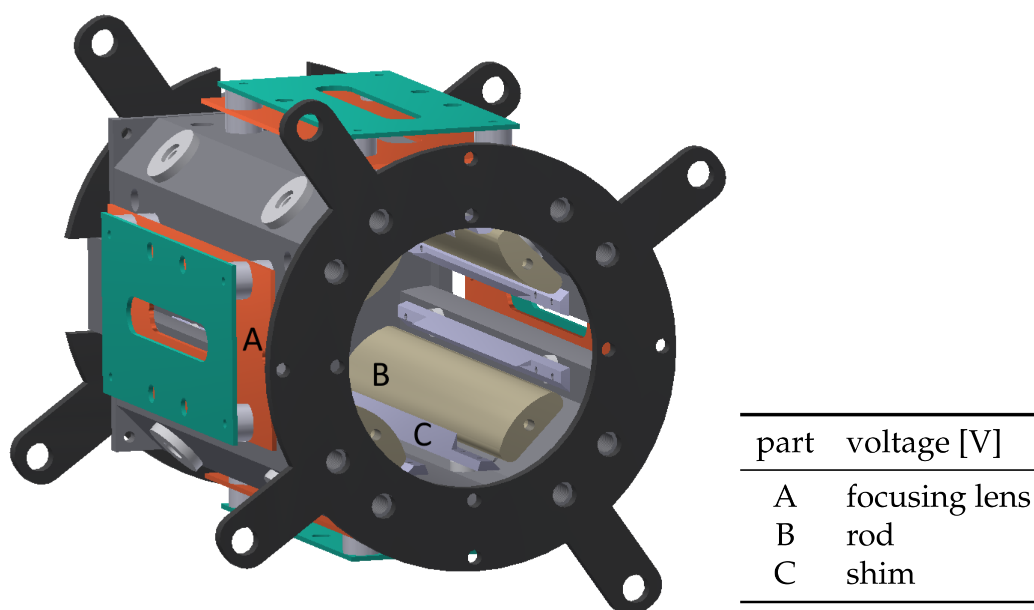

part	voltage [V]
A	focusing lens
B	rod
C	shim

Figure 22: Quadrupole bender structure

Ion optics discussed up to this point in this section form a part of the system that has optics relevant only to the vertical branch of the cross chamber. All optical elements from here on are common to all three possible input directions of the cross chamber. First of these elements is the quadrupole bender presented in figure 22. Its purpose is to bend an incoming beam of particles by 90° from horizontal to vertical direction. Alternatively it can leave the beam unchanged. This piece of equipment has not been used to bend a beam as a part of this thesis work since the glow discharge ion source is located directly above the vertical beam line. However, there are plans to expand the current system to the horizontal branches in the future. The bender has been made ready for operation as far as possible without testing bending a beam. The bender is designed to bend a beam using electric fields created by applying a voltage to shims and rods inside the frame of the bender. The bender has also metal plates at each entrance and exit that have slotted apertures. These function as focusing lenses, as

discussed in section 2.1.1. Maximum voltages for different parts of the quadrupole bender along with the rest of the system are listed in table 3.1.

After the quadrupole bender the next optical element is an Einzel lens. These were discussed in detail in section 2.1.1. It is followed by a set of parallel plate condensers known as double xy-plates. To be more precise, it is a set of four parallel plate condensers in such a configuration that there are two condenser in two sets so that the sets are both centered on the optical axis. Each of these sets have one condenser pointing in one direction, let us say x direction, and another one that is rotated 90° and points in y direction. The net result is that both of the two sets can be used to bend the beam in any direction. Path of ions inside a parallel plate condenser is discussed in more detail in section 2.1.3. If used together the two sets can also be used to move the beam parallel to its direction of travel. Both the Einzel lens and double xy-plates are presented in more detail in figure 23. The last pieces of ion optics located above the second floor ground level are cylindrical extraction electrodes. These are visible in figure 15.

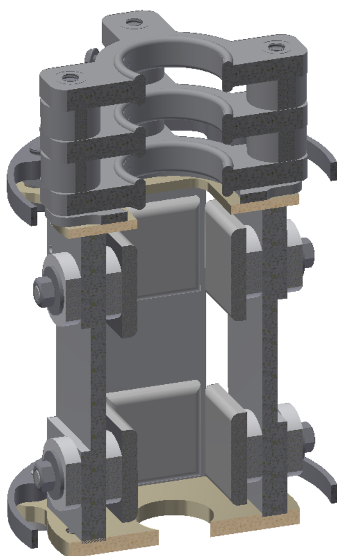

Figure 23: Internal structure of Einzel lens and double xy-plates

There are three important pieces of ion optics that remain to be discussed. These are electrostatic quadrupole triplet, cylindrical condenser and a parallel plate condenser. These have been discussed in more detail in sections 2.1.2 and 2.1.3. These three elements form the last parts of the vertical beam line. After these a beam continues its path along pre-existing parts of the IGISOL system. The quadrupole triplet and 90° bender are presented in figure 24. The figure has been partially stripped of pieces of equipment in order to better highlight the parts under discussion. A more detailed similarly stripped view of the bender is presented in figure 25. In the figure the two main parts of the bender are visible. The first one consists of the cylindrical plates that are used to bend the beam a part of the desired total deflection angle. The plates cover an angle of 65°. The second part is formed by the kicker plates. These can be used to adjust the exit angle of the beam. Typically these are used to further bend the beam so that a total deflection of 90° is achieved. The kicker plates can also be used as a selector between vertical and horizontal incoming beams. If the kicker plates are grounded no beam from the

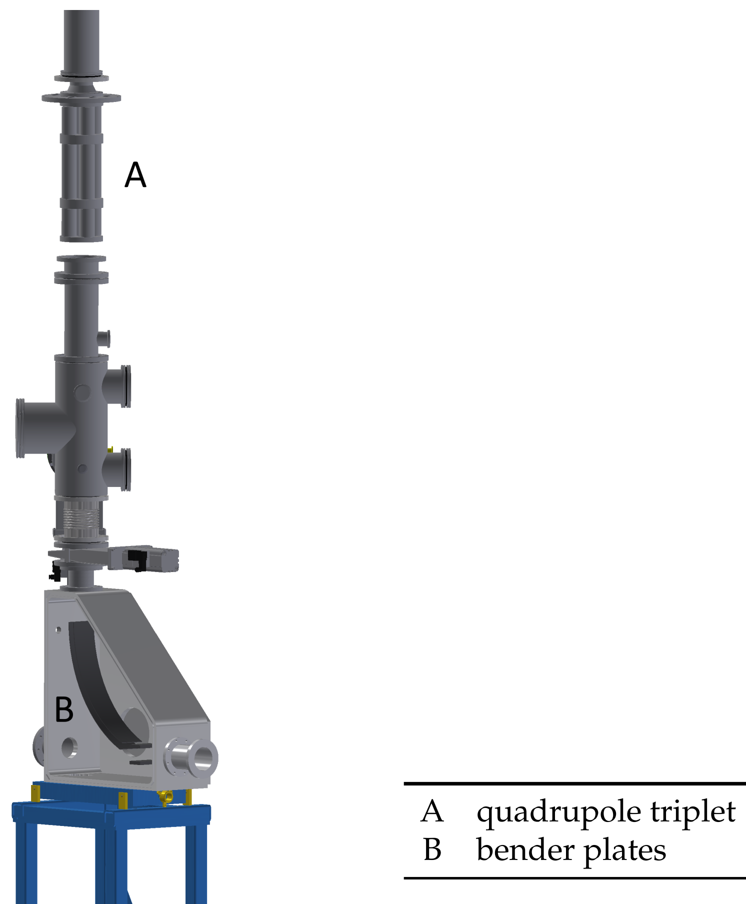

Figure 24: Core parts of the first floor set-up

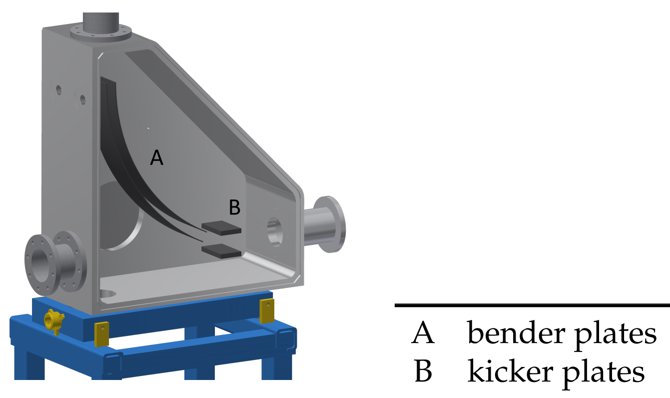

Figure 25: Structure of the 90° bender

vertical line is able to pass through the bender. In this case the horizontal beam can be passed on. It has been planned that these plates could be used to pulse the outgoing beam so that every other pulse is from vertical and every other from horizontal direction. However, this kind of use remains to be tested in practice.

Elements described above come together to form a functional beam transport line that is designed to be expanded to support three separate ion sources simultaneously. The system has been tested in practice and the equipment has been found to be functional using voltages presented in table 3.1. Values in the typical voltages column correspond to an acceleration voltage of 5000 V.

Table 3.1: Voltages of ion optical elements in the vertical line

	maximum voltage [V]	typical voltage [V]
skimmer	-1000	-290
cone	-1000	-95
chamber	-1000	-796
bender lens in	-1000	-540
bender lens out	-1000	-542
bender shims	-1000	-796
bender rods	-3000	-796
Einzel	-1000	-375
double xy: x1	-1000	-780
double xy: x2	-1000	-808
double xy: y1	-1000	-719
double xy: y2	-1000	-907
extractor	-10000	-2160
quadrupole triplet middle -	-1000	-53
quadrupole triplet middle +	-1000	0
quadrupole triplet ends -	-1000	-10
quadrupole triplet ends +	-1000	-20
upper bender plate	-3000	-283
lower bender plate	3000	-280
kicker plates	-10000	-1724
acceleration voltage	30000	5000

Ion optical elements described earlier naturally need some kind of voltage supplies and a control system to be of any use. All ion optical elements listed in table 3.1 are powered using power sources manufactured by Spellman High Voltage Electronics Ltd. Each of these is connected to circuitry that enables controlling them using voltages between $0 - 10$ V so that 0 V control signal corresponds to 0 V output and 10 V control signal to the maximum voltage of the particular power source. The control signal is produced using software described in the following section together with a Programmable Logic Controller (PLC) manufactured by WAGO. This combination works so that the software provides a set value for the PLC over a TCP/IP connection and the PLC then produces a corresponding voltage signal. One PLC along with several power sources are presented in figure 26.

Figure 26: a PLC and a part power sources of the off-line set-up

There are two PLC's used in the off-line set-up. One for the equipment upstairs and one for downstairs. These PLCs are modular in design. This means that the number of hardware connectors can be modified by adding or removing IO modules. The core part of the PLC can be seen in figure 26 as a solid white block with a number of IO modules attached to its right hand side. The IO modules can be recognized by blue or green plastic tiles at the top of each module. There exists several different types of these modules. For example, there are both analog and digital input and output modules. These were the ones used in this thesis work.

Before moving on to the software used to operate the equipment, it should be briefly mentioned that as a part of this project a safety system was designed and built to protect users from high voltages used in the system. The backbone of the system is a cage that is located around the upstairs set-up, even though it is not visible in figure 13. The safety cage is presented in figure 27. Backside of the set-up is protected by a wall that serves as the missing side of the cage. The safety cage is used as a mounting point for an electrical lock that prevents opening the cage door if high voltage is turned on. In addition, there is an automated grounding system which ensures that the set-up is always at ground potential when the door is opened. In practice this is done with a pneumatic actuator that connects high voltage parts of the system to the grounding system of the entire laboratory. Those parts of the vertical beam line that are located downstairs are inside pre-existing safety structures.

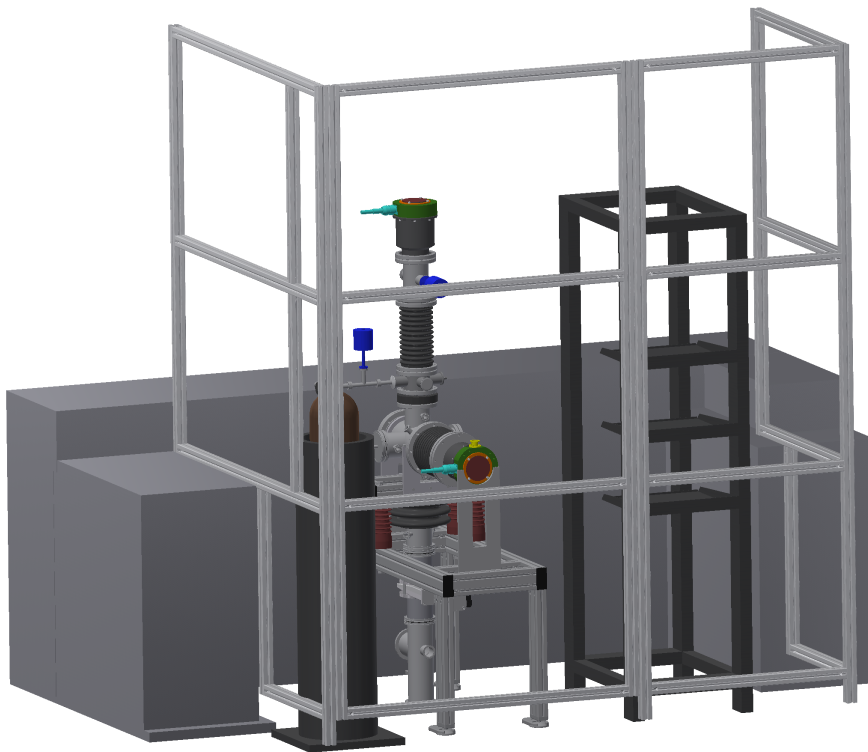

Figure 27: Safety cage surrounding the upstairs set-up

4 SOFTWARE

Most of the pieces of hardware described in previous section are such that it is either most beneficial or strictly necessary to be able to control and monitor them remotely. This is partly due to the fact that the set-up is located partly one floor higher than most of the equipment in the laboratory and partly due to safety reasons. In addition, remotely controlling the system offers a major practical benefit. Some parts of the set-up can be operated locally without losing any functionality in the system, such as helium input line needle valve, but much of the system needs to be controllable simultaneously with the rest of the IGISOL facility. For example all voltages of ion optical elements need to be adjustable remotely so that beam transportation can be optimized throughout the entire beam line as a whole.

There is a station located on the lower level of the IGISOL facility that was already used to control the previously commissioned parts of IGISOL. Therefore, it was necessary to bring controls of the new off-line ion source and the vertical beam line downstairs to this location so that both beam lines could be tuned simultaneously. This task was achieved using a software set-up modeled on pre-existing control systems at IGISOL. The most important part of this adopted system is EPICS (Experimental Physics and Industrial Control System) which provides the system software architecture and offers a set of tools needed to interface with physical equipment. In addition to EPICS, LabVIEW was chosen as a tool which provides a user friendly graphical user interface (GUI).

4.1 EPICS

4.1.1 Introduction to EPICS

The term EPICS can be though to comprise three separate parts which are also separately referred to as EPICS. One part is a collaboration of international laboratories and companies that use and develop EPICS. In 2014 there were at least 24 countries that had one or more laboratories that used EPICS [10]. The collaboration organizes a meeting twice each year which is open to anyone to discuss progress and new projects related to EPICS. There is also a website (see reference [10]) that houses a forum for discussion called Tech-Talk. This website also serves as a hub for software distribution and documentation.

Another part of the term EPICS, in addition to the collaboration, is control system architecture. This is perhaps the most significant factor behind choosing EPICS as a part of this software set-up. Defining features of the architecture are visible in EPICS logo presented in figure 28 in which boxes on the upper half can be thought of as client applications, boxes on the lower half as server applications and the line in between as channel access network protocol. This layout is useful in the sense that every client application is capable of contacting any of the servers directly. This is made possible by the fact that all clients are interconnected with each and every server by the Channel

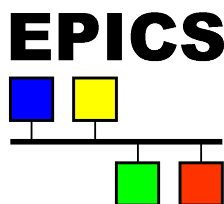

Figure 28: EPICS logo

Access protocol. In practice this means that there can be any number of client applications running and they are all usable at the same time. They do not even have to be running on the same computer. This gives the system good flexibility since the system can be controlled anywhere as long as the client computers are within the same subnetwork as the servers. This is a requirement set by the set of rules on which network routers function. This requirement can be circumvented but it was not necessary in this project. [11] This requirement will be explained further later in this section.

In this project the client application is the GUI program made using LabVIEW. This is the part of the system that provides a user friendly way of interacting with the physical equipment. However, the GUI does not interact with hardware directly, it merely conveys user input over the channel access protocol to a server application. It is this server that is then in contact with hardware over a TCP/IP connection. The server is referred to as an Input Output Controller (IOC). There is only one IOC for the entire hardware set-up commissioned as a part of this project. However, there is no reason that prevents the use of multiple servers to control parts of the same set-up. The use of just one server merely provides the simplest way to achieve all necessary functionality. EPICS IOCs are such that they need to be given exact contact information of the hardware they operate. This is done by giving the server IP address and port number of the piece of hardware that communicates with the server.

The function of all servers relies on something called Process Variables (PVs). These are usually objects that provide a specific piece of data related to hardware. For instance, PVs can be used to store voltage of some ion optical element. In general PVs can be used to hold for example set-point values, read-back values, status information, system parameter, etc. Additionally, there are PVs that do not hold any specific piece of information themselves but act as a logical or computational operators. For example, these can be PVs that perform calculations. In general each PV has a type that defines the way it can be used. For instance, a type can be analog output or input. In this project there are PVs designed for, just to name a few, inputting analog values, outputting analog and digital values and making calculations using other PVs. More specifically, each process variable is a record of a certain type, i.e. each process variable is one occurrence of a certain record and it is these records that are of the type analog output or input etc.

As mentioned above, often these PVs hold a value that describes some property of the system. These are the output and input PVs. Analog outputs are used to provide the system a specific value to be applied to hardware, for example a voltage. Inputs are used to read data from the hardware. It is useful to think about inputs and outputs from the point of view of the PV itself rather than client or server. If the PV is used to get data from hardware its type is input and if the PV is used to put data into hardware

its type is output. In this project there are several process variables that are linked in series in such a way that one gives information to another before passing information to the final variable that actually feeds the data into the hardware. Here the direction of flow of data is the significant part: if information travels towards hardware PVs involved are outputs and if it flows towards a user PVs are inputs. Analog inputs used in this project are formally records of the type "ai", analog outputs "ao", binary outputs "bo" and the variables used for calculations "calcout". These names describe adequately the direction of information passing through them. There are also some records in this project that do not follow this logic but they are used only once during the initialization of the server to provide system stability in case of server failures.

In addition to type and value PVs can have other attributes. Some attributes are specific to a certain record type and some are common to many different types. These attributes can be for example engineering units string, time stamp, output location, operational limits for PV value etc. These attributes are referred to as fields. An example of calcout record is presented in figure 29. Each field has two parts in the code. The first part

```
1 record(calcout,"$(P)$(R)") {
2   field(INPA,"$(INPVALUE)")
3   field(INPB,"$(INPONOFF)")
4   field(CALC,"B=1?A:0")
5   field(OOPT,"Every Time")
6   field(DOPT,"Use CALC")
7   field(OUT,"$(OUT)")
8   field(PINI, "$(PINI)")
9 }
```

Figure 29: An example of calcout record

is for example INPA which defines the purpose of the field. This particular field is used to specify the record that is used as input A when the calcout record is processed. The second part $(INPVALUE) is a reference to the record that is to be used as input. Another example is the CALC field which computes a value for OUT field. The value is determined according to "B=1?A:0" which means that if B equals 1, OUT is set to equal value of INPA and if B is not equal to 1 OUT is set as 0. Each of the fields in figure 29 serve a specific function. Other records used in this project have some other set of fields depending on the purpose of the record in question. In addition to different record types having different field sets, every occurrence of a record type, i.e. PV, can have a different set of fields compared to another process variable of the same record type. Each occurrence of a record is tied to one template file that determines which fields are in use. For example, figure 29 is just one of many possible calcout records and the figure presents an entire template file. There are three different sets of fields that are used with calcout records in this project and they are all stored in separate template files. A complete set of template files used in this project is presented in appendix A. For detailed explanations of all fields available in this version of EPICS the reader is referred to EPICS record reference manual [12]. The manual also serves as a primary source of information for the following discussion related to EPICS.

The system naturally needs a way to determine which records are used in the set-up as well as how many of each are needed. This is done using a substitutions file that contains all this information. The substitutions file used in this project is presented in appendix A. The substitutions file has one section for each template file. As an example, the beginning of one section is presented in figure 30. Each section begins with

declaring the location of the template file. After this there is a line that determines which values are used to substitute which variables in the template files followed by a number of lines containing the actual variable values. For example, template named aoOffline is an analog output record which begins with a similar line as the calcout template in figure 29. This means that "$(P)" in the template file is replaced with "Offline:" when the record is processed. Similarly, $(DRVH) in the template file is replaced with "1000". Each of the fields in a template file that have variables of the format "$(P)" are such that they get replaced once the value corresponding to P is retrieved from substitutions file. It is possible to initialize a field's value inside the template file by leaving out the dollar sign and the parenthesis. However, initializing the values using the substitutions file is a very easily scalable way of performing the task. Given that there are 162 PVs that are needed to control the off-line set-up it is highly justified to use a substitutions file. There can by any number of lines containing values for the variables listed in the pattern line. Each of these lines will generate one Process Variable when the IOC is started up.

Figure 30 serves as an example of an important safety feature of EPICS, namely DRVL and DRVH fields. These fields in the template files provide safety limits for the values a Process Variable can obtain. If these fields are specified EPICS will only allow the user to input a value that is at least as large as DRVL and not larger than DRVH. The use of these fields enables a developer to make sure that users cannot do any harm to the hardware using a client. If a user tries to input a value that is lower than DRVL EPICS will adjust the Value field to equal DRVL. Similarly the user can only get the Value field to go as high as DRVH.

```
1 file "templates/aoOffline.template" { pattern
2 {P,      R,              FLNK,                          DRVL,   DRVH,   PREC,   VAL,  PINI}
3 {Offline:,  Foc1:VSet,  "Offline:Foc1-IL:calcout NMS PP",   0,    1000, 3,     0,     "NO"}
```

Figure 30: A part of the substitutions file

There is one more major part to be discussed before having all the parts needed to start up an IOC. This remaining part is the cmd file which is responsible for a number of tasks. The off-line set-up needs one extension to be installed with EPICS in order to function, called SynApps. These extensions are distributed via the EPICS home page. It is the cmd file that is responsible for telling EPICS to use all needed additional parts. In addition to this the cmd file is used to specify the hardware that is controlled with this particular IOC. For example, in this project the file determines that a part of the hardware is found at the IP address and port "wago-offline.igisol:502". The file is also used to specify what kind of device is receiving the data and how it should react to communication. A majority of equipment related to this project is controlled with a Wago PLC (Programmable Logic Controller) located upstairs in the IGISOL hall. The cmd file states that 20 analog input channels and 14 analog output channels are connected to that PLC. The cmd file also tells EPICS to use the substitutions file discussed earlier and finally starts up the IOC. The cmd file used is presented in appendix A. Only a small part of that file belongs to this thesis work. There were multiple Wago PLCs in use throughout the IGISOL facility and therefore it was decided to include the new PVs into the pre-exisiting IOC controlling all other Wago PLCs.

Now that Process Variables have been introduced one more note on the restrictions asserted by network configuration to the use of EPICS: The requirement that client software must be operated within the same subnetwork as the server arises from the fact that Channel Access uses broadcast messages in its operation. A good example of this is the procedure a client program uses to make contact with the server that houses a particular PV. This begins with the client sending an UDP broadcast into the network it is connected to. This broadcast is used to send a query to all servers whether they have the PV in question. If a server that has that particular PV receives the query it then replies to the client using a unicast UDP message, saying it has the PV. After this the client and server switch from a UDP connection to TCP connection. This is done in order to have reliable communication between the to parties. It is this TCP connection that is then used in transferring all data a user inputs into the LabVIEW GUI, i.e. client program, to the server. In this procedure the UDP broadcast is the part that prevents access to Process Variables outside the IGISOL subnetwork due to the fact that broadcasts are not allowed to pass between the subnetwork and the rest of the facility. Given that both the client and server are within the same subnetwork, this procedure allows for a flexible and reliable data transfer between devices. The biggest advantage of the current system is that all that is needed to control the equipment is access to the IGISOL subnetwork and the names of PVs a user wishes to control. EPICS comes with a line user interface that can be used on any computer that has EPICS installed. Therefore, the essential parts needed to operate the equipment are already pre-installed on many of the computers in the laboratory and the LabVIEW GUI is not absolutely necessary, it is merely a matter of convenience. It can be transferred between computers rather easily as well. All that is necessary is to have LabVIEW runtime environment installed on the client machine and then simply copy the labview program into the memory of that computer.

4.1.2 EPICS with the off-line ion source

Control system of the off-line ion source uses several EPICS Process Variables. There are 6 record types and 10 template files in use and they form a total of 162 PVs in the system. The record types in use are analog input, analog ouput, binary output, calcout, calc and fanout. These are sufficient to form a system which provides stable operation under all situations.

There are 8 Process Variables for each voltage source in the system. One of these PVs in an analog input and it provides a read-out of voltage supplied by that particular source. The rest are for outputting values from client to hardware. A schematic of the PVs is presented in figure 31. The blue boxes inside the Server represent PVs. The template type of every PV is indicated in parenthesis, leaving out the text "Offline" for clarity, preceded by a short description without parenthesis. Here the IL suffix stands for Internal Logic, meaning only that users are not supposed to interact with this type of PV directly. The blue box labeled Wago PLC is the interface between power sources and EPICS server. Furthermore, each arrow represents the flow of numeric data describing the state of the hardware or set values. PVs that are interconnected have additional communication between them but hardware related data is transferred only according to the arrows. The additional data transfer consist of e.g. requests to other PVs to send a specific piece of data. For example the Switch PV is capable of asking Set Value and On/Off PVs for the values of their Value fields even though the

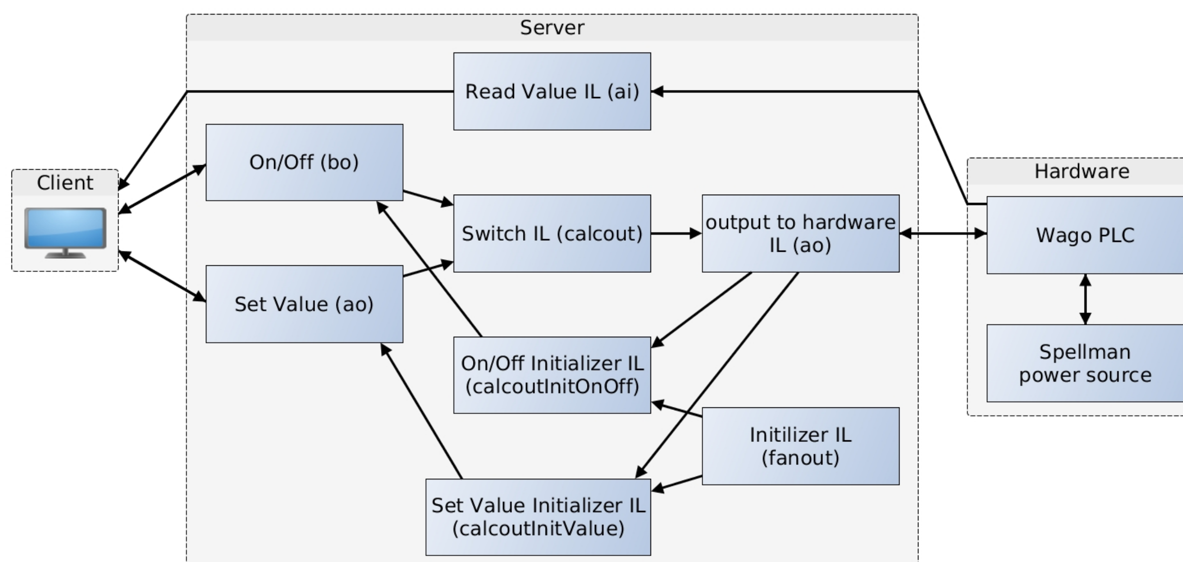

Figure 31: Schematic of EPICS PVs used in the control system

arrows between those PVs all point towards hardware.

This PV structure is currently a new addition to the IGISOL facility. Previous PLC control systems have been implemented using some other structure. The reason behind designing a new PV layout was the desire to have the ability to switch a power source either on or off without losing the set value. The chosen layout provides users with this possibility. Purpose of the On/Off Process Variable is to dictate whether the corresponding power source is on or off. Naturally, the Set Value PV holds the set value for the same power source. These PVs are unaware of the client and are designed to only hold a numerical value and to have a reference to the Switch. In other words these PVs do not have the ability to alter the state of the power source directly. The purpose of the Switch is to be the logical operator who decides whether the power source should be on. The template file of the Switch is presented in figure 29. In the figure it is visible that the Switch uses two input values, INPVALUE and INPONOFF. These are the Set Value and On/Off PVs, respectively. Each time the Switch is processed, it asks both of the preceding PVs for the values in their Value fields and stores them as A (INPA) and B (INPB). Then the calcout record performs the comparison in its CALC field and outputs either A or 0, depending on the result.

The outgoing value serves two purposes in this set-up. Firstly, it gives the desired output value to the next PV which is responsible for delivering it to the PLC. Secondly, it serves as a trigger for the next PV telling it to process itself. This triggering property turns out to be of crucial significance in designing this kind of Process Variable configurations. This will be discussed in detail later on. The Process Variable after the Switch is the one that actually has all information needed to communicate with the Wago PLC. Its main purpose is to deliver values from Switch to PLC. Additionally, it serves as a linear scaling operator that takes in a value and converts it to be within a range from 0 to 10. This scaled value is then given off to the PLC which forwards the value to the corresponding power source as a voltage equal in magnitude to the value the PLC receives from the PV. The Spellman power sources used in this project are such that they take a voltage input ranging from 0 V to 10 V and linearly convert it to range from

0 V all the way up to the maximum voltage that source is designed to provide. Finally, a path from client to power source is complete.

The rest of the PVs in figure 31, excluding the analog input, are such that they get processed just once each time the server is booted up. This is the part where the previously mentioned triggering becomes crucial. As previously hinted, each EPICS Process Variable has two ways of exchanging information with other PVs. They can either ask for a piece of information stored in one of the fields within another PV, or they can input a piece of information into a field. In other words, PVs can push or pull data between one another. Additionally, both push and pull can be done in two ways. A connection can be made in such a way that the second PV is either told to process itself before giving out a value or told not to process itself and simply provide the value that was asked for. More generally, this is a property of all links in EPICS that connect two PVs. There are a number of different links in numerous records. The shared property of all links is that they are all fields which hold the name of another PV, possibly even the name of a specific field also. Links can be used, for example, to provide a PV the identity of another PV it is supposed to give its Value to or the identity of a PV it is supposed to tell to process itself after the original one has finished processing. These links are called output link (OUT in templates) and forward link (FLNK in templates), respectively. These are the most important ones, along with Desired Output Location (DOL) and Input links (INPA, for example), when it comes to this project.

The property the links have, to either trigger processing of another PV or not to trigger it, is used to carefully control the sequence in which all PVs are initialized when the server is started up. The only two Process Variable types that are allowed to process themselves at start up are the analog inputs and fanouts. This is done using a field common to all records called PINI, or process at initialization. It determines the time at which a PV is processed for the first time, for example the default value "YES" means that a PV is processed once right after it is created and value "NO" means that a PV is processed only when some link connected to it tells it to. There is also another option, "RUNNING", which results in the record being processed once after all records have been initilized. One type of record is allowed to processed itself at server start up. These are the analog inputs. They are not connected to any other PVs and therefore they are not capable of doing any harm to the rest in any situation. This means that there is no reason to delay their initialization and processing which effectively creates a PV, makes it ready for normal operation and processes it once. In the case of the analog inputs, this translates to creation of the PVs and making them fetch a value into their Value field from the PLC.

In the case of fanout records the situation is quite different. These PVs are connected to all remaining PVs via a chain of records. If a record is allowed to process itself usually all links are activated. Calcout records, for example, can be configured to activate their OUT link only if a certain criterion is met, but in the case of this project all links are activated once per each time a record is processed. This means that if all PVs were processed at server start up and all links were allowed to activate a PV that is at the other end of the link there would be no way of knowing in which order the records got processed for the first time. This was discovered to be an unwanted situation.

The reason behind this is the fact that the PLC used in this project is such that it upholds all values given to it by a server even in the case that the server crashes or is shut down

for some reason. Additionally, the analog output record connected to the PLC has a property that it retrieves the value being upheld by the PLC and stores it in its Value field. This all happens as a part of the initialization of the PV rather than as a part of its initial processing. Altogether, this set of properties provides a possibility to make the control system such that it recovers from temporary server crashes without human intervention. However, taking advantage of this possibility requires a careful sequence of initial processing of PVs. For example, in the case of Switch being the first PV to get processed the value upheld by the PLC would be lost. This is due to the fact that the Switch would pull values from both Set Value and On/Off PVs and output the resulting value to the last analog output record which would then forward it to the PLC. The problem here lies in the fact than if the Set Value and On/Off records are not initialized to have values matching that of the PLC's original upheld value, the Switch would trigger their initial processing at a time when both other records have Value equal to zero. This results in the PLC receiving a value of 0, effectively shutting down the entire system. This would also mean that the applied voltage value would be lost entirely if there is no client upholding it. In order to make the system as robust as possible this kind of uncertainty needs to be addressed. If the server is constructed in such a way that programmers building client applications have no need to be aware of the possibility of temporary server crashes, the system becomes considerably more robust.

This is the reason behind taking the effort to control the order in which PVs are processed for the first time as the server is started up. With careful control over the sequence the server is able to recover on its own from crashes withour losing previous set values. This is the sole purpose of the fanout and the other two initializer PVs in figure 31. The purpose of the fanout record is to provide a simultaneous signal for both of the initializer calcout records telling them to process themselves. The fanout has its PINI value set to RUNNING and therefore this set up makes sure that once the initializer calcouts get processed they receive an updated value from the last analog output fetched earlier from the PLC. This value is then forwarded to Set Value PV. The value is also analyzed to determine whether On/Off should be 1 or 0 and then the correct binary state is forwarded to On/Off PV. These values are transferred, both to and from the calcouts, using links that do not cause either receiving PV to get processed. One can see this choice in the substitutions file as a text that says, for example, "NMS NPP". This abbreviation stands for Non-Maximize Severity and No Process Passive. NMS is related to the possibility of attaching an alarm severity to each link. This system could be used to notify the users each time a specific link is activated, for example. Alarms are not currently used in this set up. However, the safest choice in this situation is to make sure that each and every link is configured not to set off an alarm, i.e. Non-Maximize Severity. This way there is no risk of false alarms. The latter part is more self explanatory. No Process Passive means that the PV at the other end of the link will not be processed due to this link being activated. The other alternative for this is PP which means that the other PV would get processed. Both PP and NPP are such that the receiving PV must have its SCAN field set to PASSIVE in order for the two abbreviations to have any effect.

This set of Process Variables used to initialize the first two PVs with their desired values is processed only once per each time the server is started up. All PVs, excluding the inputs, have their SCAN fields set to PASSIVE. In practice this means that the server

does not do anything with those records unless the users asks for it. The inputs have SCAN field set to "I/O Intr" which means that they are updated based on events generated by the PLC. This is an effective way of taking care of updating new values to the input PVs. This way the server does not have to poll the PLC for the new values at given intervals. Instead, the PLC tells the server each time the value has changed. This method saves computational resources and helps make EPICS a highly scalable solution for larger control systems. This is the same method that is used in updating the client values. The server generates an event each time one of the input, Set Value or On/Off PVs change their value and the client application then reacts to these events.

The system described above is highly passive. Almost all of the PVs are not processed at server start up and even after that they remain dormant if set values remain the same. The entire process begins with the fanout records. They get processed after the server has been started up and they awaken the calcout records that initialize the Set Value and On/Off records. This process does not trigger the processing of the PV chain between the client and PLC. Only when there is a change of value in the Set Value or On/Off PVs, the Switch processes and then forwards a value to the last analog output which then updates the PLC. Fanout and the initializer calcouts are processed only once whereas the rest of the PVs await for changes as long as the server is running. To sum up, the input PVs rely on events generated by the PLC and the Set Value and On/Off PVs on ones generated by users. All resulting changes on the server generate additional events that are monitored using the client described in the following subsection.

In order to justify a peculiar choice related to fanout records it should be said that the fanout records could be removed without changing the functionality of the system. This would require changing the PINI field of initializer calcouts to RUNNING. The reason behind choosing to leave extra Process Variables to the system is the initial processing of the PV chain from client to PLC. As the system is currently set up with mostly NPP links the Set Value, On/Off, Switch and output to hardware PVs are not processed at all and partly not initialized to any value until the users interacts with the first two PVs. In operation anticipated to be normal once the system is taken into use this will not have any significance. The client will be fully functional regardless of this fact. However, given that these PVs are not processed at server start up there is a possible nuisance with using the shell based line user interface client of EPICS. If these PVs were processed at start up users would be able to use caget and camonitor commands to check the Value field of the Switch PV, for debugging resons, for example. Now that they are not processed caget and camonitor are not functional before manually changing the value of either Set Value or On/Off which triggers the processing of the rest of the PV chain. Caget and camonitor are unable to return a value from a PV that has not been initialized to some definite value. This is not a critical shortcoming since the processing can easily be triggered manually, merely something that is worth remembering in case the server needs debugging.

This shortcoming could be removed using the fanout record. Currently the fanout record provides a simultaneous signal to both calcouts to process themselves. This is not necessary in the current set up. However, if one was to remove the debugging nuisance then the property would be useful. One could set Set Value initializer calcout to have PP links and then On/Off initializer calcout to have NPP links and to activate the PP forward link with a suitable time delay. A simultaneous trigger would be needed

for both calcouts in this case. It would be provided by the fanout. This would result in the server regaining the value from the PLC just the same it does now, but it would also mean that the PV chain from client to PLC would be processed once and the nuisance would be gone. This was shortly tested and it seemed to work adequately during testing. However, this alternative set up relied on the assumption that the processing of PVs happens in the easily assumable way, Set Value initializer at least the length of the time delay earlier than the On/Off initializer. This assumption is most likely something that can be made reasonable since the time delay can be modified but it cannot be guaranteed to hold true. It is possible to have some sort of hick up in the processing of PVs that could compromise the sequence. Therefore, it was decided that the Switch PVs shall be unprocessed until a user interacts with the first two PVs in the chain. The fanout records were left in place in case this decision is revised at a later time. There is no significant harm in having them there since they do not consume any processing power once the server reaches normal operation and even during start up they do not slow down the system enough to notice.

There is one other place where computational burden was discovered to be of higher significance. It was found that the client application, discussed in the following subsection, is rather sensitive to high update frequencies of input values. If the server is allowed to update the Value field of each input PV each time a PLC creates an event, the client struggles to process the changes fast enough. This is most likely a matter related to the implementation of the client. However, the easiest way to solve this was found to be limiting the amount of data passed on to the client by introducing a dead band to the input PVs. The dead band was set to a value of 0.3 V, which means that the input PV is processed only if an event is detected that changes the Value field by at least 0.3 V. This effectively reduces the amount of events the client application needs to be able to handle in any given period of time. The value of 0.3 V was found to be sufficient to ensure smooth operation of the client.

4.2 Graphical User Interface

The system described in the previous section is a stand-alone system even on its own without adding a custom client application. However, a client designed specifically for the purpose of operating this equipment is a highly useful tool since it is cumbersome to try and tune the beam line using the line user interface provided by EPICS. There are numerous parts of the IGISOL facility that were remotely controlled using EPICS already at the time this thesis work begun. Many of those system are operated using client applications that have been built using LabVIEW as programming language. This offers a way of introducing a new piece of software into the collection of user interfaces already present in a way that the new client will not seem unfamiliar to users. In addition, LabVIEW is a practical choice of programming platform due to the fact that there is an open source interface between LabVIEW and EPICS available on the internet. These were the motivations behind choosing to develop a graphical user interface for the control system and choosing LabVIEW as the programming language for the task.

The interface between LabVIEW and EPICS is called CA Lab and it is supported on Windows and Linux and it works on all LabVIEW versions since 7.0 [13]. CA Lab was chosen to provide a link between the client application and EPICS. CA Lab provides

virtual instruments (VIs) that can be used to, among other things, read and write Process Variable fields and also listen to events from EPICS servers. These are the tools used in this project provided by CA Lab. In addition to CA Lab, only basic LabVIEW components were needed to build a client application with a graphical user interface. Finished client is presented in figure 33. The client needs the names of Process Variables it controls as an input, naturally. The names have been already saved into the first column in the program. However, they are modifiable by users in case the PVs are renamed. In addition to being used directly to retrieve values from the EPICS server these names are also processed into corresponding on-off switch and analog input PV names. This enables the program to retrieve the measured values and present them in the second column. The third column is used to input voltages and the fourth contains all on-off switches for the voltages. The client application consist of five main parts of source code. The purpose and operation of each part is discussed in detail in the rest of this section. The entire code is presented in appendix B.

The first thing needed in the program is the Process Variable names of on-off switches and inputs. These are obtained using a structure presented in figure 32. The outermost layer in the figure is a while loop. As a default it is a loop that runs continuously until a certain termination criterion is met. In this case termination of the loop is set to happen once the loop has been processed once. This is implemented with a component in the lower right hand side corner of figure 32 that compares whether the number of loop iterations "i" is larger than 0. If it is, the loop is terminated by sending a boolean value true to the connected Loop Condition terminal.

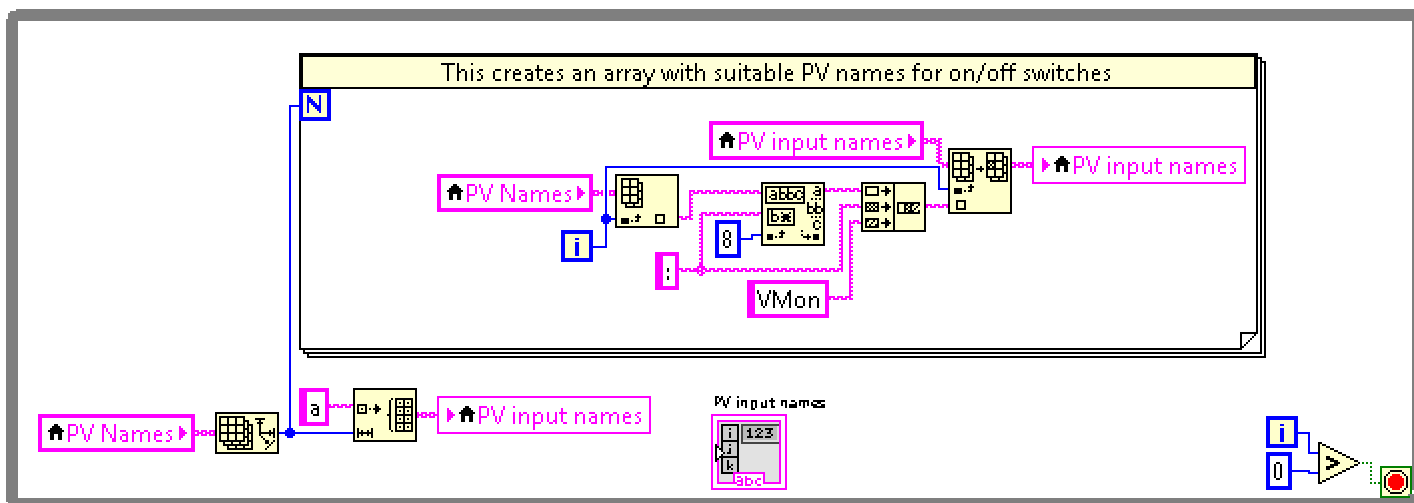

Figure 32: Measured Value Process Variable name generator

The rest of the code inside the loop is dedicated to creating the input Process Variable names. First the list "PV Names", i.e. the PV names in the first column in figure 33, is used to initialize another array of the same size called "PV input names". The size of the initial array is acquired using an Array Size Function. The size itself is then transferred along the blue wire to an Initialize Array Function and to a For Loop. This For Loop processes "PV Names" one element at a time replacing a substring following the last colon with the string "VMon". This is done by taking the *i*th element of the initial array and then searching for a colon after the string "Offline:" which is 8 characters

Vertical Line

PV Names	Measured Value	Set Voltage	On/Off
Offline:Skimmer:VSet	9	160	
Offline:Cone:VSet	10	600	
Offline:QPChamber:VSet	9	800	
Offline:QPL1:VSet	10	440	
Offline:QPL2:VSet	8	425	
Offline:QPS:VSet	7	0	
Offline:QPR:VSet	7	0	
Offline:Foc1:VSet	11	540	
Offline:STT1X:VSet	9	839	
Offline:STT1Y:VSet	9	642	
Offline:STT2X:VSet	9	770	
Offline:STT2Y:VSet	10	980	
Offline:Extr:VSet	29	2340	
Offline:QTA-:VSet	9	0	
Offline:QTA+:VSet	7	0	
Offline:QTB-:VSet	9	35	
Offline:QTB+:VSet	7	0	
Offline:Bender_upper:VSet	12	442	
Offline:Bender_lower:VSet	7	0	
Offline:Kicker:VSet	22	1050	

Save Load

Figure 33: Graphical user interface client application

long. Once the second colon is found a substring from the beginning of the string up to the colon is concatenated with another colon (the first one is excluded in the process) and "VMon" to form the new PV name. This is then used to replace the initial element in "PV input names" array. The resulting array is used to retrieve measured voltages from the EPICS server and to present them in the second column in the GUI. This code structure is also used to create a third array that holds the PV names of the On/Off switches in the fourth column in figure 33. The reader is referred to figure 45 in appendix B for a detailed schematic of this process.

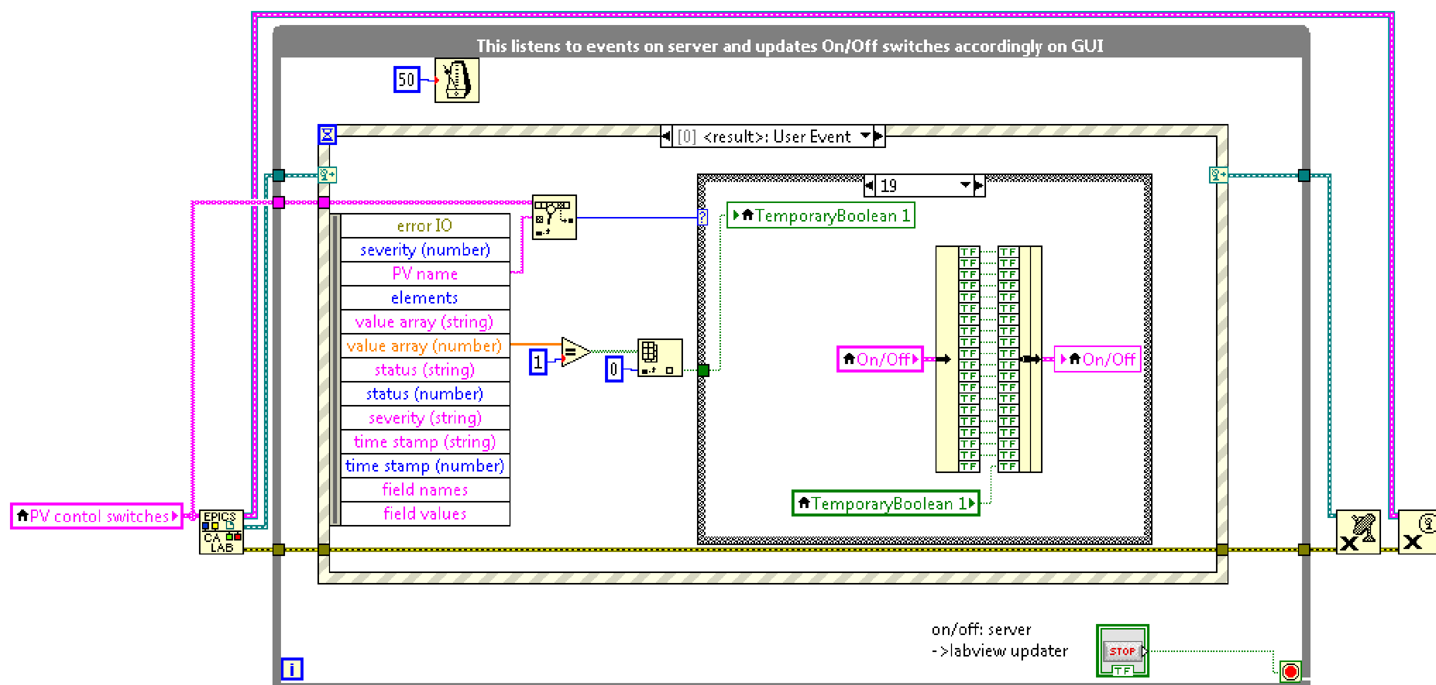

Figure 34: Event listener for On/Off switches

The second main structure in the source code is presented in figure 34. This is used to listen to events created by the EPICS server. The server is capable of informing client applications of any relevant changes to its Process Variables by creating events. This removes the need to have the client poll the server for changes, which is computationally beneficial. This piece of code uses an event function provided by CA Lab. It can be seen on the left side in figure 34 connected to "PV control switches". The event function listens to the server for any events related to Process Variables defined in the inputted array of PV names. Once this function receives an event it passes it on through a While Loop to an Event Structure which provides a way to access specific pieces of data carried by the detected event. In the case of figure 34 each event holds a binary integer representing a boolean value. This integer is converted into a boolean value. To be specific, each event carries an array of numbers that contains the information of interest in this case. It is stored in the first element of this array. Once the first element is separated from the entire array it is first stored into "TemporaryBoolean 1" and right away further inputted into the cluster containing all on-off switches visible in the GUI. A cluster can be described as a generic array which can hold a multitude of different types of components. Some components cannot be stored in arrays which results in the need to use clusters, just as in this case.

The temporary boolean is necessary due to the fact that the "On/Off" cluster holds on-off switches rather than boolean values. All switches naturally have a boolean value attached to them but the cluster will not accept anything else than a switch as its element whereas an individual on-off switch accepts a boolean value as input. The correct element to be replaced by the temporary switch is determined by finding the index of the the PV that generated the event in the "PV control switches" array. The index also represents the row of the switch in the GUI. Once the index is determined it is transeferred along the blue wire in figure 34 to a Case Structure which holds one case for each possible index value, suitable for replacing a corresponding switch in the "On/Off" cluster. The code structure presented in figure 34 is also used to listen to events related to "Measured Value" and "Set Voltage" columns in figure 33. They are updated analogously upon server events. Measured values are updated using a slightly more simple structure due to the fact that arrays have functional prebuilt tools for replacing a single element. Therefore, the case structure in figure 34 is not necessary for measured values. The reader is referred to figures 48 and 49 in appendix B for a detailed schematic of the two thusfar unpresented schematics.

The third main part of the source code is the initializers. They make use of the same Case Structure method for replacing elements within a cluster as described above. Initializer for "Set Voltage" column in the GUI is presented in figure 35. The backbone of the initializers is formed by a While Loop that is executed once, just as described earlier related to figure 32, and a For Loop which is executed once per each PV being operated by the client application. In the upper left corner of figure 35 the For Loop is given the number of times it is to be executed by wiring the size of the "PV Names"

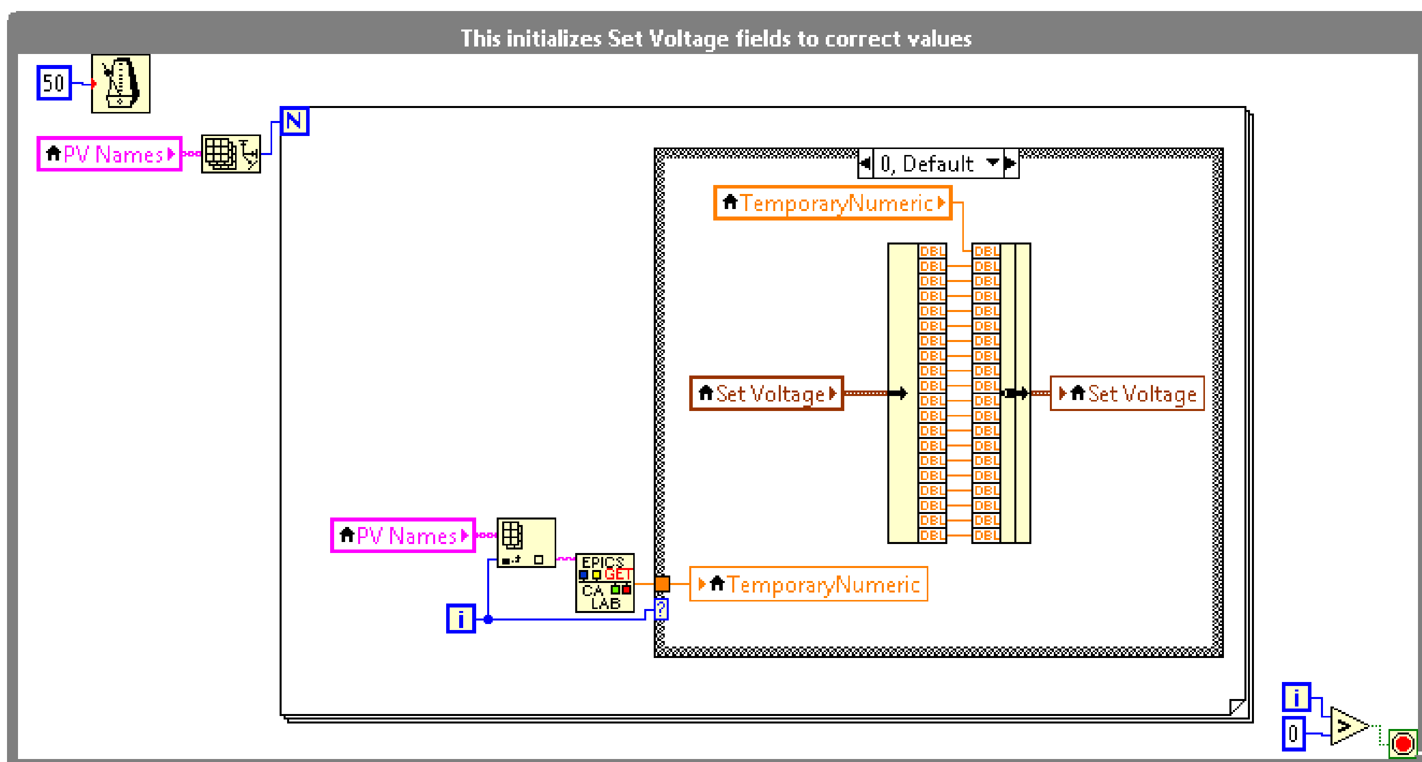

Figure 35: Initializer for Set Voltages

array to the terminal labeled "N". Once this information is provided the For Loop is ready to start. Inside the loop each element of "PV Names" is used in conjunction with a Get Function provided by CA Lab to retrieve the "Set Voltage" used by the EPICS server for each PV. This value is then inputted into the GUI similarly as described earlier in the case of on-off switches. The reader is referred to figure 51 in appendix B for a detailed schematic of the remaining initializer used to initialize on-off switches to the same values as the server.

The fourth main part of the source code is the events listeners that react to events generated by GUI components due to user interaction. For example, if a user adjusts a voltage set value it is necessary to convey the new value to the EPICS server. This is done using code presented in figure 36. This structure forms around yet another While Loop which contains an Event Structure. In contrast to the previously presented Event Structures, in this case there is no visible part representing an event, for example a wire connected to the structure. This Event Structure can be described as a Case Structure for which each case is programmed in the same way as for the actual Case Structure but with the difference that any execution of the Structure is triggered by an event created by a component of the GUI rather than an input wire connected to the Structure in the source code. Each event is connected to a different piece of code which is executed once the event is detected. The connection is defined using LabVIEW development environment and there is no visible trace of this connection in figure 36. All cases in the code of figure 36 are identical bar the integer number inside the blue box.

Previously it was necessary to use a Case Structure to access "Set Voltage" elements but in this case it is possible to use the NewVal field provided by the Event Structure. Each element of the "Set Voltage" cluster triggers an event that is customized to that particular element, i.e. has the right integer in the blue box. Therefore the NewVal field gives the desired piece of data. The corresponding PV name is then selected using the integer in the blue box and the set value is uploaded into the EPICS server. To sum up,

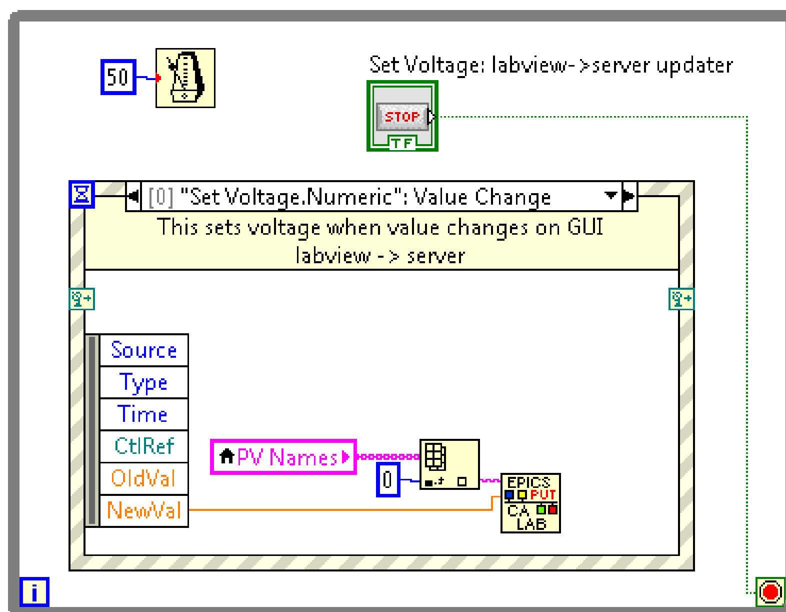

Figure 36: Set Voltage value uploader

the code effectively takes the ith element of "PV Names" and "Set Voltage" and uses CA Lab provided function to upload the value to the EPICS server. This code structure is also used to update server values of on-off switches. The reader is referred to figure 52 in appendix B for a detailed schematic of the on-off switch updater.

In addition to these four main parts that provide all the functions the client must have in order to be reliable, there is one more part to the client. This remaining part provides a possibility to save and reload set values to and from .xml files. Code used to save data into a file is presented in figure 37. The outermost layer of the code is a while loop. This is used to merely keep the "Save" button active on the GUI. Inside the loop there is a Case Structure that detects whether the button has been pressed. If the button has been pressed the code generates a name suggestion for the new file. This is done in the upper left corner of the Case Structure where a text "vertical-line-settings" is concatenated with a timestamp and a proper file extension. This file name is then forwarded to the next element that opens up a dialog box on the screen that can be used to select a folder and name for the file. The name suggestion is offered to the user but it can be overwritten. This information is then forwarded to another Case Structure that converts the data in the "Set Value" cluster into xml format and then actually saves the data into the file depending on whether a user clicked "OK" or "Cancel" in the dialog box. This selection can be seen as the Case Structre with the text "False" visible in figure 37. Loading a saved file happens similarly. Instead of saving a file the code converts the data back from xml format into a cluster and displays the information on the GUI. For a schematic of the loading code the reader is referred to figure 55 in appendix B.

All pieces of code described above together form a functional graphical user interface to control the new equipment. They provide a tool for users that keeps itself up-to-date with server values so that it is possible to have any number of copies of the GUI

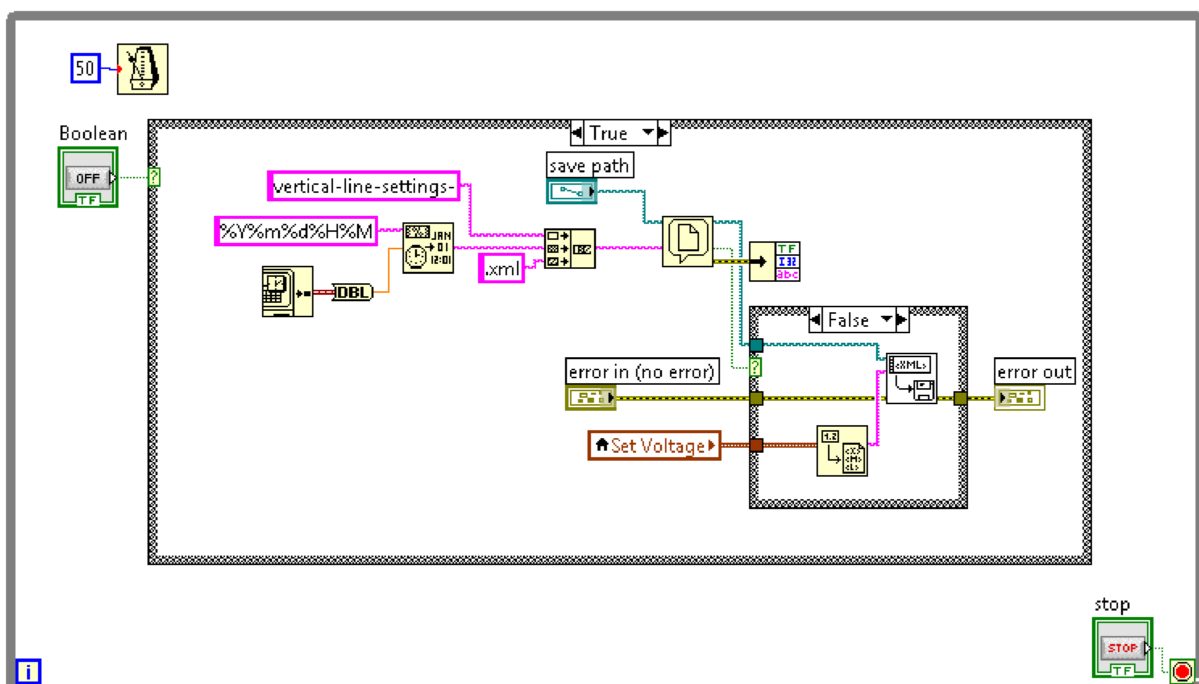

Figure 37: Set Value saver

client running at the same time, even on different computers. Therefore, it is a reliable tool even in case there is a computer failure in the normally used IGISOL control system set-up. Users can simply switch to another computer that has LabVIEW runtime environment installed.

5 EQUIPMENT TEST RESULTS

In the previous sections hardware and software were described along with a theoretical framework to support the use of the set-up. Now that the design of these systems have been covered we may move on to discuss test results. Naturally, the system was put through a set of tests in order to determine whether the design and implementation of the system, as a whole, was up to par. These tests include measurements related to the vacuum system, high voltage operational limits and, of course, a beam produced and transported by the system.

The first test were done on the vacuum system. As explained in section 3, the ion source needs a stream of helium in order to operate. This helium exits the ion source through a small hole at the bottom of the source entering a volume above the skimmer. That volume has one set of vacuum pumps evacuating the gas and one vacuum gauge. There is another set of pumps evacuating the volume below the skimmer along with a separate vacuum gauge. Gas pressure in these chambers was measured as a function of helium input pressure. This data is presented in figure 38.

The measurement was started with the gas input line closed. The system was allowed to pump down for a couple of days before the measurement. Therefore, the 0 mbar

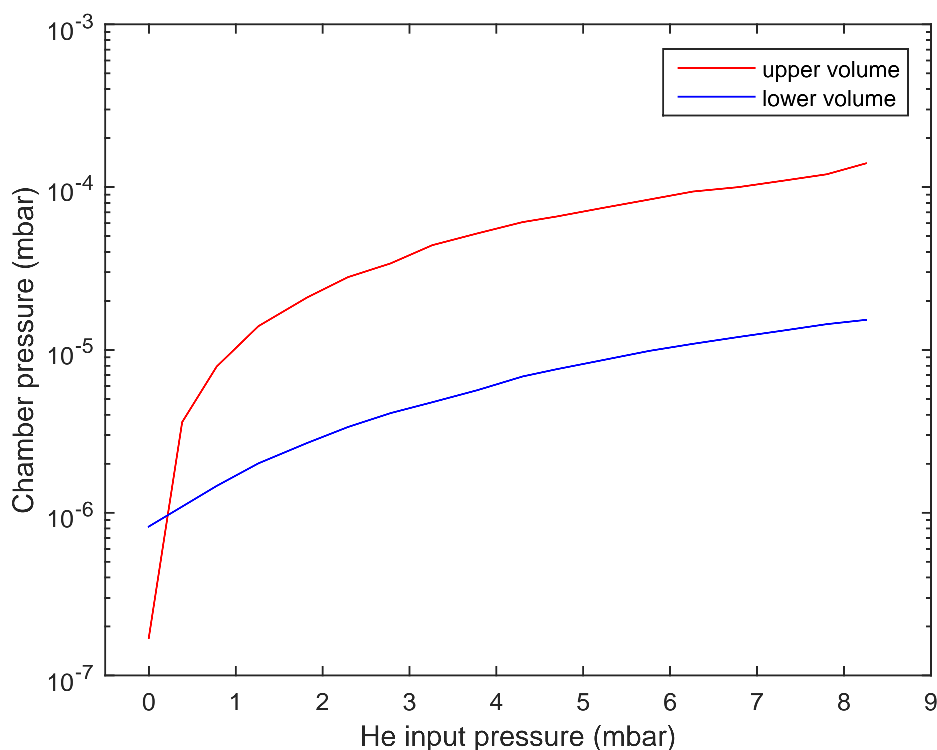

Figure 38: Gas pressures in two uppermost chambers of the vertical line

input pressure represent the best vacuum achievable with the currently assembled system. Pressure in the upper volume rises faster than in the lower as the input pressure is increased. However, the ratio of pressures becomes roughly constant around 2 mbar, being roughly an order of magnitude. Both volumes have turbomolecular pumps (upper pump: Edwards STP-301, lower pump: STP-451) with a maximum working pressure of $6.7 \cdot 10^{-4}$ mbar [14]. Data in figure 38 is raw data from the vacuum gauges. These values need to be corrected according to the gas the pressure of which they are measuring, in this case helium. Suitable correction factor was not readily available for the upper vacuum gauge (Edwards WRG-S). However, for the lower one (Varian FRG-700) a value of 5.9 was reported by the manufacturer [15]. Using the same value for both of the gauges, it can be seen that an input pressure of 8 mbar corresponds roughly to the maximum working pressure of the upper pump. Therefore, the data set in figure 38 was not extended further.

It was found that the input pressure is a highly significant factor in the amount of ionization taking place in the ion source. Production of ions was measured from two electrodes simultaneously, from the skimmer and cone electrodes. The cone was modified for this measurement so that the hole in the middle of the electrode was blocked. This ensured that all ions produced are measured. The two electrodes were kept at the same voltage compared to each other and the voltage was scanned from 0 V to 60 V. At the time of this measurement there were no reliable estimates on the voltages to be applied to these electrodes under normal operation of the set-up. Therefore, maximum voltage had to be chosen without any significant argument to support the choice. The voltage was chosen so that it was considered to be without a risk of sparking under any circumstances, it was chosen to be 60 V. Total measured current for different input pressures is presented in figure 39.

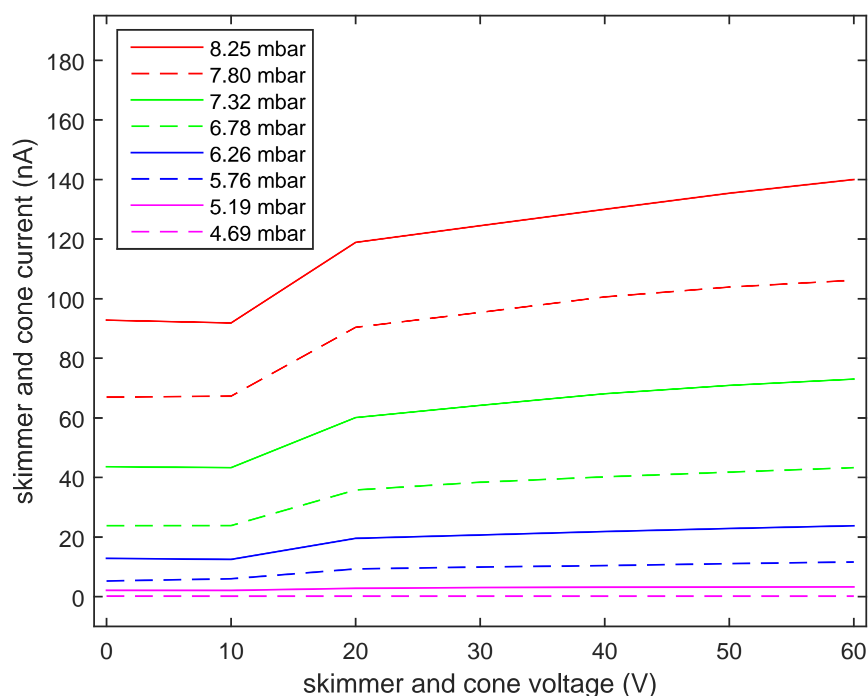

Figure 39: Total current measured from the skimmer and cone electrodes

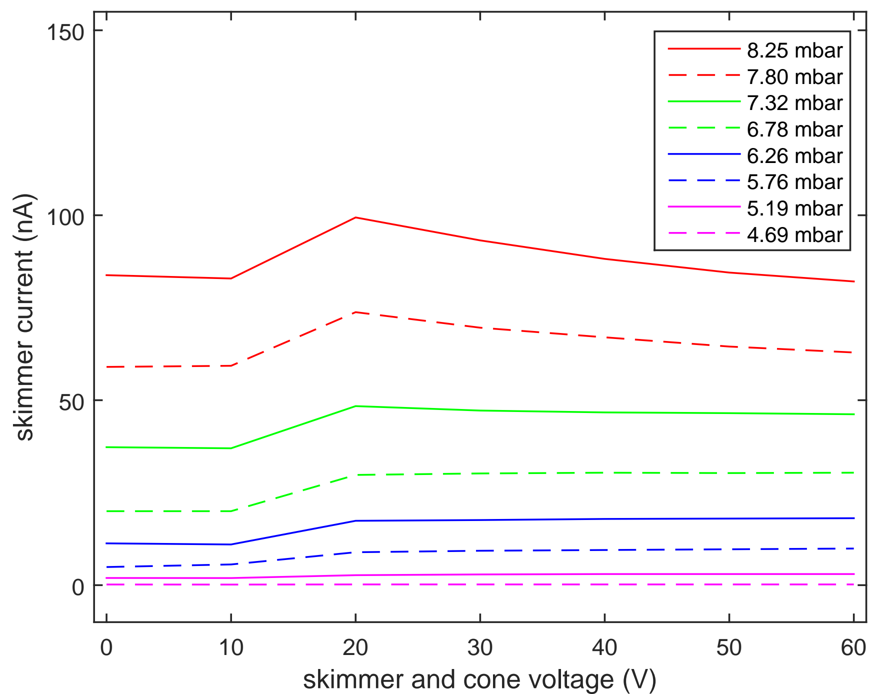

Figure 40: Current measured from the skimmer electrode

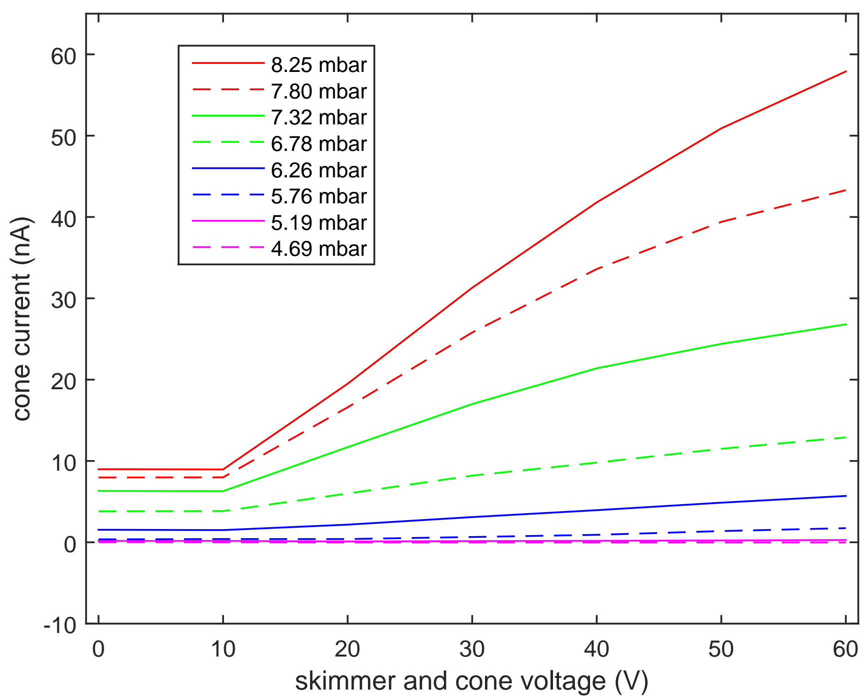

Figure 41: Current measured from the cone electrode

Figure 39 shows a clear trend of growing current with increasing voltage. The current starts to grow rather quickly after 10 V but then the slope starts to even out. The effect of increasing the input pressure was found to be an increase in the current in all pressure ranges. Data in figure 39 was collected with one ammeter for each of the electrodes. Currents measured separately from the skimmer and cone electrodes are presented in figures 40 and 41, respectively.

Skimmer current in figure 40 reveals an interesting property of the system. The skimmer electrode first starts to pull ions from the surrounding gas to itself as the voltage increses. However, after 20 V the behavior changes and the skimmer starts to let ions through more and more, as shown by the falling skimmer current and raising total current. Current measured from the cone electrode exhibits a more simple shape. Figure 41 shows that current increases steadily with increasing voltage, showing sings of slowly evening out at higher voltages. The effect of increasing the input pressure was similar for both electrodes, i.e. higher pressure corresponds to higher current.

As shown by figure 41, input pressure and electrode voltage are important factors in the amount of current passing through the system. The input pressure was pushed to its limits in these measurements, the vacuum pumps are not safe to be operated in any higher pressures. However, after these measurements during testing of the entire set-up as a whole, it was discovered that the skimmer and cone voltages can and should be raised much higher than 60 V. Regardless, it was decided that measurements behind figures 39, 40 and 41 would not be repeated since the figures were thought to demonstrate credible and explainable behavior. This lead to the conclusion that it was considered not to be justified to vent the system and once again modify the cone electrode to have a blocked aperture. After all, it is the amount of current that can be transmitted through the entire system which is of true significance, not the amount in the first two electrodes. The total transmitted current can be measured regardless of the shortcomings of figures 39-41.

In addition to the previously discussed current measurements, the entire system was tested as a whole. This was done so that the ion source was operated with different pressures and the created beam was passed through the beam line all the way up to the switchyard, presented in figure 11. The beam was mass separated using a dipole magnet. In addition to different input pressures, also different voltage set-ups were tried in the beam line as well as in the ion source itself. Five mass scan were conducted in such a way that current was measured at the switchyard while field strength of the magnet was swept from low to high. Results of the last four scans are presented in figure 42. The first scan was used to find a suitable mass peak for optimizing beam line voltages. Mass 28 u was chosen for this. Two closer views of figure 42 are presented in figures 43 and 44.

The last four scans were done in such a way that the first scan was with the lowest ion source voltage 0.7 kV, i.e. voltage between copper electrodes inside the source. Regardless of the fact that an input pressure close to the maximum safe pressure was used the first scan (red line in figures) did not reveal any copper within the beam. Copper has two naturally abundant isotopes with masses 63 u and 65 u. Their terrestrial abundances are 69.15 % and 30.85 %, respectively [16]. Figure 44 shows peaks for these masses only in the last two mass scans.

Once the first scan turned out not to have copper in significant amounts it was decided

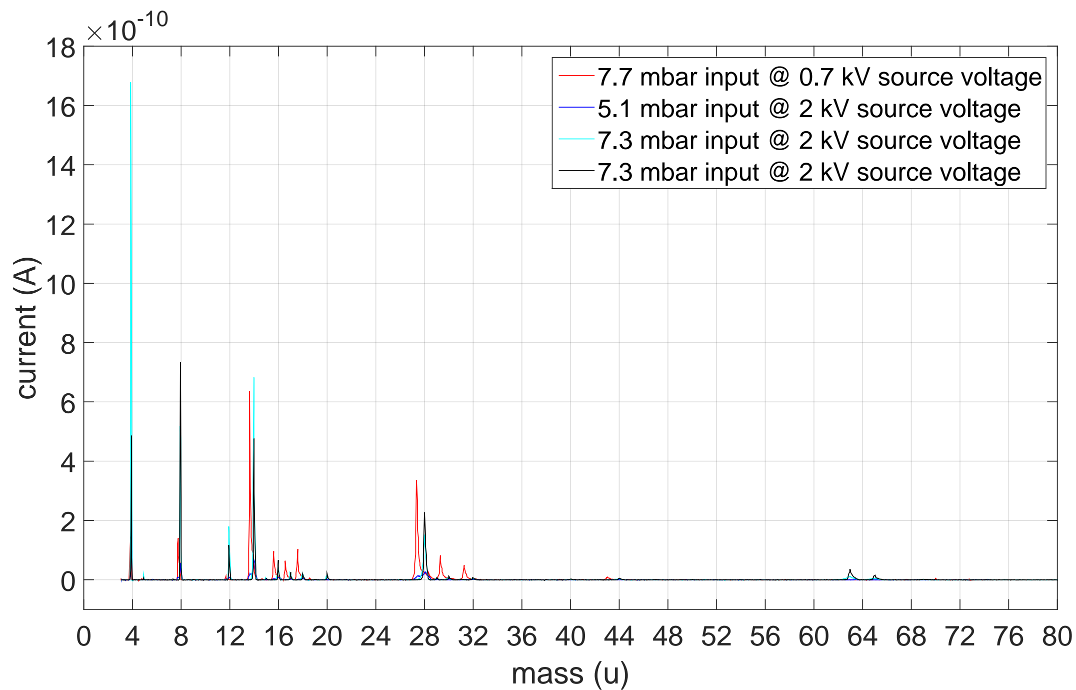

Figure 42: Current measured at switchyard with different masses set to pass the dipole magnet.

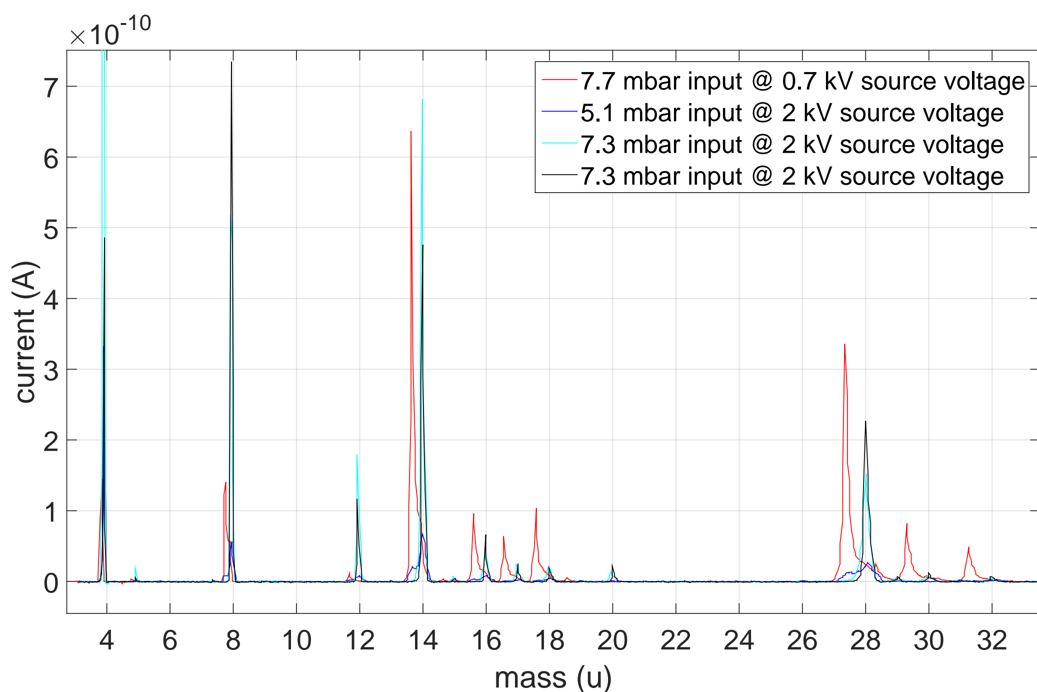

Figure 43: Current measured at switchyard with different masses set to pass the dipole magnet in mass region 4 u - 32 u.

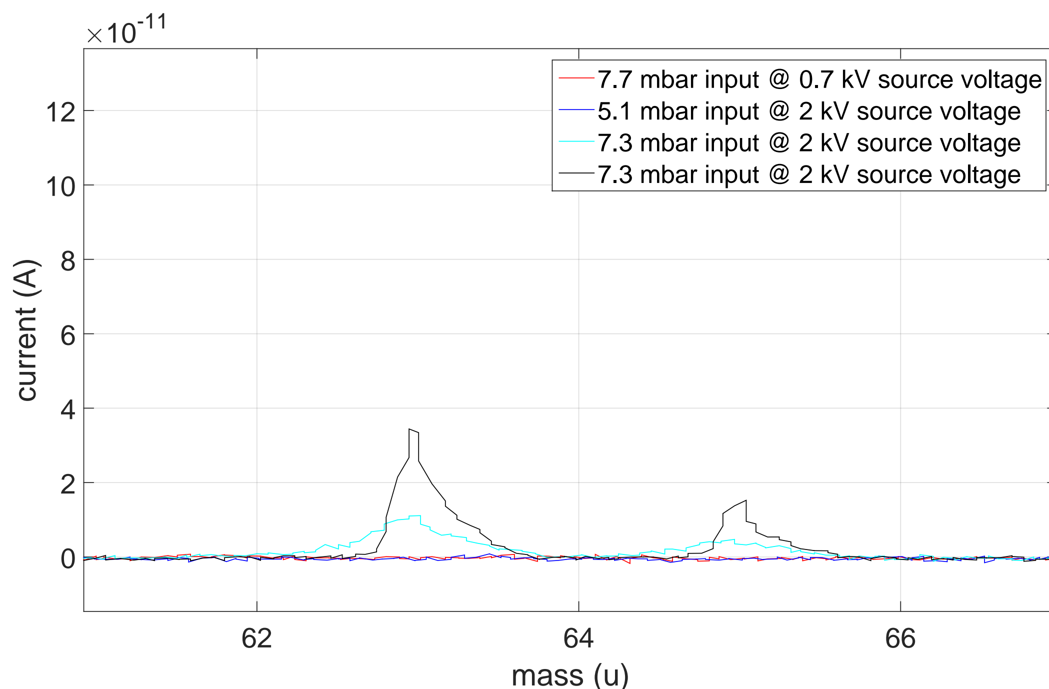

Figure 44: Current measured at switchyard with different masses set to pass the dipole magnet in mass region 62 u - 66 u.

to raise the inter-electrode voltage within the ion source. This decision was justified in section 2.2 by the fact that higher total voltage also increases the voltage used to accelerate ions towards the cathode. Since it is these ions that sputter copper from the electrode it was considered to be beneficial to increase the voltage. However, the first scan with higher source voltage (blue line in figures) did not reveal any copper either. This scan was done with an input pressure of 5.1 mbar.

After the first scan with higher source voltage turned out not to have copper, the input pressure was raised. This resulted in the second 2 kV scan (cyan line in figures). This was the first scan to have high enough amounts of both copper isotopes for them to be visible on a linear scale. However, the amount of copper was very small compared to the rest of the peaks. This scan proved to be very useful, regardless. The previous scans were done with the beam line optimized for mass 28 u. Given that a small amount of copper was detected it became possible to tune the beam line using mass 63 u. This turned out to improve the measured amount of copper by more than a factor of 2. This last scan (black line in figures) had the largest amount of copper ever measured from the new off-line ion source. All scans revealed a range of other masses besides copper. Sources of all mass peaks that could be indentified are listed in table 5.1.

There is one more notable aspect in the measured mass scans. The first plotted mass scan is shifted towards low masses, roughly 0.5 u in the mid mass range, compared to the last three scans. The mass scans were calibrated so that mass peaks in the last scans matched integer mass numbers. Mass peaks in the first scan are similarly positioned in comparison to other peaks in the same scan as in the last three scans. The shift could be explained in two ways. One is that ions could have been formed in a different location in the first scan than in the rest of the scans. If ions were formed in the gap between the skimmer electrode and ion source in the last three scans the observed behavior could

Table 5.1: Sources of different mass peaks

mass (u)	substance	mass (u)	substance
4	He^+	20	Ne^+
8	$2He^+$	28	N_2^+
12	C^+	30	NO^+
14	N^+	32	O_2^+
16	O^+	44	CO_2^+
17	HO^+	63	$^{63}Cu^+$
18	H_2O^+	65	$^{65}Cu^+$

be explained. The gap has lower potential than the ion source itself. This would result in the last three scan exhibiting slightly larger masses. Starting with equating a force exerted by a magnetic field on a charged particle and normal acceleration in circular motion, the needed voltage difference between mass scans can be calculated. Starting from

$$qvB = m\frac{v^2}{r} \tag{5.1}$$

and

$$v = \sqrt{\frac{2E}{m}} \tag{5.2}$$

one arrives at

$$m = \frac{(qrB)^2}{2E}. \tag{5.3}$$

Let us examine a case where charge q, radius r and magnetic flux density B are constant. Let us then examine two pairs of mass and energy and calculate which energy would be needed in the second case in order to for the particles to traverse the same path as the ones in the first case. A mass shift of 0.5 u at mass 18 u corresponds in this case to a voltage of

$$\frac{m_{red}}{m_{black}} = \frac{E_{black}}{E_{red}} = \frac{17.5\,\mathrm{u}}{18\,\mathrm{u}} = 0.9722 \tag{5.4}$$

$$E_{black} = 0.9722 \cdot E_{red} = 0.9722 \cdot 5\,\mathrm{keV} = 4861\,\mathrm{keV}. \tag{5.5}$$

This results in a voltage difference of roughly 140 V needed to explain the observed behavior. Skimmer voltage compared to the ion source was roughly 300 V in all of the scans. Therefore, the needed voltage difference is well achievable. This reasoning leads to a situation where constant voltage difference between scan shows up as a constant ratio of masses of corresponding peaks. All mass peaks in the presented figures seem to follow this reasoning. This finding supports different acceleration voltages as the source of the observed shift. However, there is another plausible explanation to the shift besides different ion formation locations.

The second possible reason behind the shift is the high voltage level of the upstairs set-up. High voltage had to be shut down each time either the input pressure or ion source voltage was adjusted. Therefore, it is possible that the high voltage level was unintentionally altered between the scans. The only way to determine the voltage was to read a scale on the side of a potentiometer used to adjust the voltage. The voltage

was set to the same value each time but it was not measured in any direct way from the set-up. Therefore, the high voltage level could very well have changed between the scans. This would shows up in results similarly as different positions of ion formation.

The latter explanation was considered to be the most likely one. Given that the last scans were the only ones to have detectable amounts of copper in them, it would seem unlikely that the ions were generated outside the ion source since the inside of the source was the only place where copper was present. In addition, the ion source itself should act as a Faraday cage around the copper electrodes and thus shield the source-skimmer gap from the effects of ion source electrode voltage. This shielding should result in similar conditions in the source-skimmer gap in the first and two last scans, making it unlikely that in only one of those scans the ions were created outside the ion source. This leaves the high voltage level as a more likely source of the shift.

There is one more factor that might be enough on its own to cause the observed shift or it might partially explain the shift together with the difference in acceleration voltage. It is possible that the entrance angle between the beam and the dipole magnet did not stay constant throughout the measurements. Beam line voltages were slightly adjusted between the measurements to maximize throughput of the system. It is possible that at the same time the entrance angle was altered, which would result in a need to calibrate each measurement separately. Data sets in figures 42 - 44 were all calibrated at the same time. Therefore, it could be that data from all four measurements is valid and merely erroneously calibrated.

Even though copper was detected in the second-to-last mass scan and the last scan was a clear improvement to that one in the amount of copper, the total amount is still lower than what was hoped for. The largest total current before the dipole magnet that could be seen with a pressure of 7.3 mbar was roughly 100 nA. In the light of this the total amount of copper seemed very small.

6 DISCUSSION

Motivation behind this thesis work was to commission a length of beam line that would provide a possibility to switch from using an older version of a glow discharge ion source to a new version. This switch offers several benefits. As mentioned earlier, the old ion source was problematic due to the fact that it needed to be installed in the target chamber which receives significant amounts of radiation during experiments. This made it necessary to wait for a period of time before entering the target chamber area to install the ion source. The new set-up improves this situation in two ways: A waiting period is no longer necessary and scientists do not a get any more radiation exposure due to operating the new ion source than what is received due to background radiation.

There is also one more significant benefit to be gained by using the new off-line set-up. Two of the more important pieces of equipment in the IGISOL set-up are the Penning traps. They are devices used to measure masses to a high precision. In order to achieve as high a precision as possible the traps require calibration. This is best done with known reference masses close to the mass region in which elements to be studied lie. Since the new off-line set-up can be operated parallel to the front end, it is possible to get a mass reference from an off-line ion source upstairs and then quickly switch to taking a beam from the front end. The intersection of vertical and horizontal beam lines is designed so that it should be possible to rapidly switch between both beam sources, even so that the source is switched continually back and forth in rapid succession by altering the voltage applied to the kicker plates, labeled B in figure 25. However, an opportunity to test this mode of operation did not present itself during testing of the vertical line. This is something to be pursued in the future.

In other respects all commissioned parts of the system were tested as far as possible with only one ion source available upstairs. Bending a beam with the quadrupole bender was not tested since no beam was available from either of the suitable horizontal branches of the cross chamber. There are plans to install two more ions sources to the remaining mounting points, one for each. Once they are installed it will be possible to finish testing the quadrupole bender. The glow discharge ion source was successfully used to test the beam line and verify that it is operational. However, no reliable estimates on the transmission percentage of the system were acquired since there were no current measurement points with identical cross sectional areas. Therefore, all current measurements done along the beam line are incomparable against each other. This situation could be rectified with relative ease and low costs in the future by replacing thus far used Faraday cups with identical ones.

The shape of the beam could also be studied using fluorescent plates installed in the beam line and viewing them with a suitable camera. This was done at one location right after the kicker plates in order to ensure that the newly installed plates did not obstruct the path of a horizontal beam from the front end. The method was found to provide a useful measure of understanding on the behavior of a beam when different

optical elements are adjusted. For example, it was found that a quadrupole triplet preceding the kicker plates had the effect of rotating the beam around the optical axis. This was considered to be caused by the beam traversing the triplet slightly off-center. Similar observations on the vertical line would most likely prove useful.

Test done on the vertical line and ion source showed that copper was ionized and transported to the switchyard. However, the amount of copper was not as high as was hoped for. It was observed that increasing helium pressure inside the ion source improved the situation as well as increasing inter-electrode voltage within the source. The measured amount of copper leaves yet another goal for the future: to increase the yield, naturally. The previous glow discharge ion source used at IGISOL was proven to provide significantly higher yields of copper with 0.7 kV source voltage than what was measured with any tested configuration with the new source. This was considered to be a matter of helium pressure.

Previously it has been possible to use much higher pressures inside a source since the pumping system at the front end is vastly more powerful than the one upstairs. Current financial situation of the research group supports only modifying the ion source, rather than constructing a more capable pumping set-up upstairs. Therefore, it has been planned that the exit hole of the ion source will be made smaller in order to increase helium pressure without putting more strain on the pumping system. This is expected to increase the production of copper ions. However, there lies a possibility that an increase in the evacuation time of the ions from the source could adversely compensate for the increased production. The higher the evacuation time the more recombination of ions takes place. All in all, this was considered to be a modification worth the effort since it comes with minimal financial costs and a very reasonable amount of labor. This modification is to be pursued in the future.

In addition to the above discussed improvements to the performance of the system some room for improvement remains on the usability side of the set-up. Currently the input pressure of the ion source can only be adjusted manually inside the safety cage surrounding the upstairs set-up. This could be computerized and made controllable using EPICS. The software side requires only little development but the hardware requirements are a bit more challenging. A suitable servo motor and drive belt would be needed and a matching mounting structure would have to be designed and built. This is entirely doable but would require some working hours to complete. In addition to this, there are two pressure gauges that are not yet remotely readable. This should be corrected at the same time as the needle valve is made remotely controllable. It would also enable more sophisticated safety functions to be put in place for opening valves in the beam line. For example, it would be possible to ensure that both sides of a valve are roughly at the same pressure before a valve would respond to a user trying to open it.

On the software side of this project there is less to be done in the future. The commissioned software architecture and graphical user interface have thus far functioned without any problems. In addition, up to this point no need to update or add any functionality to the system has been discovered. There is one function in EPICS that would be beneficial to take into active use. This is the alarm system. It would be possible to have EPICS servers to post alarms under certain conditions, such as a too high pressure in some part of the beam line. This possibility was not utilized in this work. In addi-

tion, it has not been utilized in the rest of EPICS servers that were already operational at the time this thesis work begun. It would be beneficial to update all of these servers so that the entire IGISOL set-up would make the most of the control system software architecture. However, this would require detailed knowledge of the entire IGISOL set-up and a considerable amount of work. This is still something to be considered in the future.

All in all, this thesis project has thus far at least partially achieved goals set before its beginning. The vertical beam line is operational and has been tested to a reasonable extent. Some room for further testing still remains. Importantly, the beam line has been tested enough to allow for additional ion sources to be installed and taken into active use. The glow discharge ion source has been proven to produce a good amount of ions, even some copper ions. This will hopefully be improved by introducing a smaller exit hole to the ion source. Software needed to control the system has proven to be reliable and it has introduced a more robust EPICS PV set-up in case of server failures. As is the case with many other systems, work shall continue with the commissioned set-up.

References

[1] Helmut Liebl. *Applied Charged Particle Optics*. Springer, 2007.

[2] Hermann Wollnik. *Optics of Charged Particles*. Academic Pr, 1987.

[3] Yuri P. Raizer. *Gas Discharge Physics*. Springer, 2001.

[4] Brian Chapman. *Glow Discharge Processes: Sputtering and Plasma Etching*. Wiley-Interscience, 1980.

[5] Kim Taeman. *Buffer Gas Cooling of Ions in a Radio Frequency Quadrupole Ion Guide*. PhD thesis, McGill University, Montreal, 1997, unpublished.

[6] A. Nieminen, J. Huikari, A. Jokinen, J. Äystö, P. Campbell, and E.C.A. Cochrane. Beam cooler for low-energy radioactive ions. *Nuclear Instruments and Methods in Physics Research Section A: Accelerators, Spectrometers, Detectors and Associated Equipment*, 469(2):244–253, aug 2001.

[7] T. Eronen, V. S. Kolhinen, V.-V. Elomaa, D. Gorelov, U. Hager, J. Hakala, A. Jokinen, A. Kankainen, P. Karvonen, S. Kopecky, I. D. Moore, H. Penttilä, S. Rahaman, S. Rinta-Antila, J. Rissanen, A. Saastamoinen, J. Szerypo, C. Weber, and J. Äystö. JYFLTRAP: A Penning trap for precision mass spectroscopy and isobaric purification. In Juha Äystö, Tommi Eronen, Ari Jokinen, Anu Kankainen, Iain D. Moore, and Heikki Penttilä, editors, *Three decades of research using IGISOL technique at the University of Jyväskylä: A Portrait of the Ion Guide Isotope Separator On-Line Facility in Jyväskylä*, pages 61–81. Springer Netherlands, Dordrecht, 2014.

[8] B. Cheal and D. H. Forest. Collinear laser spectroscopy at the new IGISOL 4 facility. In Juha Äystö, Tommi Eronen, Ari Jokinen, Anu Kankainen, Iain D. Moore, and Heikki Penttilä, editors, *Three decades of research using IGISOL technique at the University of Jyväskylä: A Portrait of the Ion Guide Isotope Separator On-Line Facility in Jyväskylä*, pages 287–294. Springer Netherlands, Dordrecht, 2014.

[9] SIMION website. `http://simion.com/`, accessed 3.7.2016.

[10] EPICS website. `http://www.aps.anl.gov/epics/`, accessed 3.7.2016.

[11] Channel Access Reference Manual. `http://www.aps.anl.gov/epics/base/R3-14/12-docs/CAref.html#Environmen`, accessed 3.7.2016.

[12] EPICS record reference manual. `https://wiki-ext.aps.anl.gov/epics/index.php/RRM_3-14`, accessed 3.7.2016.

[13] CA Lab website. `http://www-csr.bessy.de/control/SoftDist/CA_Lab/`, accessed 3.7.2016.

[14] STP-301/451 series turbomolecular pump manual. `https://www.lesker.com/newweb/vacuum_pumps/pdf/manuals/stp301~451%20manual.pdf`, accessed 3.7.2016.

[15] Varian FRG-700 inverted magnetron pirani gauge manual. http://ridl.cfd.rit.edu/products/manuals/Varian/FRG-700%20Short%20Operating%20Instructions.pdf, accessed 3.7.2016.

[16] National Nuclear Data Center, Chart of Nuclides. http://www.nndc.bnl.gov/chart/, accessed 3.7.2016.

Appendices

A EPICS configuration files

Analog input:

```
1  # ai record template for register inputs
2  record(ai, "$(P)$(R)") {
3      field(DTYP,"asynInt32")
4      field(INP,"@asynMask($(PORT) $(OFFSET) $(BITS))MODBUS_DATA")
5      field(LINR,"LINEAR")
6      field(EGUL,"$(EGUL)")
7      field(EGUF,"$(EGUF)")
8      field(HOPR,"$(EGUF)")
9      field(LOPR,"$(EGUL)")
10     field(PREC,"$(PREC)")
11     field(SCAN,"$(SCAN)")
12     field(EGU, "Volt")
13     field(MDEL, "$(MDEL)")
14 }
```

Analog input with smoothing:

```
1  # ai record template for register inputs
2  record(ai, "$(P)$(R)") {
3      field(DTYP,"asynInt32")
4      field(INP,"@asynMask($(PORT) $(OFFSET) $(BITS))MODBUS_DATA")
5      field(LINR,"LINEAR")
6      field(EGUL,"$(EGUL)")
7      field(EGUF,"$(EGUF)")
8      field(HOPR,"$(EGUF)")
9      field(LOPR,"$(EGUL)")
10     field(PREC,"$(PREC)")
11     field(SCAN,"$(SCAN)")
12     field(SMOO,"0.9")
13     field(MDEL,"0.0025")
14     field(FLNK,"$(FLNK)")
15 }
```

Analog output for Set Value:

```
1  record(ao, "$(P)$(R)") {
2    field(FLNK,"$(FLNK)")
3      field(DRVH,"$(DRVH)")
4      field(DRVL,"$(DRVL)")
5      field(PREC,"$(PREC)")
6      field(VAL, "$(VAL)")
7      field(PINI, "$(PINI)")
8  }
9
10
11 # TODO: varmista toimiiko VAL = 1 alustus kunnolla siten, etta caput ja get toimivat ok. ja ↩
       sit kanssa etta VSet PV:T toimii kunnolla
```

Analog output for communication with the PLC:

```
1  # ao record template for register outputs
2
3  # I tested that additional fields here do not cause any harm in the case where substitutions↩
        file doesn't have any mention of them.
```

```
4  # i.e. this file can be swapped with the older one that was on qad without a need to update ↩
       other IOCs.
5  # — Markus Vilen, December 2015
6
7  record(ao, "$(P)$(R)") {
8      field(DTYP,"asynInt32")
9      field(OUT,"@asynMask($(PORT) $(OFFSET) $(BITS))MODBUS_DATA")
10     field(LINR,"LINEAR")
11     field(EGUL,"$(EGUL)")
12     field(EGUF,"$(EGUF)")
13     field(HOPR,"$(EGUF)")
14     field(LOPR,"$(EGUL)")
15     field(PREC,"$(PREC)")
16     field(DRVH,"$(EGUF)")
17     field(OMSL,"$(OMSL)")
18     field(DOL, "$(DOL)")
19     field(PINI, "$(PINI)")
20 }
```

Binary output for On/Off:

```
1  # bo record template for register outputs
2  record(bo,"$(P)$(R)") {
3      field(FLNK,"$(FLNK)")
4    field(ZNAM,"$(ZNAM)")
5      field(ONAM,"$(ONAM)")
6      field(VAL, "$(VAL)")
7      field(PINI, "$(PINI)")
8  }
```

Calcout for initializing On/Off:

```
1  record(calcout,"$(P)$(R)") {
2    field(INPA,"$(INPVALUE)")
3    field(CALC,"A<0.1?0:1")
4    field(OOPT,"Every Time")
5    field(DOPT,"Use CALC")
6    field(OUT, "$(OUT)")
7    field(SCAN, "Passive")
8    field(PINI, "$(PINI)")
9  }
```

Calcout for initializing Set Value:

```
1  record(calcout,"$(P)$(R)") {
2    field(INPA,"$(INPVALUE)")
3    field(CALC,"1=1?A:A")
4    field(OOPT,"Every Time")
5    field(DOPT,"Use CALC")
6    field(OUT, "$(OUT)")
7    field(SCAN, "Passive")
8    field(PINI, "$(PINI)")
9  }
```

Calcout for Switch:

```
1  record(calcout,"$(P)$(R)") {
2    field(INPA,"$(INPVALUE)")
3    field(INPB,"$(INPONOFF)")
4    field(CALC,"B=1?A:0")
5    field(OOPT,"Every Time")
6    field(DOPT,"Use CALC")
7    field(OUT,"$(OUT)")
8    field(PINI, "$(PINI)")
9  }
```

Calc for pressure monitoring:

```
record(calc,"$(P)$(R)") {
  field(INPA,"$(INPVALUE)")
  field(CALC,"10^(1.667*A-11.33)")
  field(PINI, "YES")
  field(EGU, "mbar")
}
```

Fanout for initialization:

```
record(fanout, "$(P)$(R)") {
  field(SCAN, "Passive")
  field(SELM, "All")
  field(LNK1, "$(LNKVALUEINIT)")
  field(LNK2, "$(LNKONOFFINIT)")
  field(PINI, "$(PINI)")
}
```

Substitutions file:

```
# OFFLINE.SUBSTITUTIONS



##### IL-marked records are ones that are NOT ment to be interacted with by users.


# OUTPUT TO HARDWARE ##########################################################

## let the right side of the set up be called the positive X-direction
## there is one channel that does not seem to work. It puts out a constant 15V -> offset 8

# TODO: varmista, etta taa template tulee talla nimella qadiin!!
file "/epics/synApps/synApps_5_8/support/modbus-2-7/db/aoOfflineIL.template" { pattern
{P,          R,               PORT,          OFFSET,   BITS,   EGUL,   EGUF, PREC,   OMSL↩
    ,      DOL,                   PINI}
{Offline:,    Foc1-IL:VSet,         Offline_AO,       0,      15,     0,      1000, 3,    "↩
    closed_loop",  "Offline:Foc1-IL:calcout NMS PP",    "NO"}
{Offline:,    Extr-IL:VSet,         Offline_AO,       1,      15,     0,      10000 3,    "↩
    closed_loop",  "Offline:Extr-IL:calcout NMS PP",    "NO"}
{Offline:,    STT2X-IL:VSet,      Offline_AO,       2,      15,     0,      1000, 3,    "↩
    closed_loop",  "Offline:STT2X-IL:calcout NMS PP",    "NO"}
{Offline:,    STT2Y-IL:VSet,        Offline_AO,       3,      15,     0,      1000, 3,    "↩
    closed_loop",  "Offline:STT2Y-IL:calcout NMS PP",    "NO"}
{Offline:,    Skimmer-IL:VSet,      Offline_AO,       4,  15,   0,      1000, 3,    "↩
    closed_loop",  "Offline:Skimmer-IL:calcout NMS PP",    "NO"}
{Offline:,    QPChamber-IL:VSet,    Offline_AO,       5,  15,   0,      1000, 3,    "↩
    closed_loop",  "Offline:QPChamber-IL:calcout NMS PP",    "NO"}
{Offline:,    QPR-IL:VSet,      Offline_AO,       6,  15,   0,      3000, 3,    "closed_loop↩
    ",  "Offline:QPR-IL:calcout NMS PP",    "NO"}
{Offline:,    QPS-IL:VSet,      Offline_AO,       7,  15,   0,      3000, 3,    "closed_loop↩
    ",  "Offline:QPS-IL:calcout NMS PP",    "NO"}
{Offline:,    QPL1-IL:VSet,     Offline_AO,       9,      15, 0,      1000, 3,    "↩
    closed_loop",  "Offline:QPL1-IL:calcout NMS PP",    "NO"}
{Offline:,    Cone-IL:VSet,         Offline_AO,       10,     15, 0,      1000, 3,    "↩
    closed_loop",  "Offline:Cone-IL:calcout NMS PP",    "NO"}
{Offline:,    QPL2-IL:VSet,         Offline_AO,       11,     15, 0,      1000, 3,    "↩
    closed_loop",  "Offline:QPL2-IL:calcout NMS PP",    "NO"}
{Offline:,    STT1X-IL:VSet,      Offline_AO,   12, 15, 0,  1000, 3,    "closed_loop",  "↩
    Offline:STT1X-IL:calcout NMS PP",    "NO"}
{Offline:,    STT1Y-IL:VSet,      Offline_AO,   13, 15, 0,  1000, 3,    "closed_loop",  "↩
    Offline:STT1Y-IL:calcout NMS PP",    "NO"}
#
{Offline:,    QTA--IL:VSet,     Cave_AO,        0,  15,   0,      1000, 3,    "closed_loop",↩
      "Offline:QTA--IL:calcout NMS PP",    "NO"}
{Offline:,    QTA+-IL:VSet,     Cave_AO,        1,  15,   0,      1000, 3,    "closed_loop",↩
      "Offline:QTA+-IL:calcout NMS PP",    "NO"}
```

```
32 {Offline:,    QTB−−IL:VSet,     Cave_AO,        2,      15, 0,      1000, 3,    "closed_loop↩
       ",  "Offline:QTB−−IL:calcout NMS PP",   "NO"}
33 {Offline:,    QTB+−IL:VSet,         Cave_AO,        3,      15, 0,      1000, 3,    "↩
       closed_loop",  "Offline:QTB+−IL:calcout NMS PP",   "NO"}
34 {Offline:,    Bender_upper−IL:VSet,   Cave_AO,        4,      15, 0,      3000, 3,    "↩
       closed_loop",  "Offline:Bender_upper−IL:calcout NMS PP", "NO"}
35 {Offline:,    Bender_lower−IL:VSet,   Cave_AO,    5,  15, 0,  3000, 3,    "closed_loop",  "↩
       Offline:Bender_lower−IL:calcout NMS PP", "NO"}
36 {Offline:,    Kicker−IL:VSet,     Cave_AO,    6,  15, 0,  10000,  3,    "closed_loop",  "↩
       Offline:Kicker−IL:calcout NMS PP",   "NO"}
37
38 }
39
40
41
42
43
44 # INPUT FROM HARDWARE ##########################################################
45
46
47 file "/epics/synApps/synApps_5_8/support/modbus−2−7/db/ai.template" { pattern
48 {P,       R,    PORT,   OFFSET, BITS, EGUL,   EGUF,   PREC,   SCAN,   MDEL}
49 {Offline:,      Foc1:VMon,      Offline_AI,     0,      15,     0,      1000,   2,    "1 ↩
       second", "0.3"}
50 {Offline:,      Extr:VMon,      Offline_AI,     1,      15,     0,      10000,  2,    "1 ↩
       second", "0.3"}
51 {Offline:,      STT2X:VMon,     Offline_AI,     2,      15,     0,      1000,   2,    "1 ↩
       second", "0.3"}
52 {Offline:,      STT2Y:VMon,     Offline_AI,     3,      15,     0,      1000,   2,    "1 ↩
       second", "0.3"}
53 {Offline:,      QPS:VMon,     Offline_AI,     4,      15,     0,      3000,   2,    "1 ↩
       second", "0.3"}
54 {Offline:,      QPChamber:VMon,     Offline_AI,     5,      15,     0,      1000,   2,    "1↩
        second", "0.3"}
55 {Offline:,      QPR:VMon,     Offline_AI,     6,      15,     0,      3000,   2,    "1 ↩
       second", "0.3"}
56 {Offline:,      Skimmer:VMon,     Offline_AI,     7,      15,     0,      1000,   2,    "1 ↩
       second", "0.3"}
57 # tahan lisattiin kapasitiivisen lukemiseksi yksi pakka
58 #{Offline:,     Skimmer:IMon,     Offline_AI,     9,  15,     #0,     0.003,    15,   "1 ↩
       second", "0.000000000001"}
59 {Offline:,      QPL2:VMon,      Offline_AI,     12, 15,     0,      1000,   2,    "1 second↩
       ", "0.3"}
60 {Offline:,      Cone:VMon,      Offline_AI,     14, 15,     0,      1000,   2,    "1 second↩
       ", "0.3"}
61 {Offline:,      QPL1:VMon,      Offline_AI,     15,     15,     0,      1000,   2,    "1 ↩
       second", "0.3"}
62 {Offline:,      STT1X:VMon,     Offline_AI,     16,     15,     0,      1000,   2,    "1 ↩
       second", "0.3"}
63 {Offline:,      STT1Y:VMon,     Offline_AI,     17,     15,     0,      1000,   2,    "1 ↩
       second", "0.3"}
64 #
65 {Offline:,      QTA−:VMon,      Cave_AI,      0,      15,     0,      1000,   2,    "1 ↩
       second", "0.3"}
66 {Offline:,      QTA+:VMon,      Cave_AI,      1,      15,     0,      1000,   2,    "1 ↩
       second", "0.3"}
67 {Offline:,      QTB−:VMon,      Cave_AI,      2,  15,     0,      1000,   2,    "1 second", ↩
       "0.3"}
68 {Offline:,      QTB+:VMon,      Cave_AI,      3,  15,     0,      1000,   2,    "1 second", ↩
       "0.3"}
69 {Offline:,      Bender_upper:VMon,    Cave_AI,      4,      15,     0,      3000,   2,    "1↩
        second", "0.3"}
70 {Offline:,      Bender_lower:VMon,    Cave_AI,      5,      15,     0,      3000,   2,    "1↩
        second", "0.3"}
71 {Offline:,      Kicker:VMon,      Cave_AI,      6,      15,     0,      10000,  2,    "1 ↩
       second", "0.3"}
72
73 }
74
75 file "/epics/synApps/synApps_5_8/support/modbus−2−7/db/ai_smooth.template" { pattern
76 {P,   R,        PORT,   OFFSET, BITS, EGUL,   EGUF,     PREC,     SCAN,   FLNK}
77 {Pressure:,     Offline:LowerRaw,   Offline_AI,     8,  15,     0,      10,     4,      ".5 ↩
       second",  "Pressure:Offline:Lower NMS PP"}
```

```
78  }
79
80
81  file "/epics/synApps/synApps_5_8/support/modbus-2-7/db/calcPressure.template" { pattern
82  {P,   R,        INPVALUE}
83  {Pressure:,     Offline:Lower,      "Pressure:Offline:LowerRaw"}
84  }
85
86  # BINARY OUTPUT(SOFTWARE ONLY) #######################################################
87
88
89  file "/epics/synApps/synApps_5_8/support/modbus-2-7/db/boOffline.template" { pattern
90  {P,     R,              FLNK,                   ZNAM, ONAM, VAL,  PINI}
91  {Offline:,  Foc1:OnOff,       "Offline:Foc1-IL:calcout NMS PP",   "Off",  "On", 0,    "NO"}
92  {Offline:,  Extr:OnOff,       "Offline:Extr-IL:calcout NMS PP",   "Off",  "On", 0,    "NO"}
93  {Offline:,  STT2X:OnOff,      "Offline:STT2X-IL:calcout NMS PP",    "Off",  "On", 0,    "NO↩
        "}
94  {Offline:,  STT2Y:OnOff,      "Offline:STT2Y-IL:calcout NMS PP",    "Off",  "On", 0,    "NO↩
        "}
95  {Offline:,  Skimmer:OnOff,      "Offline:Skimmer-IL:calcout NMS PP",  "Off",  "On", 0,    "↩
        NO"}
96  {Offline:,  QPChamber:OnOff,    "Offline:QPChamber-IL:calcout NMS PP",  "Off",  "On", 0,    ↩
        "NO"}
97  {Offline:,  QPR:OnOff,        "Offline:QPR-IL:calcout NMS PP",    "Off",  "On", 0,    "NO"}
98  {Offline:,  QPS:OnOff,        "Offline:QPS-IL:calcout NMS PP",    "Off",  "On", 0,    "NO"}
99  {Offline:,  QPL1:OnOff,       "Offline:QPL1-IL:calcout NMS PP",   "Off",  "On", 0,    "NO"}
100 {Offline:,  QPL2:OnOff,       "Offline:QPL2-IL:calcout NMS PP",   "Off",  "On", 0,    "NO"}
101 {Offline:,  Cone:OnOff,       "Offline:Cone-IL:calcout NMS PP",   "Off",  "On", 0,    "NO"}
102 {Offline:,  STT1X:OnOff,      "Offline:STT1X-IL:calcout NMS PP",    "Off",  "On", 0,    "NO↩
        "}
103 {Offline:,  STT1Y:OnOff,      "Offline:STT1Y-IL:calcout NMS PP",    "Off",  "On", 0,    "NO↩
        "}
104 #
105 {Offline:,  QTA-:OnOff,       "Offline:QTA--IL:calcout NMS PP",   "Off",  "On", 0,    "NO"}
106 {Offline:,  QTA+:OnOff,       "Offline:QTA+-IL:calcout NMS PP",   "Off",  "On", 0,    "NO"}
107 {Offline:,  QTB-:OnOff,       "Offline:QTB--IL:calcout NMS PP",   "Off",  "On", 0,    "NO"}
108 {Offline:,  QTB+:OnOff,       "Offline:QTB+-IL:calcout NMS PP",   "Off",  "On", 0,    "NO"}
109 {Offline:,  Bender_upper:OnOff,   "Offline:Bender_upper-IL:calcout NMS PP",   "Off",  "On", ↩
        0,    "NO"}
110 {Offline:,  Bender_lower:OnOff,   "Offline:Bender_lower-IL:calcout NMS PP",   "Off",  "On", ↩
        0,    "NO"}
111 {Offline:,  Kicker:OnOff,     "Offline:Kicker-IL:calcout NMS PP",   "Off",  "On", 0,    "NO↩
        "}
112 }
113
114
115 # ANALOG OUTPUT(SOFTWARE ONLY) #######################################################
116
117
118 file "/epics/synApps/synApps_5_8/support/modbus-2-7/db/aoOffline.template" { pattern
119 {P,     R,      FLNK, DRVL,   DRVH,   PREC,   VAL,  PINI}
120 {Offline:,  Foc1:VSet,        "Offline:Foc1-IL:calcout NMS PP",   0,    1000, 3,    0,    "↩
        NO"}
121 {Offline:,  Extr:VSet,        "Offline:Extr-IL:calcout NMS PP",   0,    10000,  3,    0,    ↩
        "NO"}
122 {Offline:,  STT2X:VSet,       "Offline:STT2X-IL:calcout NMS PP",    0,    1000, 3,    0,    ↩
        "NO"}
123 {Offline:,  STT2Y:VSet,       "Offline:STT2Y-IL:calcout NMS PP",    0,    1000, 3,    0,    ↩
        "NO"}
124 {Offline:,  Skimmer:VSet,     "Offline:Skimmer-IL:calcout NMS PP",  0,    1000, 3,    0,    ↩
        "NO"}
125 {Offline:,  QPChamber:VSet,     "Offline:QPChamber-IL:calcout NMS PP",  0,    1000, 3,    0,↩
            "NO"}
126 {Offline:,  QPR:VSet,       "Offline:QPR-IL:calcout NMS PP",    0,    3000, 3,    0,    "NO↩
        "}
127 {Offline:,  QPS:VSet,       "Offline:QPS-IL:calcout NMS PP",    0,    3000, 3,    0,    "NO↩
        "}
128 {Offline:,  QPL1:VSet,        "Offline:QPL1-IL:calcout NMS PP",   0,    1000, 3,    0,    "↩
        NO"}
129 {Offline:,  QPL2:VSet,        "Offline:QPL2-IL:calcout NMS PP",   0,    1000, 3,    0,    "↩
        NO"}
130 {Offline:,  Cone:VSet,        "Offline:Cone-IL:calcout NMS PP",   0,    1000, 3,    0,    "↩
        NO"}
```

```
131 {Offline:,  STT1X:VSet,       "Offline:STT1X-IL:calcout NMS PP",    0,    1000, 3,    0,    ↩
        "NO"}
132 {Offline:,  STT1Y:VSet,       "Offline:STT1Y-IL:calcout NMS PP",    0,    1000, 3,    0,    ↩
        "NO"}
133 #
134 {Offline:,  QTA-:VSet,        "Offline:QTA--IL:calcout NMS PP",   0,    1000, 3,    0,    "↩
        NO"}
135 {Offline:,  QTA+:VSet,        "Offline:QTA+-IL:calcout NMS PP",   0,    1000, 3,    0,    "↩
        NO"}
136 {Offline:,  QTB-:VSet,        "Offline:QTB--IL:calcout NMS PP",   0,    1000, 3,    0,    "↩
        NO"}
137 {Offline:,  QTB+:VSet,        "Offline:QTB+-IL:calcout NMS PP",   0,    1000,   3,    0,    ↩
        "NO"}
138 {Offline:,  Bender_upper:VSet,    "Offline:Bender_upper-IL:calcout NMS PP",   0,    3000,    ↩
        3,    0,    "NO"}
139 {Offline:,  Bender_lower:VSet,    "Offline:Bender_lower-IL:calcout NMS PP",   0,    3000,    ↩
        3,    0,    "NO"}
140 {Offline:,  Kicker:VSet,      "Offline:Kicker-IL:calcout NMS PP",   0,    10000,  3,    0,  ↩
          "NO"}
141 }
142
143
144
145
146 # CALCOUT (SOFTWARE ONLY) ########################################################
147
148
149 file "/epics/synApps/synApps_5_8/support/modbus-2-7/db/calcoutOffline.template" { pattern
150 {P,       R,              INPVALUE,               INPONOFF,               OUT,              ↩
           PINI}
151 {Offline:,      Foc1-IL:calcout,      "Offline:Foc1:VSet NMS NPP",      "Offline:Foc1:OnOff ↩
        NMS NPP",       "Offline:Foc1-IL:VSet NMS PP",        "NO"}
152 {Offline:,      Extr-IL:calcout,      "Offline:Extr:VSet NMS NPP",      "Offline:Extr:OnOff ↩
        NMS NPP",       "Offline:Extr-IL:VSet NMS PP",        "NO"}
153 {Offline:,      STT2X-IL:calcout,     "Offline:STT2X:VSet NMS NPP",     "Offline:STT2X:OnOff↩
         NMS NPP",      "Offline:STT2X-IL:VSet NMS PP",       "NO"}
154 {Offline:,      STT2Y-IL:calcout,     "Offline:STT2Y:VSet NMS NPP",     "Offline:STT2Y:OnOff↩
         NMS NPP",      "Offline:STT2Y-IL:VSet NMS PP",       "NO"}
155 {Offline:,      Skimmer-IL:calcout,     "Offline:Skimmer:VSet NMS NPP",     "Offline:Skimmer↩
        :OnOff NMS NPP",      "Offline:Skimmer-IL:VSet NMS PP",     "NO"}
156 {Offline:,      QPChamber-IL:calcout,   "Offline:QPChamber:VSet NMS NPP",   "Offline:↩
        QPChamber:OnOff NMS NPP",    "Offline:QPChamber-IL:VSet NMS PP",     "NO"}
157 {Offline:,      QPR-IL:calcout,       "Offline:QPR:VSet NMS NPP",       "Offline:QPR:OnOff ↩
        NMS NPP",        "Offline:QPR-IL:VSet NMS PP",       "NO"}
158 {Offline:,      QPS-IL:calcout,       "Offline:QPS:VSet NMS NPP",       "Offline:QPS:OnOff ↩
        NMS NPP",        "Offline:QPS-IL:VSet NMS PP",       "NO"}
159 {Offline:,      QPL1-IL:calcout,      "Offline:QPL1:VSet NMS NPP",      "Offline:QPL1:OnOff ↩
        NMS NPP",       "Offline:QPL1-IL:VSet NMS PP",        "NO"}
160 {Offline:,      QPL2-IL:calcout,      "Offline:QPL2:VSet NMS NPP",      "Offline:QPL2:OnOff ↩
        NMS NPP",       "Offline:QPL2-IL:VSet NMS PP",        "NO"}
161 {Offline:,      Cone-IL:calcout,      "Offline:Cone:VSet NMS NPP",      "Offline:Cone:OnOff ↩
        NMS NPP",       "Offline:Cone-IL:VSet NMS PP",        "NO"}
162 {Offline:,      STT1X-IL:calcout,     "Offline:STT1X:VSet NMS NPP",     "Offline:STT1X:OnOff↩
         NMS NPP",      "Offline:STT1X-IL:VSet NMS PP",       "NO"}
163 {Offline:,      STT1Y-IL:calcout,     "Offline:STT1Y:VSet NMS NPP",     "Offline:STT1Y:OnOff↩
         NMS NPP",      "Offline:STT1Y-IL:VSet NMS PP",       "NO"}
164 #
165 {Offline:,      QTA--IL:calcout,      "Offline:QTA-:VSet NMS NPP",      "Offline:QTA-:OnOff ↩
        NMS NPP",       "Offline:QTA--IL:VSet NMS PP",        "NO"}
166 {Offline:,      QTA+-IL:calcout,      "Offline:QTA+:VSet NMS NPP",      "Offline:QTA+:OnOff ↩
        NMS NPP",       "Offline:QTA+-IL:VSet NMS PP",        "NO"}
167 {Offline:,      QTB--IL:calcout,      "Offline:QTB-:VSet NMS NPP",      "Offline:QTB-:OnOff ↩
        NMS NPP",       "Offline:QTB--IL:VSet NMS PP",        "NO"}
168 {Offline:,      QTB+-IL:calcout,      "Offline:QTB+:VSet NMS NPP",      "Offline:QTB+:OnOff ↩
        NMS NPP",       "Offline:QTB+-IL:VSet NMS PP",        "NO"}
169 {Offline:,      Bender_upper-IL:calcout,  "Offline:Bender_upper:VSet NMS NPP",  "Offline:↩
        Bender_upper:OnOff NMS NPP",   "Offline:Bender_upper-IL:VSet NMS PP",    "NO"}
170 {Offline:,      Bender_lower-IL:calcout,  "Offline:Bender_lower:VSet NMS NPP",  "Offline:↩
        Bender_lower:OnOff NMS NPP",   "Offline:Bender_lower-IL:VSet NMS PP",    "NO"}
171 {Offline:,      Kicker-IL:calcout,      "Offline:Kicker:VSet NMS NPP",      "Offline:Kicker:↩
        OnOff NMS NPP",       "Offline:Kicker-IL:VSet NMS PP",      "NO"}
172 }
173
```

```
174
175
176
177 # CALOUT_FOR_INITIALIZATION (SOFTWARE ONLY) ######################################
178
179
180 file "/epics/synApps/synApps_5_8/support/modbus-2-7/db/calcoutInitValueOffline.template" { ↩
    pattern
181 {P,        R,                  INPVALUE,                  OUT,                    PINI}
182 {Offline:,      Foc1-IL:calcout_init_value,     "Offline:Foc1-IL:VSet NMS NPP",     "Offline↩
    :Foc1:VSet NMS NPP",      "NO"}
183 {Offline:,      Extr-IL:calcout_init_value,     "Offline:Extr-IL:VSet NMS NPP",     "Offline↩
    :Extr:VSet NMS NPP",      "NO"}
184 {Offline:,      STT2X-IL:calcout_init_value,    "Offline:STT2X-IL:VSet NMS NPP",    "Offline↩
    :STT2X:VSet NMS NPP",     "NO"}
185 {Offline:,      STT2Y-IL:calcout_init_value,    "Offline:STT2Y-IL:VSet NMS NPP",    "Offline↩
    :STT2Y:VSet NMS NPP",     "NO"}
186 {Offline:,      Skimmer-IL:calcout_init_value,    "Offline:Skimmer-IL:VSet NMS NPP",    "↩
    Offline:Skimmer:VSet NMS NPP",     "NO"}
187 {Offline:,      QPChamber-IL:calcout_init_value,  "Offline:QPChamber-IL:VSet NMS NPP",  "↩
    Offline:QPChamber:VSet NMS NPP",   "NO"}
188 {Offline:,      QPR-IL:calcout_init_value,      "Offline:QPR-IL:VSet NMS NPP",      "Offline↩
    :QPR:VSet NMS NPP",       "NO"}
189 {Offline:,      QPS-IL:calcout_init_value,      "Offline:QPS-IL:VSet NMS NPP",      "Offline↩
    :QPS:VSet NMS NPP",       "NO"}
190 {Offline:,      QPL1-IL:calcout_init_value,     "Offline:QPL1-IL:VSet NMS NPP",     "Offline↩
    :QPL1:VSet NMS NPP",      "NO"}
191 {Offline:,      QPL2-IL:calcout_init_value,     "Offline:QPL2-IL:VSet NMS NPP",     "Offline↩
    :QPL2:VSet NMS NPP",      "NO"}
192 {Offline:,      Cone-IL:calcout_init_value,     "Offline:Cone-IL:VSet NMS NPP",     "Offline↩
    :Cone:VSet NMS NPP",      "NO"}
193 {Offline:,      STT1X-IL:calcout_init_value,    "Offline:STT1X-IL:VSet NMS NPP",    "Offline↩
    :STT1X:VSet NMS NPP",     "NO"}
194 {Offline:,      STT1Y-IL:calcout_init_value,    "Offline:STT1Y-IL:VSet NMS NPP",    "Offline↩
    :STT1Y:VSet NMS NPP",     "NO"}
195 #
196 {Offline:,      QTA--IL:calcout_init_value,     "Offline:QTA--IL:VSet NMS NPP",     "Offline↩
    :QTA-:VSet NMS NPP",      "NO"}
197 {Offline:,      QTA+-IL:calcout_init_value,     "Offline:QTA+-IL:VSet NMS NPP",     "Offline↩
    :QTA+:VSet NMS NPP",      "NO"}
198 {Offline:,      QTB--IL:calcout_init_value,     "Offline:QTB--IL:VSet NMS NPP",     "Offline↩
    :QTB-:VSet NMS NPP",      "NO"}
199 {Offline:,      QTB+-IL:calcout_init_value,     "Offline:QTB+-IL:VSet NMS NPP",     "Offline↩
    :QTB+:VSet NMS NPP",      "NO"}
200 {Offline:,      Bender_upper-IL:calcout_init_value, "Offline:Bender_upper-IL:VSet NMS NPP", ↩
    "Offline:Bender_upper:VSet NMS NPP",  "NO"}
201 {Offline:,      Bender_lower-IL:calcout_init_value, "Offline:Bender_lower-IL:VSet NMS NPP", ↩
    "Offline:Bender_lower:VSet NMS NPP",  "NO"}
202 {Offline:,      Kicker-IL:calcout_init_value,   "Offline:Kicker-IL:VSet NMS NPP",   "Offline↩
    :Kicker:VSet NMS NPP",      "NO"}
203 }
204
205
206 file "/epics/synApps/synApps_5_8/support/modbus-2-7/db/calcoutInitOnOffOffline.template" { ↩
    pattern
207 {P,        R,  INPVALUE, OUT,  PINI}
208 {Offline:,      Foc1-IL:calcout_init_OnOff,     "Offline:Foc1-IL:VSet NMS NPP",     "Offline↩
    :Foc1:OnOff NMS NPP",     "NO"}
209 {Offline:,      Extr-IL:calcout_init_OnOff,     "Offline:Extr-IL:VSet NMS NPP",     "Offline↩
    :Extr:OnOff NMS NPP",     "NO"}
210 {Offline:,      STT2X-IL:calcout_init_OnOff,    "Offline:STT2X-IL:VSet NMS NPP",    "Offline↩
    :STT2X:OnOff NMS NPP",      "NO"}
211 {Offline:,      STT2Y-IL:calcout_init_OnOff,    "Offline:STT2Y-IL:VSet NMS NPP",    "Offline↩
    :STT2Y:OnOff NMS NPP",      "NO"}
212 {Offline:,      Skimmer-IL:calcout_init_OnOff,    "Offline:Skimmer-IL:VSet NMS NPP",    "↩
    Offline:Skimmer:OnOff NMS NPP",    "NO"}
213 {Offline:,      QPChamber-IL:calcout_init_OnOff,  "Offline:QPChamber-IL:VSet NMS NPP",  "↩
    Offline:QPChamber:OnOff NMS NPP",    "NO"}
214 {Offline:,      QPR-IL:calcout_init_OnOff,      "Offline:QPR-IL:VSet NMS NPP",      "Offline↩
    :QPR:OnOff NMS NPP",      "NO"}
215 {Offline:,      QPS-IL:calcout_init_OnOff,      "Offline:QPS-IL:VSet NMS NPP",      "Offline↩
    :QPS:OnOff NMS NPP",      "NO"}
```

```
216 {Offline:,      QPL1-IL:calcout_init_OnOff,     "Offline:QPL1-IL:VSet NMS NPP",     "Offline↩
        :QPL1:OnOff NMS NPP",     "NO"}
217 {Offline:,      QPL2-IL:calcout_init_OnOff,     "Offline:QPL2-IL:VSet NMS NPP",     "Offline↩
        :QPL2:OnOff NMS NPP",     "NO"}
218 {Offline:,      Cone-IL:calcout_init_OnOff,     "Offline:Cone-IL:VSet NMS NPP",     "Offline↩
        :Cone:OnOff NMS NPP",     "NO"}
219 {Offline:,      STT1X-IL:calcout_init_OnOff,    "Offline:STT1X-IL:VSet NMS NPP",    "Offline↩
        :STT1X:OnOff NMS NPP",      "NO"}
220 {Offline:,      STT1Y-IL:calcout_init_OnOff,    "Offline:STT1Y-IL:VSet NMS NPP",    "Offline↩
        :STT1Y:OnOff NMS NPP",      "NO"}
221 #
222 {Offline:,      QTA--IL:calcout_init_OnOff,     "Offline:QTA--IL:VSet NMS NPP",     "Offline↩
        :QTA-:OnOff NMS NPP",     "NO"}
223 {Offline:,      QTA+-IL:calcout_init_OnOff,     "Offline:QTA+-IL:VSet NMS NPP",     "Offline↩
        :QTA+:OnOff NMS NPP",     "NO"}
224 {Offline:,      QTB--IL:calcout_init_OnOff,     "Offline:QTB--IL:VSet NMS NPP",     "Offline↩
        :QTB-:OnOff NMS NPP",     "NO"}
225 {Offline:,      QTB+-IL:calcout_init_OnOff,     "Offline:QTB+-IL:VSet NMS NPP",     "Offline↩
        :QTB+:OnOff NMS NPP",     "NO"}
226 {Offline:,      Bender_upper-IL:calcout_init_OnOff, "Offline:Bender_upper-IL:VSet NMS NPP", ↩
        "Offline:Bender_upper:OnOff NMS NPP", "NO"}
227 {Offline:,      Bender_lower-IL:calcout_init_OnOff, "Offline:Bender_lower-IL:VSet NMS NPP", ↩
        "Offline:Bender_lower:OnOff NMS NPP", "NO"}
228 {Offline:,      Kicker-IL:calcout_init_OnOff,   "Offline:Kicker-IL:VSet NMS NPP",   "Offline↩
        :Kicker:OnOff NMS NPP",     "NO"}
229 }
230
231
232 # FANOUT (SOFTWARE ONLY) ######################################
233
234
235 file "/epics/synApps/synApps_5_8/support/modbus-2-7/db/fanoutOffline.template" { pattern
236 {P,     R,            LNKVALUEINIT,                     LNKONOFFINIT,                     PINI↩
        }
237 {Offline:,  Foc1-IL:fanout,     "Offline:Foc1-IL:calcout_init_value NMS PP",    "Offline:↩
        Foc1-IL:calcout_init_OnOff NMS PP",      "RUNNING"}
238 {Offline:,  Extr-IL:fanout,     "Offline:Extr-IL:calcout_init_value NMS PP",    "Offline:↩
        Extr-IL:calcout_init_OnOff NMS PP",      "RUNNING"}
239 {Offline:,  STT2X-IL:fanout,    "Offline:STT2X-IL:calcout_init_value NMS PP",   "Offline:↩
        STT2X-IL:calcout_init_OnOff NMS PP",     "RUNNING"}
240 {Offline:,  STT2Y-IL:fanout,    "Offline:STT2Y-IL:calcout_init_value NMS PP",   "Offline:↩
        STT2Y-IL:calcout_init_OnOff NMS PP",     "RUNNING"}
241 {Offline:,  Skimmer-IL:fanout,    "Offline:Skimmer-IL:calcout_init_value NMS PP",   "Offline↩
        :Skimmer-IL:calcout_init_OnOff NMS PP",     "RUNNING"}
242 {Offline:,  QPChamber-IL:fanout,  "Offline:QPChamber-IL:calcout_init_value NMS PP", "Offline↩
        :QPChamber-IL:calcout_init_OnOff NMS PP",   "RUNNING"}
243 {Offline:,  QPR-IL:fanout,      "Offline:QPR-IL:calcout_init_value NMS PP",     "Offline:QPR↩
        -IL:calcout_init_OnOff NMS PP",       "RUNNING"}
244 {Offline:,  QPS-IL:fanout,      "Offline:QPS-IL:calcout_init_value NMS PP",     "Offline:QPS↩
        -IL:calcout_init_OnOff NMS PP",       "RUNNING"}
245 {Offline:,  QPL1-IL:fanout,     "Offline:QPL1-IL:calcout_init_value NMS PP",    "Offline:↩
        QPL1-IL:calcout_init_OnOff NMS PP",      "RUNNING"}
246 {Offline:,  QPL2-IL:fanout,     "Offline:QPL2-IL:calcout_init_value NMS PP",    "Offline:↩
        QPL2-IL:calcout_init_OnOff NMS PP",      "RUNNING"}
247 {Offline:,  Cone-IL:fanout,     "Offline:Cone-IL:calcout_init_value NMS PP",    "Offline:↩
        Cone-IL:calcout_init_OnOff NMS PP",      "RUNNING"}
248 {Offline:,  STT1X-IL:fanout,    "Offline:STT1X-IL:calcout_init_value NMS PP",   "Offline:↩
        STT1X-IL:calcout_init_OnOff NMS PP",     "RUNNING"}
249 {Offline:,  STT1Y-IL:fanout,    "Offline:STT1Y-IL:calcout_init_value NMS PP",   "Offline:↩
        STT1Y-IL:calcout_init_OnOff NMS PP",     "RUNNING"}
250 #
251 {Offline:,  QTA--IL:fanout,     "Offline:QTA--IL:calcout_init_value NMS PP",    "Offline:QTA↩
        --IL:calcout_init_OnOff NMS PP",      "RUNNING"}
252 {Offline:,  QTA+-IL:fanout,     "Offline:QTA+-IL:calcout_init_value NMS PP",    "Offline:QTA↩
        +-IL:calcout_init_OnOff NMS PP",      "RUNNING"}
253 {Offline:,  QTB--IL:fanout,     "Offline:QTB--IL:calcout_init_value NMS PP",    "Offline:QTB↩
        --IL:calcout_init_OnOff NMS PP",      "RUNNING"}
254 {Offline:,  QTB+-IL:fanout,     "Offline:QTB+-IL:calcout_init_value NMS PP",    "Offline:QTB↩
        +-IL:calcout_init_OnOff NMS PP",      "RUNNING"}
255 {Offline:,  Bender_upper-IL:fanout, "Offline:Bender_upper-IL:calcout_init_value NMS PP","↩
        Offline:Bender_upper-IL:calcout_init_OnOff NMS PP",  "RUNNING"}
256 {Offline:,  Bender_lower-IL:fanout, "Offline:Bender_lower-IL:calcout_init_value NMS PP","↩
        Offline:Bender_lower-IL:calcout_init_OnOff NMS PP",  "RUNNING"}
```

```
257 {Offline:,  Kicker−IL:fanout,   "Offline:Kicker−IL:calcout_init_value NMS PP",    "Offline:↩
        Kicker−IL:calcout_init_OnOff NMS PP",      "RUNNING"}
258 }
```

cmd file: TODO: update

```
1  #!/usr/bin/modbusApp
2  
3  ## You may have to change serialTest to something else
4  ## everywhere it appears in this file
5  
6  cd /shares/control/epics/wago
7  < envPaths
8  
9  ## Register all support components
10 # dbLoadDatabase("/opt/epics/modbusR2−5/dbd/modbus.dbd", 0, 0)
11 dbLoadDatabase("/usr/lib/epics/dbd/modbus.dbd", 0, 0)
12 modbus_registerRecordDeviceDriver(pdbbase)
13 
14 # Configure devices
15 # drvAsynIPPortConfigure(portName, hostInfo, priority, noAutoConnect, noProcessEos)
16 # see http://www.aps.anl.gov/epics/modules/soft/asyn/R4−7/asynDriver.html#drvAsynIPPort
17 # drvAsynIPPortConfigure("Vacuum1", "wago−vacuum.igisol:502", 0, 0, 1)
18 
19 drvAsynIPPortConfigure("SPIG", "wago−spig.igisol:502", 0, 0, 1)
20 drvAsynIPPortConfigure("Cave", "wago−valitila.igisol:502", 0, 0, 1)
21 drvAsynIPPortConfigure("SWYard", "wago−switchyard.igisol:502", 0, 0, 1)
22 drvAsynIPPortConfigure("Cooler", "wago−cooler.igisol:502", 0, 0, 1)
23 drvAsynIPPortConfigure("Trap", "wago−trap.igisol:502", 0, 0, 1)
24 drvAsynIPPortConfigure("TrapExt", "wago−trap−ext.igisol:502", 0, 0, 1)
25 drvAsynIPPortConfigure("Prog3", "wago−prog3.igisol:502", 0, 0, 1)
26 drvAsynIPPortConfigure("Offline","wago−offline.igisol:502",0,0,1)
27 
28 # modbusInterposeConfig(portName, linkType, timeoutMsec)
29 # see http://cars9.uchicago.edu/software/epics/modbusDoc.html
30 # modbusInterposeConfig("Vacuum1", 0, 1000)
31 modbusInterposeConfig("SPIG", 0, 1000)
32 modbusInterposeConfig("Cave", 0, 1000)
33 modbusInterposeConfig("SWYard", 0, 1000)
34 modbusInterposeConfig("Cooler", 0, 1000)
35 modbusInterposeConfig("Trap", 0, 1000)
36 modbusInterposeConfig("TrapExt", 0, 1000)
37 modbusInterposeConfig("Prog3", 0, 1000)
38 modbusInterposeConfig("Offline", 0, 1000)
39 
40 # drvModbusAsynConfigure(portName,
41 #        tcpPortName,
42 #      slaveAddress,
43 #      modbusFunction,
44 #      modbusStartAddress,
45 #      modbusLength,
46 #      dataType,
47 #      pollMsec,
48 #        plcType)
49 # see http://cars9.uchicago.edu/software/epics/modbusDoc.html
50 
51 # analog inputs
52 # drvModbusAsynConfigure("Vacuum1_AI",   "Vacuum1", 0, 3,   0, 4, 0, 10, "Wago")
53 # analog outputs read
54 # drvModbusAsynConfigure("Vacuum1_AO_R", "Vacuum1", 0, 3, 512, 6, 0, 10, "Wago")
55 # analog outputs write
56 # drvModbusAsynConfigure("Vacuum1_AO_W", "Vacuum1", 0, 6,   0, 6, 0, 0, "Wago")
57 
58 ### drvModbusAsynConfigure("Vacuum1_DO_R", "Vacuum1", 0, 1, 512, 24, 0, 10, "Wago")
59 
60 # digital inputs
61 # drvModbusAsynConfigure("Vacuum1_DI", "Vacuum1", 0, 1, 0, 72, 0, 100, "Wago")
62 # digital outputs
63 # drvModbusAsynConfigure("Vacuum1_DO", "Vacuum1", 0, 5, 0, 24, 0, 100, "Wago")
64 
65 # fieldbus variables
```

```
66 # drvModbusAsynConfigure("Vacuum1_FBVAR_IN", "Vacuum1", 0, 4, 512, 4, 0, 10, "Wago")
67
68 ## Load record instances
69 # dbLoadRecords("../../db/serialTest.db","user=jahakala")
70
71 ## Load record instances
72 #dbLoadRecords("/usr/lib/epics/db/asynRecord.db","P=norum:,R=asyn,PORT=WagoPort1,ADDR=24,↩
       IMAX=100,OMAX=100")
73 #dbLoadTemplate "vacuum.substitutions"
74
75 ###
76 ### SPIG/HV
77 ###
78 # digital outputs
79 drvModbusAsynConfigure("SPIG_DO", "SPIG", 0, 5, 0, 6, 0, 1, "Wago")
80 # digital inputs
81 drvModbusAsynConfigure("SPIG_DI", "SPIG", 0, 2, 0, 4, 0, 100, "Wago")
82 # analog inputs
83 drvModbusAsynConfigure("SPIG_AI", "SPIG", 0, 4, 0, 28, 0, 100, "Wago")
84 # analog outputs
85 drvModbusAsynConfigure("SPIG_AO", "SPIG", 0, 6, 0, 12, 0, 1, "Wago")
86 dbLoadTemplate "spig.substitutions"
87
88 ###
89 ### Cave
90 ###
91 # digital outputs
92 drvModbusAsynConfigure("Cave_DO", "Cave", 0, 5, 0, 4, 0, 1, "Wago")
93 # analog inputs
94 drvModbusAsynConfigure("Cave_AI", "Cave", 0, 4, 0, 32, 0, 100, "Wago")
95 # analog outputs
96 drvModbusAsynConfigure("Cave_AO", "Cave", 0, 6, 0, 32, 0, 1, "Wago")
97 dbLoadTemplate "cave.substitutions"
98
99 ###
100 ### Offline
101 ###
102 # analog inputs
103 drvModbusAsynConfigure("Offline_AI",  "Offline", 0, 4, 0, 16,    0,  100, "Wago")
104 # analog outputs
105 drvModbusAsynConfigure("Offline_AO",  "Offline", 0, 6, 0, 14,    0,  100, "Wago")
106 dbLoadTemplate "Offline.substitutions"
107
108
109 ###
110 ### SWYard
111 ###
112 # digital outputs
113 drvModbusAsynConfigure("SWYard_DO", "SWYard", 0, 5, 0, 8, 0, 1, "Wago")
114 # analog inputs
115 drvModbusAsynConfigure("SWYard_AI", "SWYard", 0, 4, 0, 34, 0, 100, "Wago")
116 # analog outputs
117 drvModbusAsynConfigure("SWYard_AO", "SWYard", 0, 6, 0, 32, 0, 1, "Wago")
118 dbLoadTemplate "swyard.substitutions"
119
120 ###
121 ### Cooler
122 ###
123 # analog inputs
124 drvModbusAsynConfigure("Cooler_AI", "Cooler", 0, 4, 0, 28, 0, 100, "Wago")
125 # analog outputs
126 drvModbusAsynConfigure("Cooler_AO", "Cooler", 0, 6, 0, 28, 0, 1, "Wago")
127 dbLoadTemplate "cooler.substitutions"
128
129 ###
130 ### Trap
131 ###
132 drvModbusAsynConfigure("Trap_AI", "Trap", 0, 4, 0, 14, 0, 100, "Wago")
133 drvModbusAsynConfigure("Trap_AO", "Trap", 0, 6, 0, 8, 0, 1, "Wago")
134 drvModbusAsynConfigure("Trap_DO", "Trap", 0, 5, 0, 12, 0, 1, "Wago")
135
136 drvModbusAsynConfigure("TrapExt_DO", "TrapExt", 0, 5, 0, 8, 0, 1, "Wago")
137 drvModbusAsynConfigure("TrapExt_AI", "TrapExt", 0, 4, 0, 16, 0, 100, "Wago")
```

```
138 drvModbusAsynConfigure("TrapExt_AO", "TrapExt", 0, 6, 0, 6, 0, 1, "Wago")
139 dbLoadTemplate "trap.substitutions"
140
141 drvModbusAsynConfigure("Prog3_AI", "Prog3", 0, 4, 0, 12, 0, 100, "Wago")
142 dbLoadTemplate "pressure.substitutions"
143
144 dbLoadRecords("calc.db")
145 dbLoadRecords("alias.db")
146
147 # epicsThreadSleep 0.5
148
149 iocInit()
150 dbpf("SPIG:Amplifier:Temperature.MDEL", "0.25")
151 <adel-values.txt
152
153 ## Start any sequence programs
154 #seq sncserialTest,"user=jahakala"
```

B Graphical user interface source code

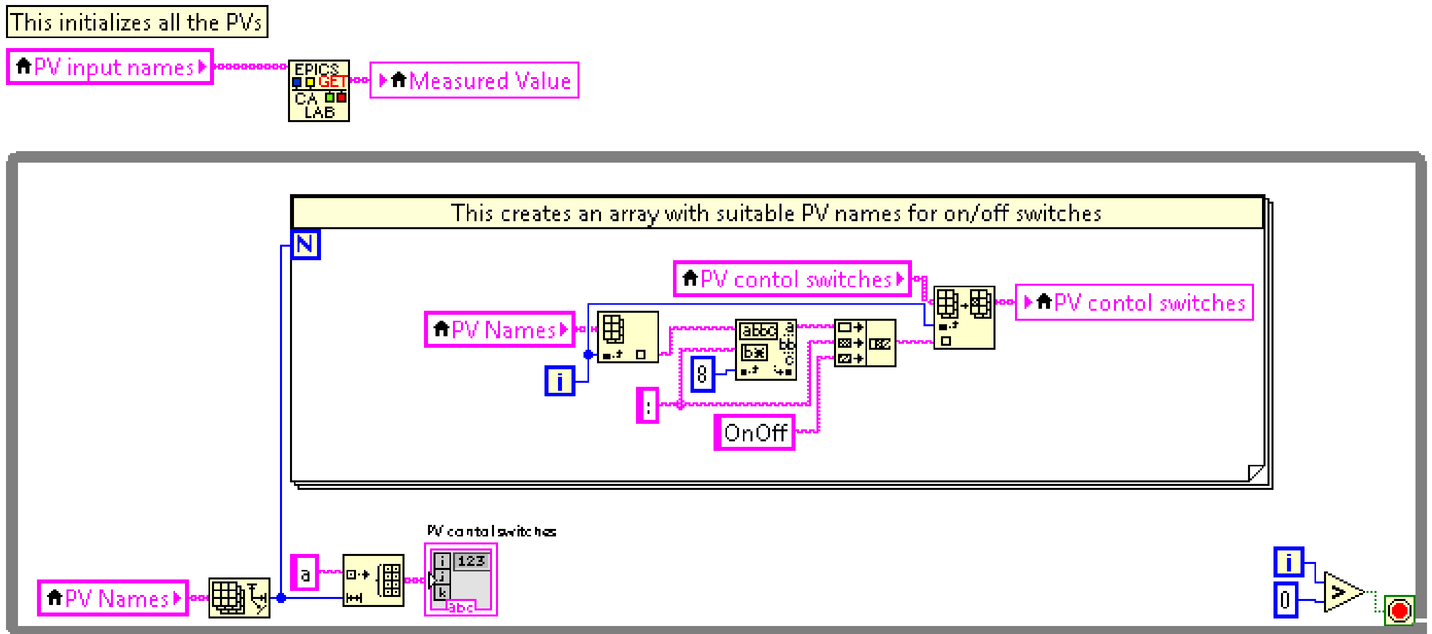

Figure 45: On/Off switch Process Variable name generator

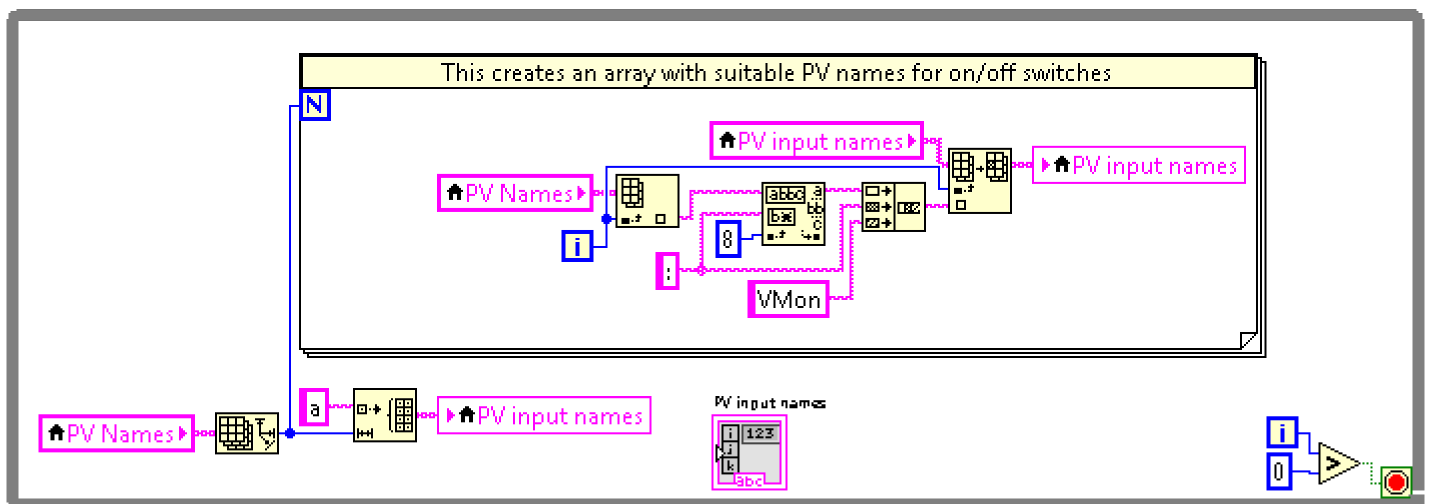

Figure 46: Measured Value Process Variable name generator

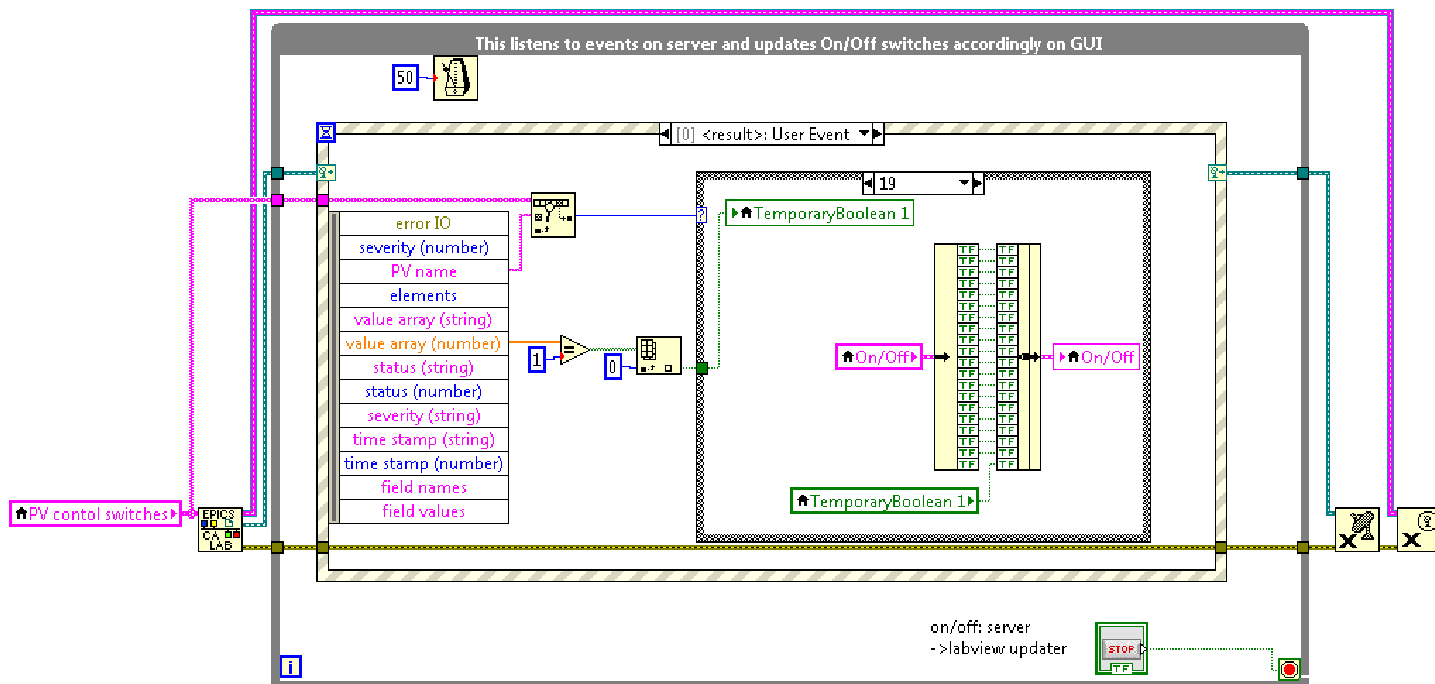

Figure 47: Event listener for On/Off switches

Figure 48: Event listener for Measured Values

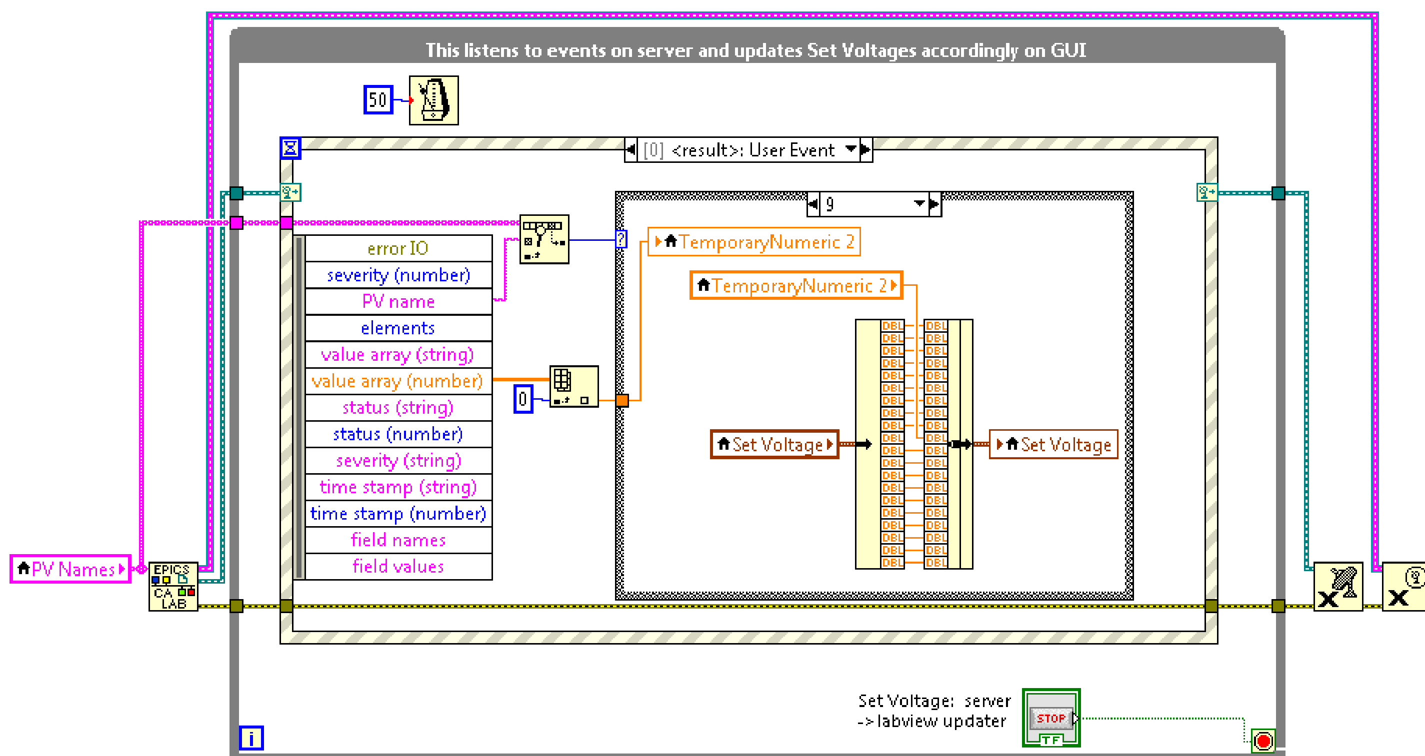

Figure 49: Event listener for Set Voltages

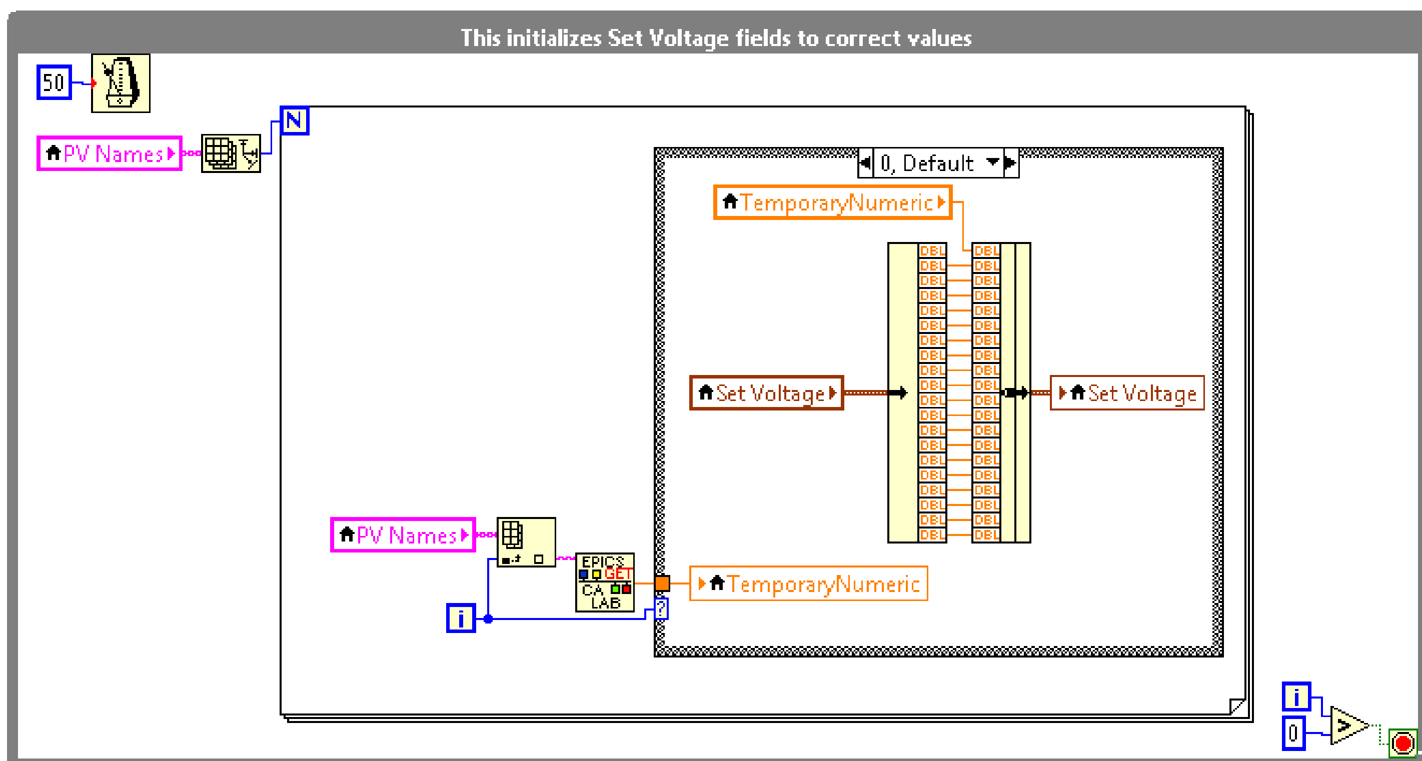

Figure 50: Initializer for Set Voltages

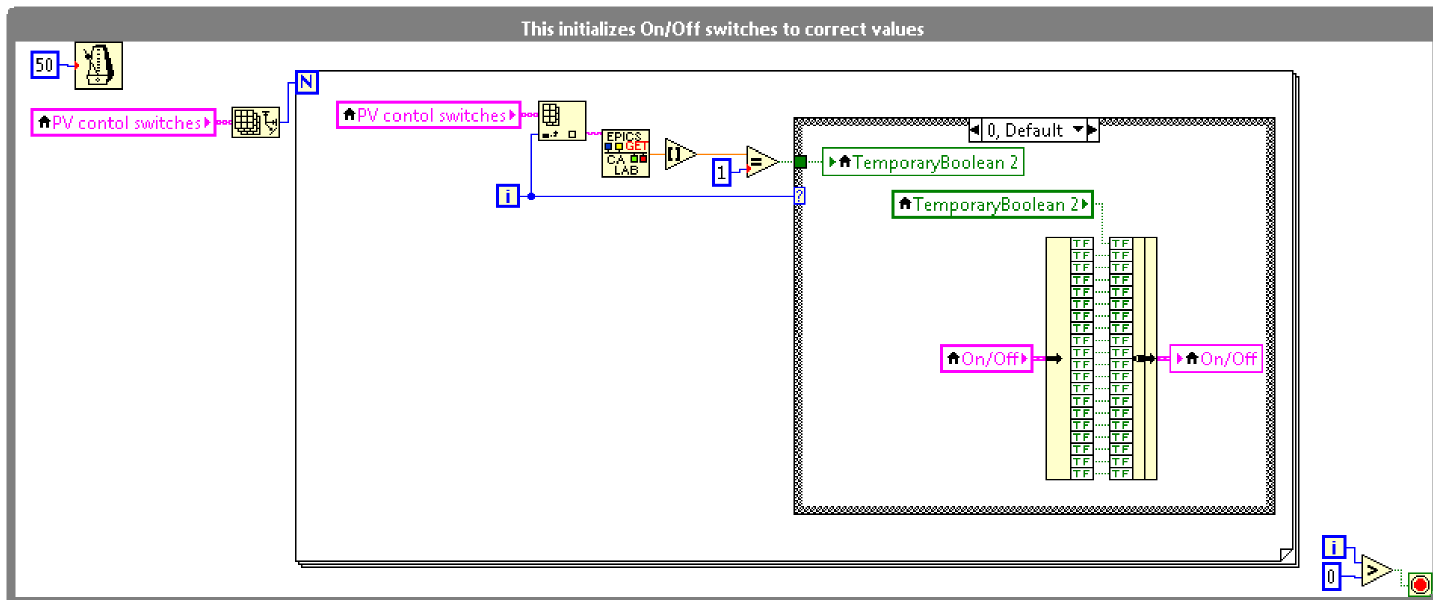

Figure 51: Initializer for On/Off switches

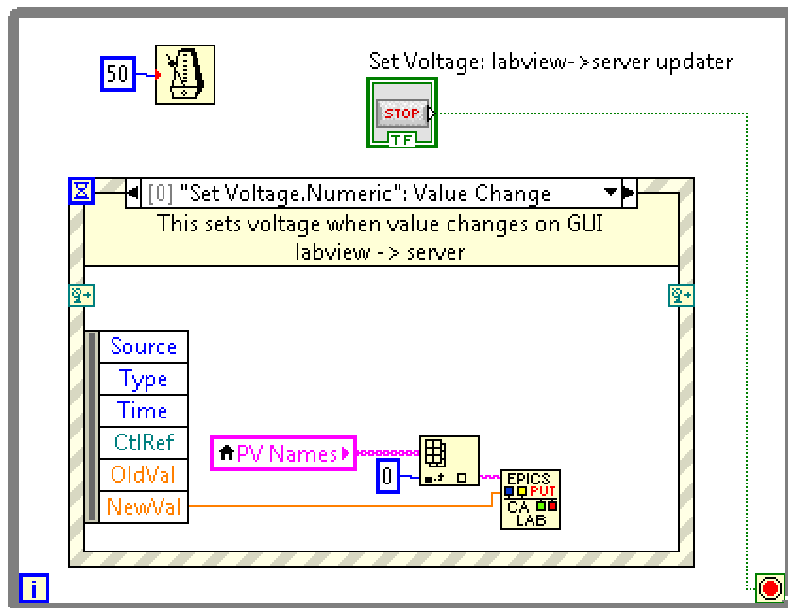

Figure 52: Set Voltage value uploader

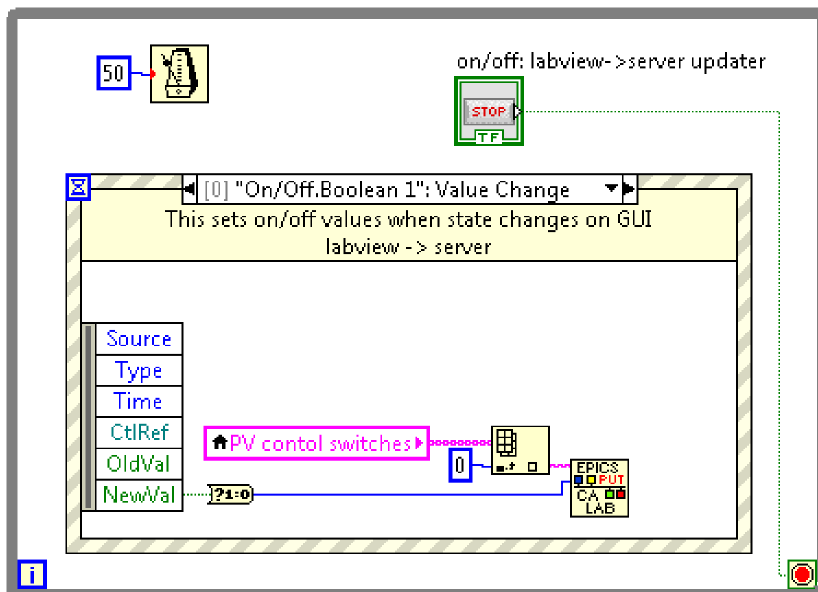

Figure 53: On/Off switch state uploader

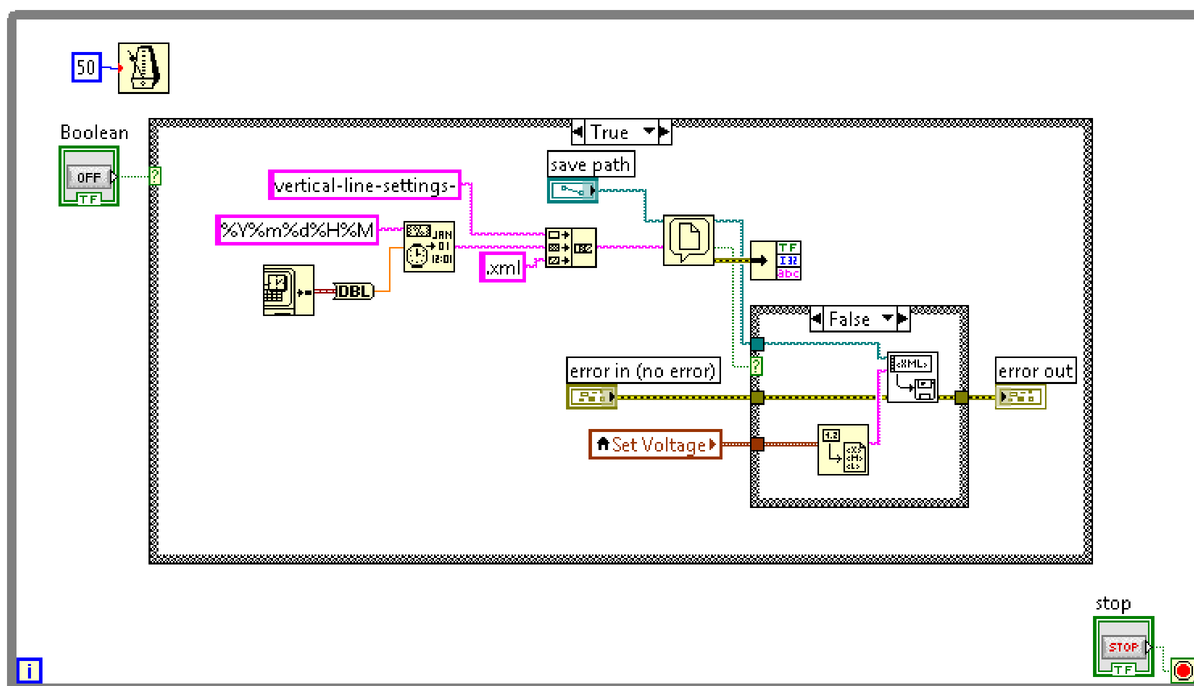

Figure 54: Set Value saver

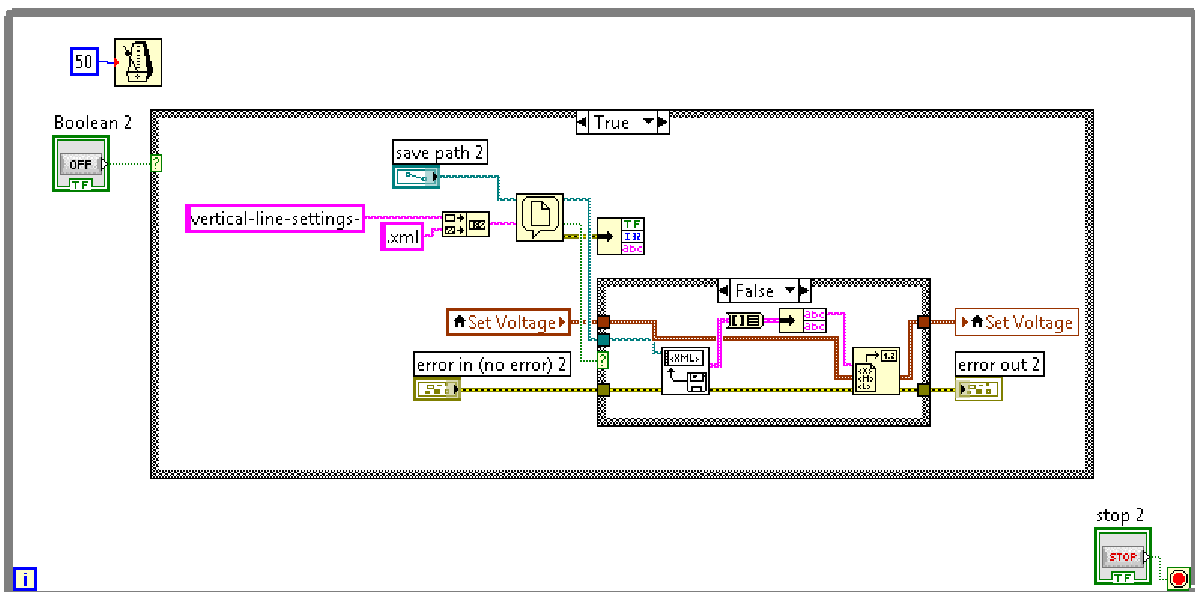

Figure 55: Set Value loader